

PHASE-SEPARATION PHENOMENA IN POLYMER SOLUTIONS

D. M. KOENIG

2

**PHASE-SEPARATION PHENOMENA IN
POLYMER SOLUTIONS**

THE UNIVERSITY OF CHICAGO
DIVISION OF THE PHYSICAL SCIENCES
DEPARTMENT OF CHEMISTRY

PHASE-SEPARATION PHENOMENA IN POLYMER SOLUTIONS

PROEFSCHRIFT

ter verkrijging van de graad van doctor in de
technische wetenschappen
aan de Technische Hogeschool Twente,
op gezag van de rector magnificus, prof. dr. I. W. van Spiegel,
volgens besluit van het College van Dekanen
in het openbaar te verdedigen
op donderdag 3 november 1977 te 16.00 uur

door

DIRK MARINUS KOENHEN

geboren op 13 juni 1949 te Lathum (gem. Angerlo)

DIT PROEFSCHRIFT IS GOEDGEKEURD DOOR PROMOTOR

PROF. DR. C.A. SMOLDERS

AAN TOOS
AAN DE NAGEDACHTENIS VAN
MIJN VADER

I wish to express my great gratitude to all those who have contributed to the work reported in this thesis.

Special reference ought to be given to Prof. M. Gordon for stimulation to work on the PICS apparatus, Dr. J. Goldsbrough and Mr. B.W. Ready (all of the University of Essex, Colchester, England) for carrying out part of the experiments.

Also to Mr. M.A. de Jongh ing, ing. L. Broens Btw, ing. M. Mulder, Ir. A. Bakker, Ir. H. Roelofs and Mr. L. v. d. Ridder for carrying out some experiments.

I am greatly indebted to Dr. D. Bargeman and Dr. H. v. d. Berg for the stimulating discussions.

For enabling me to publish in this form I also want to extend my sincere thanks to Mr. R. Arends for making the drawings and last but not least to Mrs. A. Nienhaus van Lint-Lenselink for typing the manuscript.

CONTENTS	7
CHAPTER I : INTRODUCTION	11
CHAPTER II : PHASE-SEPARATION PHENOMENA IN SOLUTIONS OF POLY (2, 6 DIMETHYL- 1, 4 PHENYLENE OXIDE). I. THERMODYNAMIC PARAMETERS OF SOLUTIONS IN TOLUENE	21
CHAPTER III: PHASE-SEPARATION PHENOMENA IN SOLUTIONS OF POLY (2, 6 DIMETHYL- 1, 4 PHENYLENE OXIDE). II. DIFFERENTIAL SCANNING CALORIMETRY OF SOLUTIONS IN TOLUENE	33
CHAPTER IV: PHASE-SEPARATION PHENOMENA IN SOLUTIONS OF POLY (2, 6 DIMETHYL- 1, 4 PHENYLENE OXIDE). III. PULSE INDUCED CRITICAL SCATTERING OF SOLUTIONS IN TOLUENE	38
CHAPTER V : PHASE-SEPARATION PHENOMENA IN SOLUTIONS OF POLY (2, 6 DIMETHYL- 1, 4 PHENYLENE OXIDE). IV. THERMODYNAMIC PARAMETERS FOR SOLUTIONS IN A SERIES OF HOMOLOGOUS SOLVENTS: TOLUENE TO HEXYLBENZENE	48
CHAPTER VI: PHASE-SEPARATION PHENOMENA IN SOLUTIONS OF POLY (2, 6 DIMETHYL- 1, 4 PHENYLENE OXIDE). V. VAPOUR PRESSURE AND MEMBRANE OSMOMETRY	61
CHAPTER VII: THE DETERMINATION OF SOLUBILITY PARAMETERS OF SOLVENTS AND POLYMERS BY MEANS OF CORRELATIONS WITH OTHER PHYSICAL QUANTITIES	72

CHAPTER VIII: PHASE-SEPARATION PHENOMENA DURING THE FORMATION OF ASYMMETRIC MEMBRANES	89
SUMMARY	106
SAMENVATTING	108
CURRICULUM VITAE	110

The Chapters II, III, IV, VII and VIII are reprinted from the Journal of Polymer Science and Journal of Applied Polymer Science with kind permission of John Wiley & Sons, Inc.

INTRODUCTION

Macromolecules have been connected with life on our planet from its very early forms. One may say that life is impossible without special chemical substances. Plants consist for a substantial part of cellulose, a macromolecule on carbohydrate basis. Man is built for an important part out of proteins, which also constitute an indispensable part of his food. Proteins are macromolecules based on polyamino acids. In this thesis we will be concerned with the behaviour of synthetic macromolecules or polymers. These synthetic polymers could be made from natural or synthetic low molecular weight substances. The first developments in this field occurred on the basis of pure luck and perseverance. The first polymer to go into (commercial) production was the famous celluloid (1869), made from nitrocellulose and camphor.

Following this one, around the turn of the century, casein resins and Bakelite (phenolformaldehyde resin) came on the market. Before 1930 quite a few well known polymers like celluloseacetate, polyvinylacetate, polyvinylchloride and some polyacrylates have been in production. The exact nature of the polymerization reactions and the structure of the polymers was not understood and the results were purely empirical. This situation started to change when in 1926, Staudinger proposed the structure of macromolecules (as he first called them), the structure which we are now used to. The essence of this structure is that the macromolecules consist of a long linear, or sometimes branched, chain with covalent bonds, in which certain structural entities are regularly repeating, the segments. This structure itself explains how the macromolecule can be built up from certain low molecular weight substances, the monomers.

After this big achievement a more systematic search was initiated which resulted in an innumerable amount of different polymers. From this vast quantity some 40 to 50 became of commercial importance. Special reference should be given to the polyamides, the polyesters, to polyethylene and its substituted derivatives.

The main areas of application for the synthetic polymers in previous years can be divided roughly in the following groups.

- Polymers used as construction materials for household apparatus etc.
- Polymers used as synthetic fibers in the textile industry and as films for packaging.
- Polymers used as elastomers replacing natural rubber in several applications.

The possibility to tailoring the chemical structure to obtain the desired mechanical thermal and chemical properties have extended the applications to a far greater field than only replacing the natural occurring macromolecules like wood, rubber, cotton, wool etc.

The polymer poly(2,6-dimethyl-1,4-phenylene oxide) to which the greater part of this thesis is devoted was developed by General Electric in the USA in the mid sixties. It is a so called "engineering" plastic. These are strong, though, abrasion resistant materials, capable of withstanding wide ranges of temperatures and resistant to attack by weather, chemicals and other hostile conditions. The price is generally higher than for "multi purpose" plastics like polyethylene and polystyrene. The better properties however, yield better end products, which allows them to compete successfully with other materials such as metals and ceramics.

The properties of macromolecules can be influenced by factors like crystallization, chain branching, copolymerization, crosslinking, molecular weight etc. Crystallization generally improves the mechanical properties by increasing the modules, and it is generally observed with highly regular macromolecular chains. A high degree of crystallization can yield a brittle material. The crystalline melting point is of course a very important factor in the applicability of crystalline polymers. Branching can reduce crystallization by rendering the chain irregular.

Crosslinking (introducing chemical links between the macromolecular chains, in contrast with physical links as in crystallization) can improve the mechanical and chemical resistance in non-crystalline materials by preventing irreversible flow; crosslinking may yield elastic properties as encountered in rubbers.

During the last decades some applications have been found which make use of, sometimes deliberately build-in, very specific physical and chemical properties of the polymers, e.g. high temperature resistant polymers in space research; the soft swollen contact lenses etc. One of these applications referred to in this thesis is the use of polymers for the manufacturing of ultra- and hyperfiltration membranes. These membranes are used in separation processes of solutes in water, which separation is pressure driven: the membranes reject solutes while water can pass. The properties of these membranes depend on the properties of the membrane. The membranes are made according

to a so called phase inversion process starting from a solution of the polymer and ending with an asymmetric structure: a thin dense skin on a porous sub-structure.

There are many other processes and physical determinations which require polymers in a certain stage to be in solution. These include:

- Solution polymerization; if the polymer is not soluble at higher molecular weight this limits the polymerization reaction.
- Coatings (paints); starting from a polymer solution an applied coating should not phase separate in the drying process.
- Wet and dry spinning of fibers.
- Molecular weight determinations to characterize the polymer.

This shows that sometimes a phase separation in a polymer solution is desired and sometimes not. In any case this marks the importance of studying phase separation behaviour in polymer solutions.

In the following paragraphs some general considerations on phase separation from polymer solutions will be presented.

PHASE RELATIONSHIPS

Substances can occur in different phases which are in thermodynamic equilibrium. The rule governing the phase relationships has been formulated by Gibbs and is known as the phase rule. The phases which are important in this thesis are the liquid and crystalline phases. Although the phase rule theory in itself applies to solutions of high molecular weight substances in a low molecular weight solvent, these solutions present additional problems compared to low molecular weight systems.

It has been discovered quite early that for a liquid-liquid miscibility gap occurring in systems with a polymer in solution this miscibility gap in the phase diagram is shifted to low solute concentrations. This phenomenon is known as the asymmetry of the miscibility gap for polymer solutions. Another complication arises from the fact that in most cases the polymer consists of chains of different molecular length or weight. All these different chains should be considered in the phase rule theory as different substances, thus causing a considerable number of degrees of freedom. The second type of phase separation studied here, crystallization from solution, is affected by these problems as well. A description of the liquid-liquid and liquid-solid phase relationships

is given below.

LIQUID-LIQUID EQUILIBRIUM

For the description of phase relationships use is made of an expression for the free enthalpy of mixing (ΔG_m). This is the free enthalpy of the mixture minus the free enthalpy of the pure components. The chemical potential $\Delta\mu$ is defined in an analogous way.

In figure 1 a typical dependence of ΔG_m on concentration is illustrated at constant temperature, which gives a completely miscible binary system (i.e. the solution will be found to be homogeneous for the whole composition range, from a thermodynamic point of view).

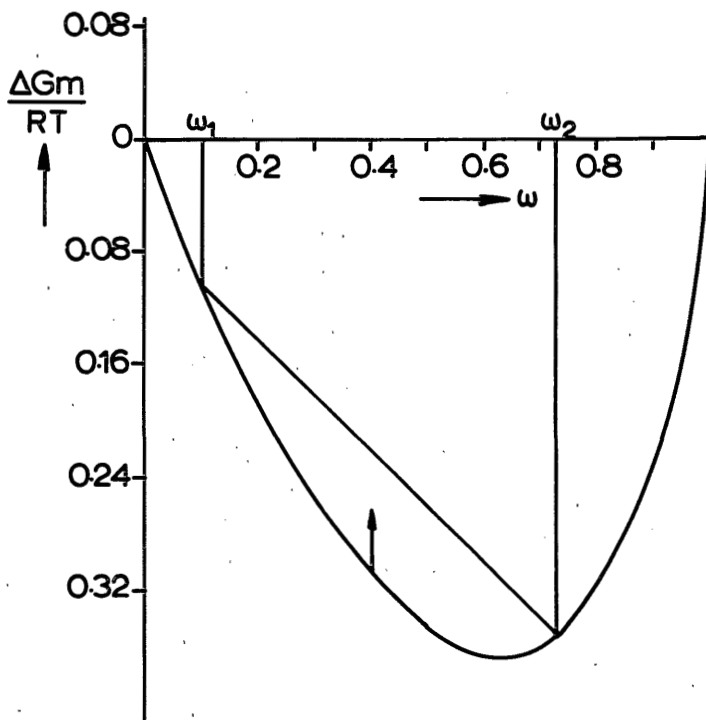


Fig. 1. Schematic diagram for the enthalpy of mixing for a polymer solution which is homogeneous at all compositions.

A phase separation into two liquids of composition w_1 and w_2 would imply an increase in ΔG_m , as is indicated in the figure. A different situation is occurring in figure 2.

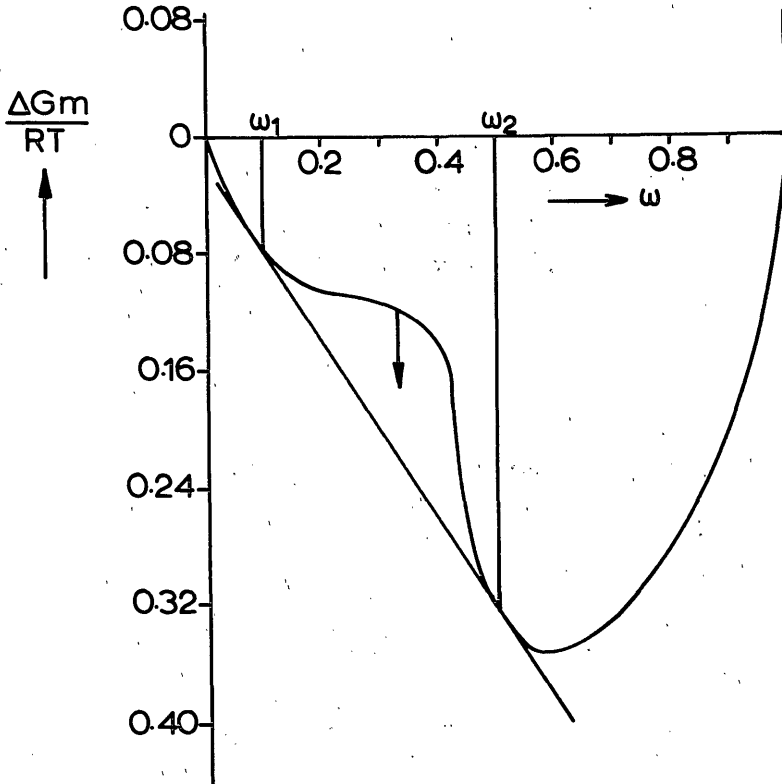


Fig. 2. Schematic diagram of the free enthalpy of mixing for a polymer solution exhibiting a miscibility gap.

Here the ΔG_m - w dependence partly shows a negative curvature and at certain concentrations the solution is experiencing a driving force to lower its free enthalpy of mixing by separating into two phases.

Figure 2 shows that the compositions of the coexisting phases will be given by the common tangent to the ΔG_m - w curve. This curve shows two points of inflection which separate two different regions of demixing.

In the two regions between the common tangent point and the inflection points the solution is metastable. The curvature is still positive and a small variation in concentration gives an increase in ΔG_m . This causes the small variation in concentration to be extinguished. Only a big jump in concentration at certain loci in the solution (a nucleus) can in principle give a phase separation. This is why separation of the solution in these areas is called nucleation and growth. Between the points of inflection the phase separation is initiated by any change in composition, however small this variation may be, because this always lowers ΔG_m . Here the mechanism of phase separation is called spinodal decomposition. Of course the ΔG_m - w curves are here given for one temperature. It is possible that, on changing the temperature the curve in figure 1 changes to a curve like that in figure 2. This gives rise to a T- w diagram which is schematically drawn in figure 3.

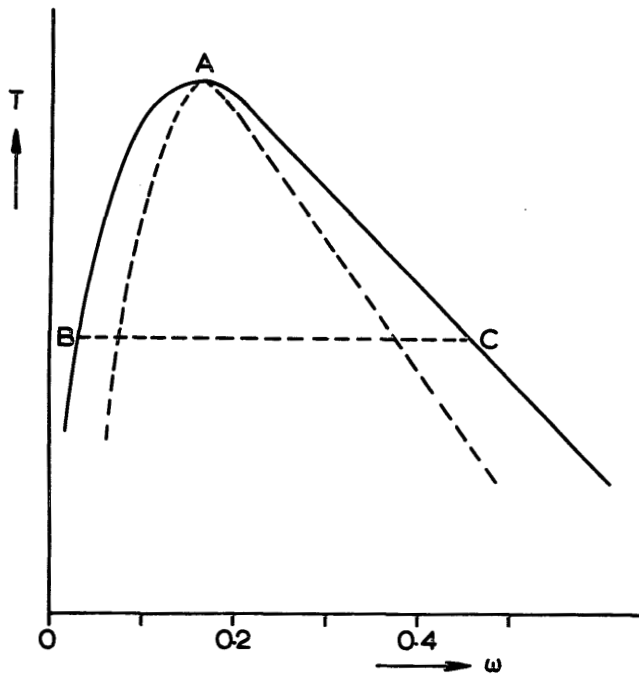


Fig. 3. Schematic representation of a phase diagram for a polymer solution exhibiting liquid-liquid phase separation.

The tie-lines connect the compositions of the phases which are in equilibrium at a certain temperature. The temperature at which the tie-lines reduce to one point yields the so called critical point. In this strictly binary system this point is given by the highest temperature at which phase separation occurs. The inflection points in figure 2 are given by $(\partial^2 \Delta G_m / \partial X^2)_{P,T} = 0$ and the collection of these points in the T-w diagram is called the spinodal curve (dotted line in figure 3).

CRYSTALLIZATION

Crystallization, the solidification of one or more of the components of a solution in the form of an ordered structure may occur when the solution temperature is lowered to below the melting point of one of the components. This situation is presented in figure 4 in a schematic ΔG_m -w curve at constant temperature T_1 , below the melting point of component B. Below its melting point the chemical potential of B is smaller in the solid state than of the mixture in the liquid state. At certain compositions the free enthalpy can thus be lowered.

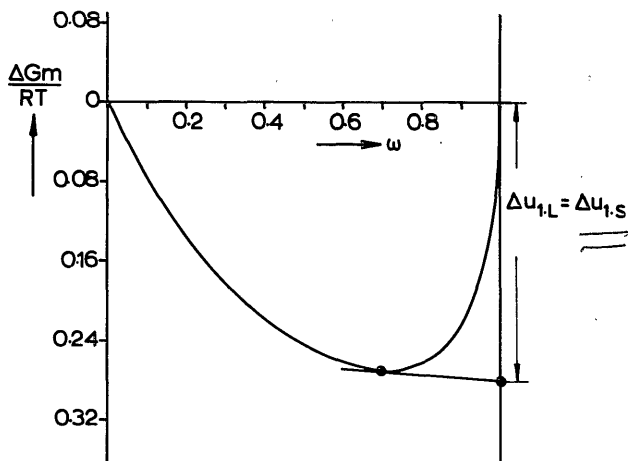


Fig. 4. Schematic representation of a free enthalpy curve for a polymer solution exhibiting phase separation by crystallization.

The composition of the liquid phase in equilibrium with solid B is given by the tangent to the ΔG_m - w curve from the $\Delta \mu$ of the solid phase.

When the melting point of the solvent is high enough a eutectic point can be observed. In most instances in polymer solutions, where the solvent melting point is a great deal lower than the melting point of the polymer, the expected eutectic composition has disappeared in the $w = 0$ axis. For this case the collection of melting points as given by figure 4 for different temperatures is given in figure 5.

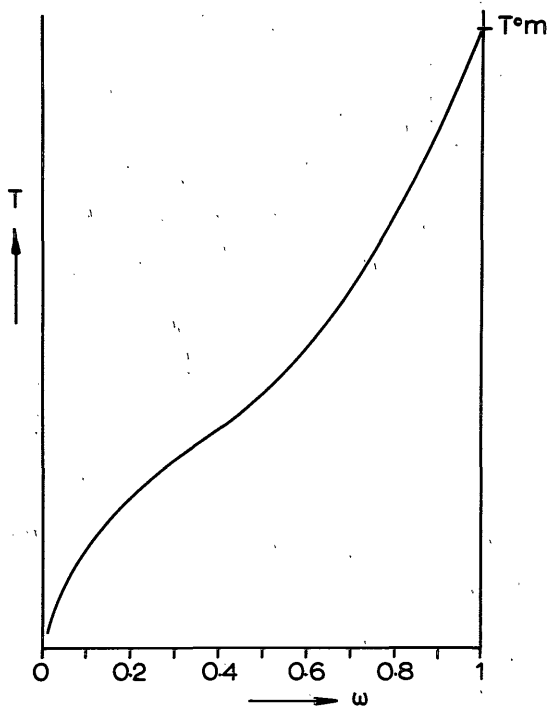


Fig. 5. Schematic melting point curve for a polymer solution.

FREE ENTHALPY EXPRESSION

The most widely used equation for the free enthalpy of mixing is the Flory-Huggins equation. This equation, derived independently by Flory and Huggins, gives essentially the entropy of mixing of a polymer with a low molecular weight substance, calculated on the basis of a lattice model. The equation has been used in a number of formulations which differ only slightly. Here we will use the one introduced by Scholte, using weight fractions.

$$\frac{\Delta G_m}{RT} = w_0 \ln w_0 + \Sigma \frac{M_0}{M_i} w_i \ln w_i + g w_0 w$$

where R is the gas constant, T the temperature, w_0 is the weight fraction of solvent, w_i is the weight fraction of polymer species i, M_0 is the molecular weight of the solvent, M_i is the molecular weight of polymer species i, w is the total weight fraction of polymer, and g is the empirical free enthalpy correction parameter.

The first two terms on the right hand side give the entropy of mixing. It is clear that when a high molecular weight substance is involved M_i will be large compared to M_0 and the term $\frac{M_0}{M_i} w_i \ln w_i$ will be negligibly small. This is the term which is responsible for the asymmetry in position of the demixing gap. Additional to the entropy of mixing term a free enthalpy term $g w_0 w$ is introduced. The Van Laar type enthalpy correction g can be used to cover all non-idealities and can be assumed to depend on any variable such as temperature, concentration, molecular weight distribution etc.

In recent years it has often been tried to improve the Flory-Huggins equation. In order to explain the high temperature phase separation in polymer solutions (LCST behaviour) theories based on the difference in free volume have been introduced. These give an entropy correction term plus an enthalpy correction. The theories are able to explain the phase separation processes qualitatively, but for quantitative descriptions even more correction parameters are necessary. One of the rather simple ways of estimating the interaction between solvents and polymers is on the basis of the solubility parameter theory, a theory which uses the heats of vaporization of the pure substances as parameters.

The investigations for this thesis have been worked out in the form of seven publications or future publications. The contents of the chapters are:

- CHAPTER II In this paper the determination of the free enthalpy correction parameter g is described for the system PPO-toluene. The method used here was light scattering for solutions of different concentrations up to 10 % and at various temperatures.
- CHAPTER III In this paper the crystallization and melting of PPO from solutions in toluene is investigated. The method used here was differential scanning calorimetry. The presence of toluene in the crystal lattice is suggested.
- CHAPTER IV This chapter described the investigations on the crystallization of PPO from toluene solutions with the novel Pulse Induced Critical Scattering technique. The kinetics of the crystallization is discussed.
- CHAPTER V In this paper the determination of the free enthalpy correction parameter from melting point curves is discussed for PPO in the homologous solvent series toluene-hexylbenzene. The influence of solvent entering the crystal lattice is discussed.
- CHAPTER VI This paper discusses two alternative methods to determine the free enthalpy correction parameter for PPO in toluene: vapour pressure osmometry and high pressure membrane osmometry. The applicability of free-volume theory and of solubility parameter concept is discussed.
- CHAPTER VII In this paper the determination of solubility parameters for solvent/polymer pairs from other physical quantities is discussed.
- CHAPTER VIII This paper described the formation mechanism of asymmetric ultra- and hyperfiltration membranes. The role of liquid-liquid phase separation (nucleation and growth, spinodal decomposition) and crystallization is discussed.
- A summary of this thesis is given in CHAPTER IX.

Phase-Separation Phenomena in Solutions of Poly(2,6-dimethyl-1,4-phenylene Oxide). I. Thermodynamic Parameters of Solutions in Toluene

D. M. KOENHEN and C. A. SMOLDERS, *Twente University of Technology, Enschede, The Netherlands*

Synopsis

New experimental data have been collected on thermodynamic properties of solutions of poly(2,6-dimethyl-1,4-phenylene oxide) (PPO) in toluene. The Flory-Huggins interaction parameters g have been determined from light scattering measurements. These values are in agreement with values obtained by osmotic measurements at low concentrations and they allow the calculation of a melting point curve which fits the experimental melting points. No liquid-liquid phase separation can be calculated, as was concluded in a preceding paper. Spinodals could not be detected by light scattering or DSC-measurements. This also indicates that liquid-liquid phase separation does not occur. The phase separation on cooling of a PPO-toluene solution is thus believed to be a crystallization phenomenon.

INTRODUCTION

When a homogeneous solution of poly(2,6-dimethyl-1,4-phenylene oxide) (PPO* resin) in toluene is cooled, the solution exhibits a phase separation visible by an increase of turbidity. This phenomenon has been explained in two different ways:

1. Crystallization of the polymer. The temperature at which turbidity appears (on slow cooling) is called the crystallization point.¹ It is possible that the solvent participates in the crystal structure.²
2. Liquid-liquid phase separation, and subsequent crystallization of polymer from the concentrated phase. In this case the temperature of appearance of turbidity with a very slow cooling rate (1°C/48 hr) has been taken as a point on the cloud point curve, and with a faster cooling rate (1°C/10 min) as a point on the spinodal.³

The melting-point curve, obtained by heating the phase-separated solutions, has the same meaning in both approaches. The first explanation is the most straightforward one. It, however, does not provide an explanation for the fact that depending on the rate of cooling there can be found two temperatures at which the solution becomes homogeneous on heating.³ The second interpretation was mainly based on the change-over of the phase boundaries of the system PPO-toluene in comparison with the ternary system PPO-toluene-ethanol.³ On and near the binary side, PPO-toluene, of the ternary diagram it was possible

* Registered trademark of General Electric Company.

to determine three phase-transition temperatures, whereas in a system with more ethanol present, only liquid-liquid phase separation occurred. It seemed that the cloud point curve of this ternary system could be extrapolated to the binary PPO-toluene side. When cooled at a fast rate the solution becomes homogeneous again at or near this cloud point curve, which also points to liquid-liquid phase separation. As a last point of this interpretation it was stated that the liquid-liquid phase separation preceded a crystallization of the polymer-rich phase. This could explain the occurrence of the three-phase boundaries which have been found in the experiments.

In the present paper some additional experiments are described which allow a better choice to be made between the proposed mechanisms.

THEORETICAL

General Thermodynamic and Kinetic Framework

In polymer solution, the free enthalpy (Gibbs free energy) of mixing is usually expressed in the form of the Flory-Huggins equation.⁴ In this paper we will write the Flory-Huggins equation using weight fractions, and with a free-enthalpy correction parameter g according to Koningsveld^{5,6}

$$\Delta G_m = RT \left[w_0 \ln w_0 + \sum_i \frac{M_0}{M_i} w_i \ln w_i + g w_0 w \right] \quad (1)$$

where ΔG_m is the free enthalpy of mixing of M_0 grams of solution; w_0 is the weight fraction of the solvent; w_i is the weight fraction of polymer component i , w is the total weight fraction of the polymer, M_0 is the molecular weight of the solvent, and M_i is the molecular weight of the polymer component i .

Equation (1) can be used to describe liquid-liquid phase separation. When the free enthalpy of mixing of a homogeneous solution of a given composition is higher than the free enthalpy of a combination of two liquid phases having the same total composition, the homogeneous mixture will separate into two phases. In a graphical representation for a binary system, the compositions are given by the common tangent to the ΔG_m versus composition curve. Between the common tangent and the points of inflection the curve is concave upwards, which means that the solution is stable towards fluctuations limited to neighboring compositions, but unstable against formation and growth of a nucleus with a composition across the instability gap. This mechanism of phase separation is called nucleation and growth. Between the points of inflection the ΔG_m curve is concave downwards. This means that the solution is unstable towards any concentration fluctuation and such a solution will separate into two phases instantaneously. This mechanism is called spinodal demixing. Therefore, upon temperature lowering in a system which shows liquid-liquid phase separation one will first pass through a region in which nucleation and growth can occur: the points at which the phase separation starts constitute the binodal. When this nucleation mechanism is retarded, spinodal demixing can occur, starting at the spinodal curve. If the empirical correction factor g is known, both binodal and spinodal curves can be determined. On the other hand, if the spinodal could be determined experimentally, it should be possible to calculate g .

In this work the g parameters have been determined by light scattering. The

g parameters obtained can be used to compute ΔG_m versus composition at several temperatures from which it can be judged, whether liquid-liquid phase separation could occur. Light scattering can also indicate the existence of a spinodal region, since the scattering intensity should increase enormously on approaching the spinodal curve. This has also been checked for the system under investigation. Furthermore, an attempt has been made to determine a spinodal temperature (if any) for the system PPO-toluene by fast-cooling experiments in differential scanning calorimetry. On increasing the cooling rate one should find a phase separation temperature for spinodal demixing which is independent of the cooling rate.

Finally, in terms of crystallization phenomena, one can also use the g parameter to calculate the lowering of the melting point of crystalline material in solutions of various polymer concentration.^{4,7,8} This allows the calculation of the melting point curve which can be compared with the experimental one.

Light Scattering

Measurement of the intensity of light scattered from a polymer solution at various concentrations and angles is a means for the determination of the chemical potential and the interaction parameters of the system.⁹

The equations derived by Scholte read:

$$-\left(\frac{\partial(\Delta\mu_0)}{\partial w}\right)_{M_n} = RT M_0 \left[\frac{2\pi^2 n_B^2}{N_A \lambda^4 R_B} \left(\frac{dn}{dw}\right)^2 \frac{w}{\rho(\alpha\Delta I)_{\theta=0}} + \frac{1}{M_n} - \frac{1}{M_w} \right] \quad (2)$$

and

$$-\left(\frac{\partial\mu}{\partial w}\right)_{MWD} = RT M_n \left[\frac{2\pi^2 n_B^2}{N_A \lambda^4 R_B} \left(\frac{dn}{dw}\right)^2 \frac{1-w}{\rho(\alpha\Delta I)_{\theta=0}} + \frac{1-w}{w} \left(\frac{1}{M_n} - \frac{1}{M_w}\right) \right] \quad (3)$$

where $\Delta\mu_0$ is the chemical potential of solvent in solution less the chemical potential of pure solvent; μ is the chemical potential of the polymer in solution; ΔI is the scattered light intensity from the solution minus that from the pure solvent, relative to the light intensity of pure benzene scattered perpendicular to the incident ray (scattering angle $\theta = 90^\circ$); α is the angle factor $(\sin \theta)/(1 + \cos^2 \theta)$; ρ is the density of the solution; n_B is the refractive index of benzene at wavelength λ of light; R_B is the Rayleigh factor of benzene; N_A is the Avogadro's number; (dn/dw) is the specific refractive index increment; and subscripts M_n and MWD indicate differentiation with respect to w at a fixed number average molecular weight and a fixed molecular weight distribution, respectively.

The right side of eqs. (2) and (3) can be determined experimentally. Integration of eq. (2) from very low values of w upwards then yields values of $\Delta\mu_0$. Differentiation of eq. (1) with respect to the number of moles of the various components yields, respectively:

$$\frac{\Delta\mu_0}{RT} = \ln(1-w) + \left(1 - \frac{M_0}{M_n}\right)w + \left\{g - (1-w)\frac{\partial g}{\partial w}\right\}w^2 \quad (4)$$

and

$$\left(\frac{\Delta\mu}{RT}\right)_{M_n} = \ln w + (1-w) - \frac{M_n}{M_0}(1-w) + \left\{g + w\frac{\partial g}{\partial w}\right\}\frac{M_n}{M_0}(1-w)^2 \quad (5)$$

It follows that the quantity

$$\chi_w = g - (1 - w) \frac{\partial g}{\partial w} \quad (5a)$$

can be calculated; χ_w is the well-known Flory-Huggins interaction parameter.

When a spinodal is approached, the light scattering can reach very high values. Scholte¹⁰ has given an extrapolation procedure to determine the spinodal by plotting values of $1/(\alpha\Delta I)_{\theta=0}$ against $1/T$ or T (when the temperature range is not too large) and extrapolating to $1/(\alpha\Delta I)_{\theta=0} = 0$.

Melting-Point Depression

The melting-point depression equation for polymer-solvent systems derived by Flory⁴ and modified by Hoffman⁹ reads:

$$\Delta\mu_{f,u} = H_u^0 \frac{(T_m^0 - T_m)T_m}{(T_m^0)^2} \quad (6)$$

where $\Delta\mu_{f,u}$ is the chemical potential change for the melting of one mole of polymer segments; ΔH_u^0 is the molar enthalpy of fusion for the polymer repeat unit; T_m is the melting point in solution; and T_m^0 is the melting point of pure polymer.

At equilibrium between polymer crystals and a polymer solution, the following relations are valid:⁴

$$\begin{aligned} \mu_u^1 - \mu_u^{(0)} &= \Delta\mu_{M,u} \\ \mu_u^c - \mu_u^{(0)} &= \Delta\mu_{f,u} \end{aligned} \quad (7)$$

and

$$-\mu_{f,u} = \Delta\mu_{M,u}$$

μ_u^c is the thermodynamic potential of one mole of repeat units for the polymer in the crystalline state; $\mu_u^{(0)}$ is the thermodynamic potential of one mole of repeat units for the polymer in the standard state; μ_u^1 is the thermodynamic potential of one mole of repeat units for the polymer in solution and M refers to mixing, f to fusion.

Using eq. (5) and inserting a temperature and concentration dependent g of the form

$$g = g_0 + \frac{g_1}{T} + g_2w \quad (8)$$

(g_0 , g_1 and g_2 are constants), we obtain the following expression for the change in chemical potential upon mixing polymer and solvent.

$$\Delta\mu_{M,u} = RT \left[\frac{M_0}{M_n} \ln w - (1-w) \frac{M_0}{M_n} - (1-w) + \left(g_0 + \frac{g_1}{T} + 2g_2w \right) (1-w)^2 \right] \quad (9)$$

Combining eqs. (6), (7), and (9) we find:

behind?

$$\Delta H_u^0 \frac{(T_m^0 - T_m) T_m}{(T_m^0)^2} = -RT_m \left[\frac{M_0}{M_n} \ln w + (1-w) \frac{M_0}{M_n} - (1-w) + (g_0 + \frac{g_1}{T_m} + 2g_2 w)(1-w)^2 \right] \quad (10)$$

By solving eq. (10) for at least three sets of melting temperature versus composition data, we have a possibility in principle to determine g_0 , g_1 , and g_2 from experimental data.

Differential Scanning Calorimetry

As has been pointed out by Van Emmerik¹⁸ it is possible to determine the phase separation temperatures in this system by differential scanning calorimetry. When the phase separation is a result of nucleation and growth a certain induction or delay time has to be expected, irrespective of the type of phase separation. These delay times should become shorter with increasing undercooling. At temperatures below a spinodal even the smallest fluctuation in concentration is sufficient to destabilize the solution and therefore demixing must occur without a delay time.^{11,12} In DSC measurements spinodal demixing is in principle detectable, since phase separation temperatures should then become independent of the cooling rate.

EXPERIMENTAL

Light Scattering

The light scattering experiments were performed with a Sofica 42000 M photogoniidiffusometer. The wavelength used was 546 nm (unpolarized light). There was no need for extra neutral filters with the intensities measured. Temperatures at which experiments were performed were 25, 55, and 75°C. Temperature control was within 0.1°C, with an external thermostat. The toluene used was Baker Analyzed Reagent p.a. grade which was distilled and dried by molecular sieves (4 Å). The PPO sample used had $\bar{M}_n = 21.600$ and $\bar{M}_w = 37.700$ as determined by osmometry and light scattering, respectively. The solutions were freed from dust by filtration through a 0.45μ Millipore filter. With this filter only solutions with $w \leq 0.1$ could be filtered because the viscosity at higher concentrations.

Melting-Point Depression

Homogeneous mixtures of PPO-toluene were made by weighing the appropriate amounts of PPO and toluene in small glass tubes, which were degassed, flushed with nitrogen, and sealed under vacuum at liquid nitrogen temperature. The sealed glass tubes were heated in an oil bath to obtain a homogeneous solution. These solutions were cooled very slowly (1°C/48 hr) in a thermostat until the solutions became turbid. Melting points were determined visually by heating the turbid solution very slowly, until the solution again became clear. The melting points were confirmed by differential scanning calorimetry measurements.

Differential Scanning Calorimetry

Solutions were made in the glass tubes as mentioned above. After the tubes were cooled and broken, samples were put into liquid type sample pans. Only those pans which showed no weight loss after 24 hr at 90°C were used. DSC measurements were performed with a Perkin Elmer DSC-2 apparatus.

RESULTS

Light Scattering

In Figure 1 a typical scattering plot is shown from which the extrapolation of $\alpha\Delta I$ to $\theta = 0$ was made. The extrapolation of $(w/(\alpha\Delta I)_{\theta=0})$ values to $w = 0$ yielded a weight average molecular weight of 37.700 which is in accordance with the previously determined value. For the calculation of $(\partial\mu/\partial w)_{MWD}$ and $[\partial(\Delta\mu_0)/\partial w]$, the following constants have been used.

$$\text{At } T = 25^\circ\text{C}; n_B = 1.502 \quad R_B = 16.3 \times 10^{-6} \text{ (cm}^{-1}\text{)}$$

The values of n_B^2/R_B occurring in eqs. (2) and (3) have been corrected for temperature effects with the Lorentz-Lorenz equation (n_B) and data of Cohen and Eisenberg¹³ (for R_B), and yield

$$(n_B^2/R_B)_{55^\circ\text{C}} = 0.908 (n_B^2/R_B)_{25^\circ\text{C}}$$

$$(n_B^2/R_B)_{75^\circ\text{C}} = 0.847 (n_B^2/R_B)_{25^\circ\text{C}}$$

The densities at 25°C and 55°C were taken from Ref. 3 and the densities at 75°C were calculated with the relations given in Ref. 1.

The calculated values $\Delta\mu_0$ and χ_w are shown in Table I. Figure 2 shows χ_w

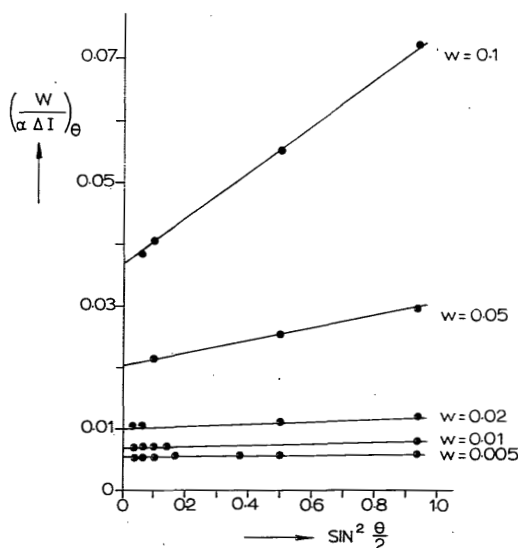


Fig. 1. Light scattering at different concentrations of PPO in toluene at 55°C.

TABLE I
Chemical Potentials and Interaction Parameters for PPO-Toluene Solutions

Temperature, °K	w	$-\Delta\mu_0 \times 10^{-6}$, erg/mole	χ_w
298	0.005	0.591	0.40
	0.01	1.305	0.40
	0.02	3.10	0.407
	0.05	11.25	0.421
	0.10	35.02	0.437
328	0.005	0.607	0.39
	0.01	1.443	0.40
	0.02	3.439	0.404
	0.05	13.00	0.412
	0.10	39.05	0.435
348	0.005	0.703	0.38
	0.01	1.58	0.38
	0.02	3.80	0.392
	0.05	14.48	0.402
	0.10	45.43	0.422

as a function of concentration and temperature. The values of χ_w at 75°C are probably somewhat too low in comparison with the values at 25°C and 55°C because the densities calculated from the equations of Shultz¹ are lower than those found by Van Emmerik³ at higher temperatures, thus yielding higher $\Delta\mu_0$ values and a lower χ_w . The concentration dependence of χ_w , however, is the same for the three temperatures. The χ_w values are in agreement with the values $\chi = 0.38 \pm 0.04$ at low concentrations, determined with osmometry in this laboratory for the determination of the number average molecular weight, and by Barrales-Rienda and Pepper.¹⁴

It can be concluded that the temperature dependence of χ_w is very small for this system, but there is a distinct concentration dependence (Fig. 2).

When g is taken as a function of concentration and temperature [eq. (8)], combination with eq. (5a) gives

$$\chi_w = g_0 + \frac{g_1}{T} + 2g_2w - g_2 \quad (11)$$

From the experimental light scattering data we thus find in a first approximation

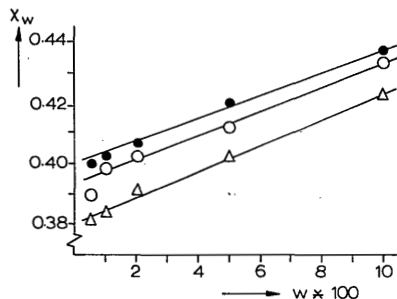


Fig. 2. The interaction parameter χ_w as a function of concentration and temperature. (●) 25°C, (○) 55°C, (△) 75°C.

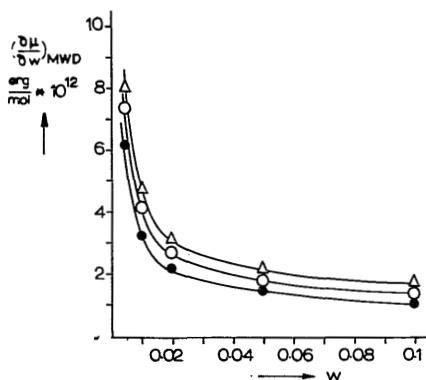


Fig. 3. $(\partial\mu/\partial w)_{MWD}$ for PPO-toluene solutions at different temperatures. (●) 25°C, (○) 55°C, (△) 75°C.

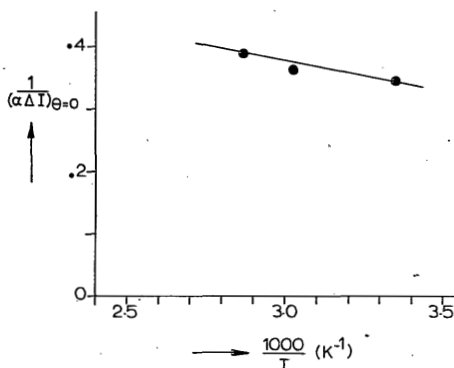


Fig. 4. Extrapolation plot to determine the spinodal.

that $g_1 = 0$. From data plotted in Figure 2, g_2 and g_0 can then be determined. The slope of the curve yields $g_2 = 0.19 \pm 0.02$ and from χ_w at $w = 0$ a value of $g_0 = 0.58 \pm 0.02$ is obtained. In Figure 3 a graphical representation of $(\partial\mu/\partial w)_{MWD}$ versus composition is shown. It can be seen from this figure that $(\partial\mu/\partial w)_{MWD}$ also has only a slight dependence on T . The spinodal (if it exists) is located at $1/(\alpha\Delta I)_{\theta=0} = 0$; this means that high-fluctuation scattering occurs on approaching a spinodal point.

From Figure 4 it appears that the extrapolation to $1/(\alpha\Delta I)_{\theta=0} = 0$ leads to an extremely low spinodal temperature; about 180°K. In the temperature range studied there is no indication for high-fluctuation scattering. Hence a spinodal curve is not present in the temperature region of interest.

Melting-Point Depression

Melting temperatures determined visually with an accuracy of $\pm 1^\circ\text{C}$ are given in Table II as a function of the polymer concentration. The results agree very well with other literature data.^{1,3} The inverse melting points plotted versus the

TABLE II
Melting Temperature of PPO Solutions in Toluene

w	$T_m, ^\circ\text{K}$
0.1	334
0.2	345
0.3	359
0.4	373
0.5	389

weight fraction of polymer in the solution, show a practically linear relation (Fig. 5), over the large concentration range covered. Therefore, the melting-point depression cannot be used to discriminate between contributions of g_1/T and g_2w in eq. (10). From the light scattering experiments it follows that g_1/T is very small and we have already concluded that $g = g_0 + g_2w$ can be used in eq. (10).

Since data on ΔH_u^0 range from 6 to 20 cal/g¹⁵ and data on T_m^0 from 510–545°K^{3,16} it is not feasible to calculate g_0 and g_2 directly from melting-point data. With the data obtained from light scattering: $g_0 = 0.58$ and $g_2 = 0.19$ a good fit of the experimental melting points was found using $T_m^0 = 545^\circ\text{K}$, $\Delta H_u^0 = 9.5$ cal/g and also using $T_m^0 = 535^\circ\text{K}$ with $\Delta H_u^0 = 9.8$ cal/g: both data sets give the "calculated" line from Figure 6. This type of experiment, obviously is not a very sensitive means of obtaining thermodynamic data. For lower g_0 values, good fits can be obtained also, but only when using somewhat higher ΔH_u^0 values. The ΔH_u^0 and T_m^0 values chosen remain within the range reported in the literature. For $g_2 = 0$ a fit can only be obtained by choosing large g_0 values. Then the normal type of liquid-liquid phase separation should occur with a maximum in the cloud point curve at low polymer concentration.⁴ This type of phase separation is not found for toluene as a solvent. It has to be concluded that g_2w contributes appreciably to the total g as was found in the light scattering results. Qualitatively, the melting point data are in agreement with the results for g from the light scattering data. Melting-point data are not very suitable to obtain quantitative information on $g(T,w)$.

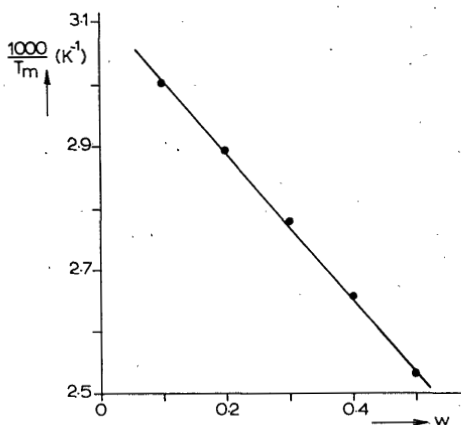


Fig. 5. Reciprocal melting points vs. concentration in the PPO-toluene system.

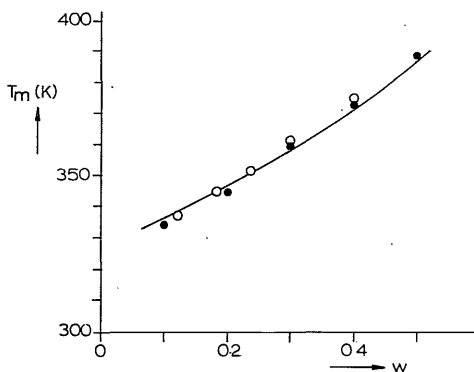


Fig. 6. Melting points for the PPO-toluene system. (—) calculated, (O) Scultz, (●) this work.

Differential Scanning Calorimetry

Phase separation upon cooling appears in DSC measurements as an exothermic peak. The temperature at which the peak begins corrected as needed,⁷ is taken as the phase separation temperature. The phase separation temperature depends largely on the scanning speed (see Fig. 7). Since phase separation temperatures decrease steadily with increase in scanning speed these experiments show that we are in the region of nucleation and growth. Thus even at the highest possible scanning speed, with temperatures far below those of the spinodal determined earlier,³ the spinodal has not been reached.

DISCUSSION

Some attempts to determine the thermodynamic parameters g and χ for the system PPO-toluene have been published previously.

The determination of the χ parameters by Shultz and McCullough¹ agrees qualitatively with the present results when their inverse temperature dependence of χ is replaced by a concentration dependence. We have shown that within the series of melting point versus concentration data it is impossible to distinguish between the two dependences. Since Shultz and McCullough assumed a χ parameter independent of concentration, only a temperature dependence was found. The light scattering experiments in his work indicate that the temperature dependence is very small and that there is a distinct concentration dependence. We believe that the light scattering experiments published earlier¹⁸ and the conclusions based on them, are erroneous. The difference in the light scattering results is probably caused in part by the pretreatment given to the solutions. We found that small amounts of water in toluene, and filtration of the solution with a filter of larger pore size, gave very high and less reproducible scattering values. Moreover, Figure 2 of Ref. 18 corresponds nearly totally with the value of $(\partial\mu/\partial w)_{MWD}$, due to the last factor inside the brackets in our eq. (3) which arises from the molecular weight distribution. This contribution is zero only at $w = 1$, so extrapolation to $(\partial\mu/\partial w)_{MWD} = 0$ to find the spinodal was not possible. Both these points, χ values and extrapolation procedure, led to the

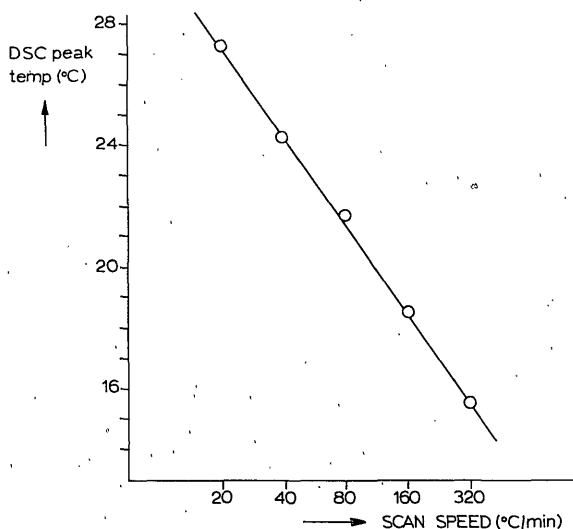


Fig. 7. Phase separation temperatures on cooling as determined by DSC at various scanning rates.

invalid conclusion that the occurrence of liquid-liquid phase separation was demonstrated by light scattering measurements.

The values for χ_{w} found in this work by light scattering agree with those from osmometry; these values can be used to derive g and describe the melting-point curve satisfactorily. These g values do not give a liquid-liquid phase separation gap in the region studied. To obtain a liquid-liquid phase separation a minimum value of χ_{w} of 0.5 must occur in a solution of a polymer of infinite molecular weight, and a χ_{w} must not depend on the concentration.⁴ For a lower molecular weight polymer and a concentration dependent χ_{w} , higher values of this parameter are needed for a liquid-liquid phase separation. In addition, when liquid-liquid phase separation occurs there should be a spinodal not too far below the cloud point curve. Because this spinodal cannot be detected, neither by light scattering nor by DSC, it is unlikely that liquid-liquid phase separation occurs in this system between 273 and 373°K.

The calculation of g parameters from the "cloud point curve" obtained by slow cooling, as was done by Van Emmerik and Smolders¹⁹ raises serious doubts, since it was incorrectly assumed that the g parameters for two cloud-point curves are the same at their point of intersection. A final comparison with other data is possible for the ternary system PPO/polystyrene/toluene where no liquid-liquid phase separation occurs.¹ Hence it can be expected that the interaction between PPO and toluene is not very different from that between polystyrene and toluene.²⁰ Indeed the χ parameters found for polystyrene-toluene⁶ are of the same magnitude as the values for PPO-toluene found in this work. This supports our conclusion that the phase-separation phenomenon observed for PPO-toluene is a crystallization phenomenon and not a liquid-liquid phase separation. The phenomenon of the two different temperatures at which a phase separated solution can become homogeneous will be dealt with in the second paper of this series.

To obtain more g values, high-pressure osmotic and vapor pressure measurements are presently being made in our laboratory. It is to be expected that a more accurate statement about the small temperature dependence of g can be made in a later stage.

The authors are indebted to J. W. A. van den Berg and G. van de Ridder for helpful discussions and suggestions.

References

1. A. R. Shultz and C. R. McCullough, *J. Polym. Sci., A-2*, **10**, 307 (1972).
2. E. P. Magré and J. Boon, *Proc. IUPAC International Symposium*, Leiden, 1970, p. 835.
3. P. T. van Emmerik and C. A. Smolders, *J. Polym. Sci., C*, **38**, 73 (1972).
4. P. J. Flory, *Principles of Polymer Chemistry*, Cornell Univ. Press, Ithaca, 1953.
5. R. Koningsveld and A. J. Staverman, *J. Polym. Sci., A-2*, **6**, 325 (1968).
6. Th. G. Scholte, *J. Polym. Sci., A-2*, **8**, 841 (1970).
7. J. D. Hoffman, *J. Chem. Phys.*, **28**, 1192 (1958).
8. P. T. van Emmerik and C. A. Smolders, *Europ. Polym. J.*, **9**, 293 (1973).
9. Th. G. Scholte, *Europ. Polym. J.*, **6**, 1063 (1970).
10. Th. G. Scholte, *J. Polym. Sci., A-2*, **9**, 1553 (1971).
11. J. W. Cahn, *J. Chem. Phys.*, **42**, 93 (1965).
12. C. A. Smolders, J. J. van Aartsen, and A. Steenbergen, *Kolloid Zu.Z. Polym.*, **243**, 14 (1971).
13. G. Cohen, H. Eisenberg, *J. Chem. Phys.*, **43**, 3881 (1965).
14. J. M. Barrales-Rienda and D. C. Pepper, *Europ. Polym. J.*, **3**, 535 (1967).
15. J. M. Barrales-Rienda and J. M. G. Fatou, *Kolloid Zu.Z. Polym.*, **244**, 317 (1971).
16. F. E. Karasz, J. M. O'Reilly, H. E. Bair, and R. A. Kluge, Paper presented at 155th Natl. ACS Meeting, 1968.
17. Perkin Elmer DSC-2 Manual.
18. P. T. van Emmerik and C. A. Smolders, *J. Polym. Sci., A-2*, **39**, 311 (1972).
19. P. T. van Emmerik and C. A. Smolders, *Europ. Polym. J.*, **9**, 157 (1973).
20. C. C. Hsu and J. M. Prausnitz, *Macromolecules*, **7**, 320 (1974).

Received January 7, 1976

Revised July 6, 1976

Phase-Separation Phenomena in Solutions of Poly(2,6-dimethyl-1,4 phenylene Oxide). II. Differential Scanning Calorimetry of Solutions in Toluene

D. M. KOENHEN and C. A. SMOLDERS, *Twente University of Technology, Enschede, The Netherlands*

Synopsis

The phase-separation phenomena observed in solutions of poly(2,6 dimethyl-1,4 phenylene oxide) in toluene have been investigated by differential scanning calorimetry. These measurements supplement the experimental evidence in favor of the concept that the phase transitions observed are crystallization and melting phenomena. The experiments suggest that two kinds of crystals can develop and that a seeded crystallization is possible.

INTRODUCTION

Homogeneous solutions of poly(2,6 dimethyl-1,4 phenylene oxide) (PPO*) in toluene, up to concentrations of 40% by weight, can be obtained by heating the mixture to a temperature of 110 °C. When such a solution is cooled, turbidity sets in at a temperature which depends on the cooling rate.¹ When this turbid solution is again heated, it becomes clear at a temperature higher than that of incipient phase separation, but always below 110 °C. In the literature two explanations have been put forth for the phase separation phenomena observed in this system: a) liquid-liquid phase separation, after which the concentrated phase undergoes crystallization.¹ b) crystallization of the polymer from the solution.²

The transitions are accompanied by a heat effect, which makes it possible to detect the transition with a differential scanning calorimeter. In this work DSC measurements are reported which supplement earlier DSC work on this system.³ The measurements were devised in such a way that the results might provide data that would help to discriminate between the two mechanisms proposed for phase separation.

EXPERIMENTAL

The apparatus used was a Perkin-Elmer DSC-1B apparatus with a liquid nitrogen subambient assembly. The solutions were made up in vacuum-sealed tubes as described earlier,¹ cooled down quickly to enable the filling of the liq-

* PPO is a trademark of the General Electric Co.

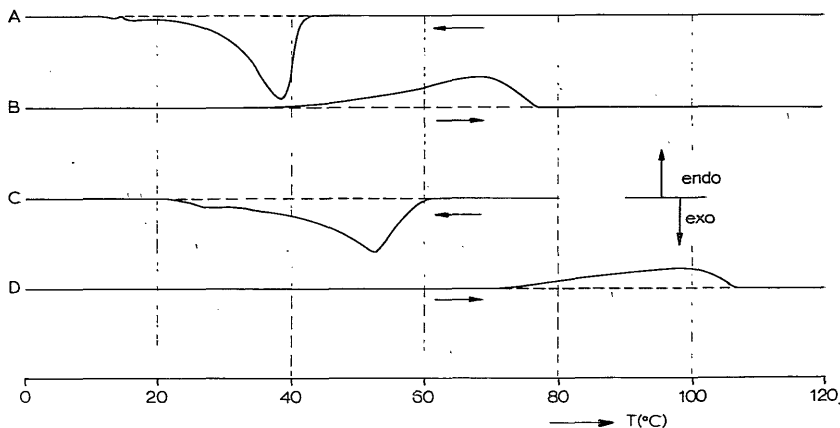


Fig. 1. DSC traces of a 40% solution of PPO in toluene.

uid-type sample pans with a semisolid polymer-solvent system. Only sample pans were used which showed no weight loss after being held at 90 °C for 3 days. The PPO used was a narrow distribution sample characterized by $\bar{M}_n = 35,800$, $\bar{M}_w = 39,500$. This sample was obtained by liquid-crystal fractionation. The toluene used was Baker Analysed Reagent p.a. grade.

RESULTS

In Figure 1 some results for a 40% w/w PPO solution are shown. Different concentrations showed parallel characteristics. The transition temperatures increase monotonically with concentration. When a solution, which has been at a temperature of 120 °C for several hours, is cooled at a rate of 16 °C/min, curve A is obtained. There is an exothermic heat effect which begins at $T = 42$ °C. Heating this solution at a rate of 16 °C/min to 120 °C produced curve B. An endotherm is shown which ends at $T = 78$ °C. When the solution heated up to 120 °C is cooled again at the same rate, curve A is reproduced. However, when the heating procedure of curve B is stopped at $T = 85$ °C (well beyond the endotherm) and the sample is cooled at a rate of 16 °C/min, curve C is obtained. When this solution is heated again, there is no endotherm ending at 78 °C but one ending at 106 °C (curve D). In this case, when heating is stopped at 85 °C and the system is cooled, no exotherm is observed.

When the solution is cooled from 120 °C to 0 °C at different cooling rates and then heated at 16 °C/min, the curves shown in Figure 2 are obtained. With a cooling rate of 0.5 °C/min curve E is obtained upon heating. This curve shows the endotherm at 106 °C. Reheating the samples directly after faster cooling (1 °C/min and 2 °C/min) produces a second endotherm (curves F and G) at lower temperatures. After cooling at a rate of 4 °C/min, reheating gives curve H with a single endotherm at 78 °C. This curve is identical with that obtained after cooling at a rate of 16 °C/min (curve B in Fig. 1). In curves F and G the lower endotherm increases in area with increasing cooling rate, whereas the other endotherm decreases. In addition the end of the lower endotherm shifts to a higher temperature. The higher endotherm ends at 106 °C in all cases.

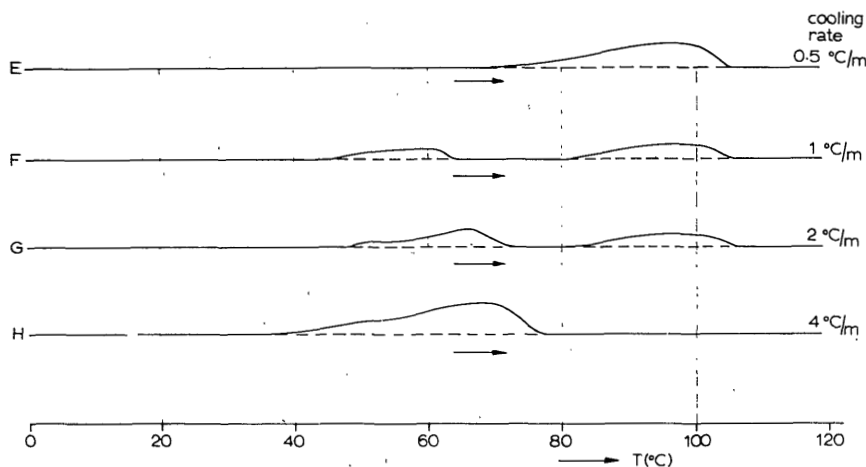


Fig. 2. DSC traces of a 40% solution of PPO in toluene. Heating after cooling at different rates.

Figure 3 shows the heating curves obtained upon cooling the sample quickly from 120 to 47 °C in the DSC apparatus and waiting for various periods of time at that temperature. The temperature of 47 °C was chosen because it is higher than the temperature of appearance of the exotherm (Fig. 1, curve A). After the waiting period the sample was cooled quickly to 0 °C and then heated at a rate of 16 °C/min. Curve K of Figure 3 is obtained after waiting for several hours at 47 °C, curve L after waiting for 10 min, curve M after waiting for 5 min and curve N with no waiting time at 47 °C. Curve N is identical with curve H in Figure 2 and with curve B in Figure 1.

As can be seen, waiting at 47 °C has approximately the same effect as a slower cooling rate (curves E to H in Fig. 2). When the waiting period was introduced at a temperature below the exotherm of curve A, Figure 1, a curve identical to curve B of Figure 1 was obtained, even after waiting for several days. Also, when a solution is cooled quickly from 120 to 0 °C (below the exotherm of 42 °C) and then brought to 47 °C during various periods of time (up to days), only the endotherm ending at 78 °C appears on heating.

At other polymer concentrations the same features are observed but the temperature of transition and the recorded heat effects differ. The transition temperatures increase by about 1.23 °C per percent concentration increase. The heat effects are larger at higher concentrations. For example, at 30% the heats involved are about 0.3 cal per g of solution and at 40% 0.9 cal per g solution.

DISCUSSION

Results equivalent to curves A and B of Figure 1 have been found in earlier work.³ The exotherm at 42 °C was assumed to be brought about by spinodal decomposition. The endotherm of 78 °C was thought to arise from the liquid-liquid separated mixture becoming homogeneous. After prolonged waiting below the phase separation temperature, the endotherm at 106 °C appeared, which was interpreted as the melting of the partly crystallized concentrated phase.

Curve A of Figure 1 is reproducible only after the solution has been reheated

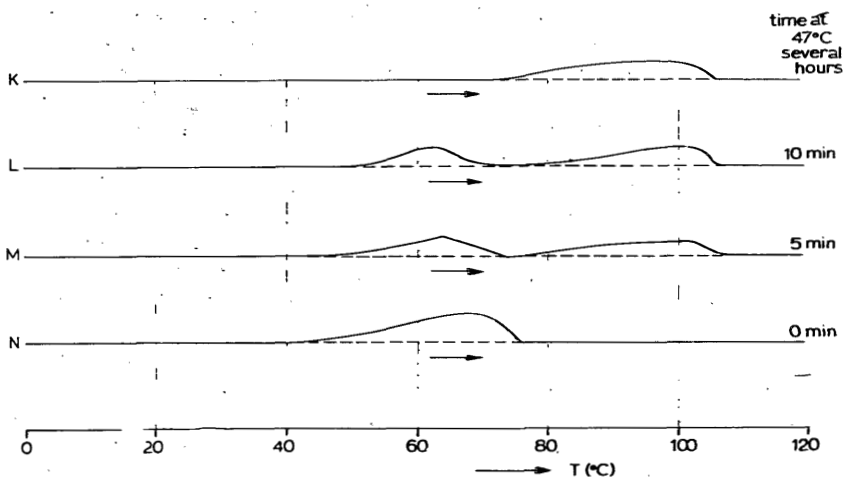


Fig. 3. DSC traces of a 40% solution of PPO in toluene. Heating after different waiting periods at 47°C.

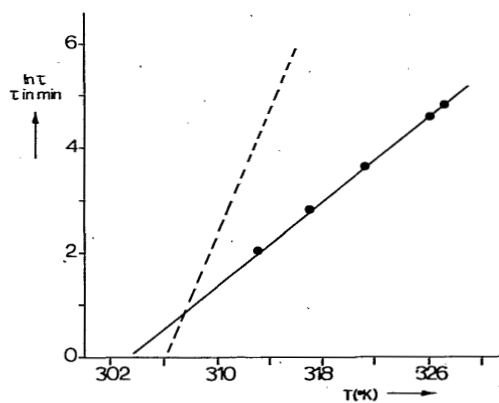


Fig. 4. Hypothetical induction times for low melting crystals (---). Measured induction times for a 30% PPO solution in toluene (•••). The induction times were obtained by visual observation by Van Emmerik and Smolders.⁴

to 120 °C. When after a cooling run the solution is only heated to 85 °C the exotherm on cooling appears at a higher temperature. An explanation can be derived from the assumption that after the first cooling run (A) some nuclei are established which are not destroyed at 85 °C and cause a "seeded" phase separation during the second cooling run (C). On reheating, the latter phase-separated mixture shows only 106 °C endotherm. This endotherm can be attributed to the melting of crystallites (pure PPO isolated from such a solution shows a melting peak at 510 °K in DSC³). With reason the nuclei may be supposed to be crystalline in nature, and the phase separation to be crystallization. A remarkable fact is the complete disappearance of the 78 °C endotherm for this seeded crystallization. This endotherm is also absent when the solution is cooled very slowly (curve E of Fig. 2), and it appears only at higher cooling rates.

The melting endotherm at 106 °C is not obtained when the exotherm at 42 °C is brought about by fast cooling, followed by prolonged storage of the phase-separated solutions. This phenomenon does not depend upon the temperature at which the phase separated solution is kept; 0 °C or 47 °C (above the temperature of the exotherm) give the same results. This is contrary to earlier findings by Van Emmerik and Smolders.³

In view of these results the phase separation at 42 °C cannot possibly be a liquid-liquid phase separation because: a) In a liquid-liquid phase-separated solution, the crystalline phase melting at 106 °C must be obtained after some time. b) The endotherm at 78 °C should not disappear completely when liquid-liquid phase separation has occurred, because only a small fraction of the polymer crystallizes in the concentrated phase.

The crystals melting at 106 °C originate directly from the solution but nucleation is slow. It now appears that at high cooling rates this nucleation can be overtaken by the nucleation and growth of a lower-melting crystal modification, which is less perfect but has a higher growth rate at the lower temperature. The induction times for the nucleation of both kinds of crystals can be represented schematically as in Figure 4. In curves *F* and *G* of Figure 2 and *L* and *M* of Figure 3 the growth of the crystals melting at 106 °C was not complete while the undercooling was proceeding so that the lower-melting crystal could also grow.

The concentration of the polymer in the solution phase has decreased at that stage because of the growth of crystals of the higher melting configuration. This causes the lowering of the melting temperature of the less perfect modification. When the growth of the high-melting modification is complete, the lower-melting one is not found in the temperature range studied (curves *E* and *K*). The phenomena observed can be explained by assuming two crystalline modifications, of which the lower-melting one consists of a less perfect crystalline material.

References

1. P. T. van Emmerik and C. A. Smolders, *J. Polym. Sci., C*, **38** 73 (1972).
2. A. R. Shultz and C. R. McCullough, *J. Polym. Sci., A-2*, **10**, 307 (1972).
3. P. T. van Emmerik and C. A. Smolders, *Europ. Polym. J.*, **9**, 293 (1973).
4. P. T. van Emmerik and C. A. Smolders, *Europ. Polym. J.*, **9**, 931 (1973).

Received January 7, 1976

Revised July 6, 1976

PHASE-SEPARATION PHENOMENA IN SOLUTIONS OF POLY(2,6-DIMETHYL-1,4-PHENYLENE OXIDE). III. PULSE INDUCED CRITICAL SCATTERING OF SOLUTIONS IN TOLUENE

D.M. KOENHEN and C.A. SMOLDERS, *Twente University of Technology, Dept. Colloid and Interface Science, Enschede, The Netherlands*

M. GORDON, *University of Essex, Institute of Polymer Science, Wivenhoe Park, Colchester CO 4.3S Q, UK.*

SYNOPSIS

For the polymer-solvent system poly(phenylene oxide) in toluene the mechanism and kinetics of crystallization have been studied with the Pulse Induced Critical Scattering technique.

It was found that after a delay-time the growth mechanism was diffusion controlled. The delay-time is thought to be connected with the nucleation of the crystallites and it disappeared in the "seeded" crystallizations studied.

After incomplete melting of crystallites the first stages of growth resemble a condensation reaction.

INTRODUCTION

With the Pulse Induced Critical Scattering method it is possible to follow isothermally the light scattering of polymer solutions, which is induced by a preceding thermal pulse (in most instances this means a cooling step). The application of this technique in the determination of the phase separation phenomena in liquid-liquid demixing systems has been reported¹. The system poly(2,6-dimethyl-1,4-phenylene oxide) (PPO* resin) in toluene exhibits a phase separation on cooling which has been shown to be a crystallization phenomenon². It was found that the crystallization occurs after a delay-time which has been measured by optical microscopy³. This delay-time is sometimes attributed to the time necessary for the growing centres to reach detectable dimensions⁴. The classical way in which these delay-times and the kinetics of crystallization can be measured is by dilatometry. This method, however, is not very sensitive

* PPO is a registered trade name of General Electric Co.

in the first stages of crystallization. An advantage of the dilatometry method is that the crystallization can be followed to completion⁵. With the purpose to improve the limit of detection to the smallest particles (the nuclei), we have used a PICS type light scattering apparatus as has been developed by Gordon and coworkers⁶.

This light scattering technique enables one to detect particles, which are smaller than the wavelength of the light used. With some assumptions the kinetics in the very first stages of the phase separation can be determined as well. Because of the very small size used in the PICS technique, assuring that rapid temperature equilibration is reached, even very fast crystallizations can be monitored.

THEORETICAL CONSIDERATIONS

LIGHT SCATTERING

The light scattering of particles with diameters small compared with the wavelength of the incident light is given by Rayleigh⁷ as:

$$i_{\theta} = \frac{8\pi^2}{r^2 \lambda'^4} v \alpha^2 I_0 (1 + \cos^2 \theta) \quad (1)$$

where i_{θ} is the light scattered at angle θ ; r is the distance to scattering volume; λ' is the wavelength of light used, divided by the refractive index of the medium; v is the number of particles; α is the polarizability of the particles and I_0 is the intensity of the incident light.

The light scattered at an angle θ thus depends on the square of the polarizability α . The polarizability α increases linearly with the volume. This means that, taking the particles as spherical, the intensity of the scattered light varies with the sixth power of the radius⁷.

When the particles are bigger but still remain smaller than the wavelength, the light scattered at larger angles decreases with a factor $P(\theta)$. This type of scattering is known as Debye scattering.

For isotropic spheres this factor is

$$P(\theta) = \frac{3}{U^3} (\sin U - U \cos U)^2 \quad (2)$$

with $U = 2\pi (L/\lambda') \sin(\theta/2)$; L is the diameter of the sphere.

Equation 2 shows that when the spherical particle is growing, the dissymmetry of intensities measured at two angles (e.g. 30° and 90°) increases rapidly. So it is easy to determine which kind of scattering is followed by monitoring the dissymmetry of the scattered light. This is important in order to determine the order of magnitude of the dimensions of the particles which one observes. From the measurements of the dissymmetry in Debye-scattering one could in principle determine the radius of the particles.

KINETICS OF CRYSTALLIZATION

The most widely used equation to describe the kinetics of crystallization from polymer melts is the Avrami-Evans equation⁵.

$$X = 1 - \exp(-kt^n) \quad (3)$$

where X is the degree of conversion; k is the rate constant; t is time; n is the Avrami exponent.

For very small conversions the first term of a series expansion of equation 3 can be used giving $X = kt^n$.

For the case of growth from a solution the kinetics of heterogeneous crystallization have been worked out mathematically by Turnbull⁸. For low conversions his equations reduce to a form equivalent to equation 3, with $n = 3/2$ for diffusion controlled growth and $n = 3$ for interface controlled growth and assuming for both types a fixed number of nuclei. When nuclei are generated during the crystallization the exponent shifts to a slightly higher value.

So if heterogeneous nucleation is assumed with a fixed number of nuclei the Rayleigh light scattering at small t values in the case of diffusion controlled growth should depend on the third power of time (since for small conversions I is proportional to X^2). For interface controlled growth Rayleigh light scattering is proportional to the sixth power of time (see tabel 1).

Table 1.

growth controlled	heterogeneous nucleation	homogeneous nucleation
by diffusion	$n = 3/2$ $q = 3$	$n = 3/2$ to 2 $q = 3$ to 4
by interface	$n = 3$ $q = 6$	$n = 3$ to 4 $q = 6$ to 8

(n is the Avrami exponent, q is the expected scattering exponent $I \sim t^q$, for Rayleigh scattering and small conversions).

Oster⁹ has considered the light scattering during various types of polymerization reactions. In some instances the crystallization from a solution could be considered as a kind of polymerization reaction. Oster finds for a condensation reaction that the light scattering is proportional to time. The light scattering in a radical polymerization depends quadratically on time.

EXPERIMENTAL

The experiments were performed with a PPO sample characterised by $M_n = 25.000$ and $M_w = 42.000$ (by GPC).

The toluene used, was of analytical grade. Stock solutions of different concentrations were made, from which the capillaries for the PICS instruments were filled with a syringe and sealed. From these stock solutions also the dilatometric measurements were made, using a digital density meter DMA 50 from Anton Paar. This apparatus measures density changes as small as 10^{-5} g/cm³.

The PICS instruments has been described in the literature^{1,6}. The light scattered by the polymer solution after a fast temperature step is recorded at angles of 30° and 90°. The laser used as light source was a He/Ne type (Spectra Physics 134).

RESULTS

The light scattering curves obtained with PICS after cooling a homogeneous solution (which was heated for 10 minutes at a temperature of 20°C above the crystalline melting point of that solution¹⁰) all show a long delay-time after which scattering increases. In analysing the curves care is taken to use only the scattering in the first stages of the crystallization process, up

to scattering intensities less than one third of that observed at the inflection point, as was ascertained by control experiments. In these curves there is no additional dissymmetry detectable which could be attributed to the growth of larger particles. The scattering curves detected at 30° and 90° are equivalent. It can therefore be concluded that Rayleigh scattering is observed.

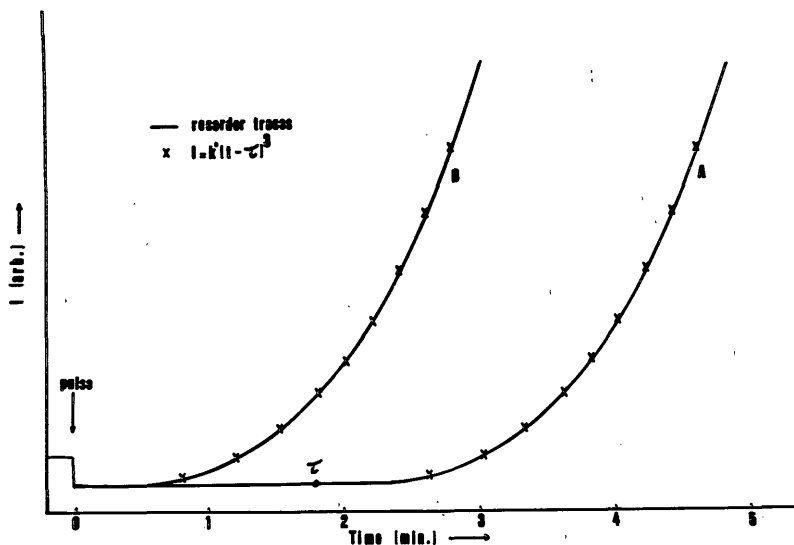


Fig. 1. PICS light scattering curves (recorder traces) for a 20 % PPO solution in toluene. Pulse temperature to 25°C .

A typical light scattering curve of this type is curve A in figure 1. When a phase separated solution is not heated at high enough temperatures (e. g. to a temperature in the region of the high end of the DSC melting endotherm) then after cooling curve B can be obtained. This form of the light scattering curve is the same as in curve A, but the delay-time has disappeared.

Thus the assumption was made that the growth of particles is the same in both experiments but in curve A there is a time lag, necessary for nucleus formation. Curve B is, therefore, interpreted as a "seeded" crystallization. Curve B could be described by a third power law. Since in curve A the growth part is identical to curve B this curve can be described by

$$\begin{aligned}
 I &= k' (t - \tau)^3 & \text{at } t > \tau \\
 I &= 0 & \text{at } t < \tau
 \end{aligned}
 \tag{4}$$

τ is the delay time

This equation gives a satisfactory fit in all experiments. Without assuming a delay-time, higher exponents were obtained with deviations especially in the first part of the curve.

In figure 2 the delay-time, obtained after fitting the curves with equation 4, are presented as a function of temperature and concentration.

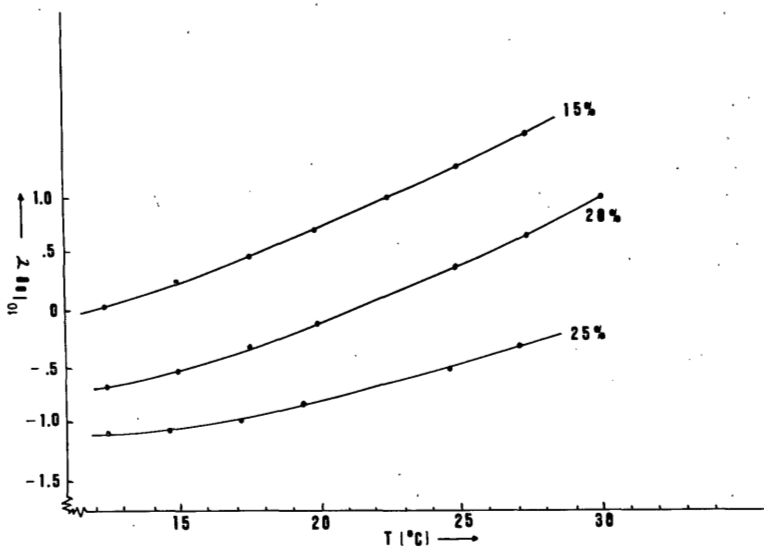


Fig. 2. Delay-time measured by PICS for solutions of PPO in toluene. τ is given in minutes.

If a phase separation is brought about to different degrees of crystallization, and the separated solution is heated until the region in which partial melting occurs, some interesting phenomena in the field of seeded crystallization can be observed. For the experiments in figure 3 the temperature of heating, after the initial phase separation, was kept constant, as was the time of this heating. The difference is in the extent of phase separation before heating.

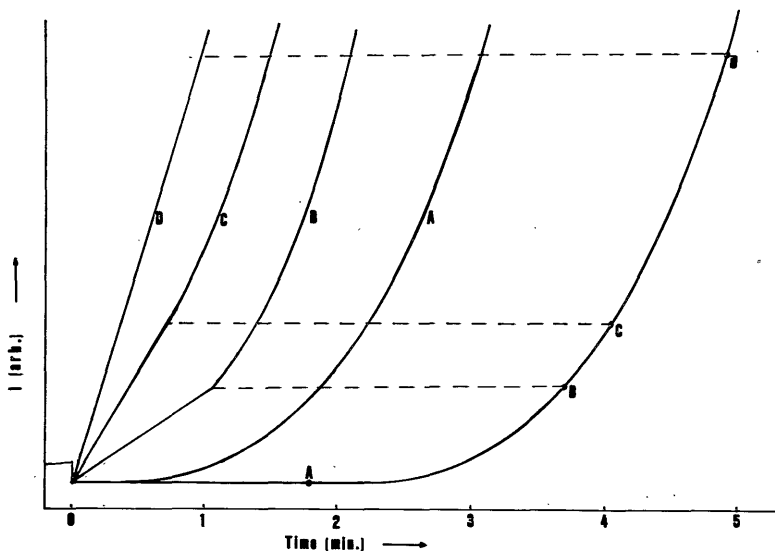


Fig. 3. PICS curves for seeding experiments on a 20 % PPO solution in toluene. Capitals refer to original extent of crystallization as indicated on the outer right curve. Pulses to 25°C, intermediate heating to 60°C for 30 minutes.

Finally in figure 4 a typical curve obtained by density measurements is shown.

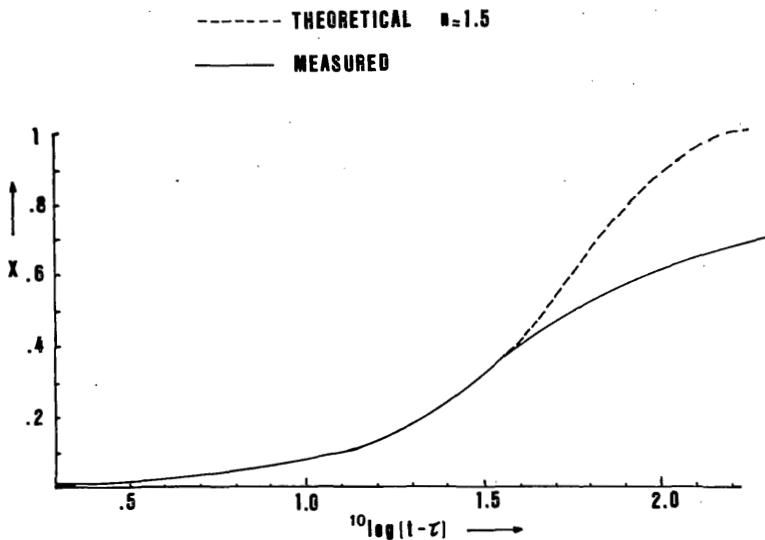


Fig. 4. Density measurements with DMA 50 for 20 % solution of PPO in toluene at 30°C. The theoretical curve (with $\tau = 0$) has been shifted horizontally to obtain coverage of the experimental curve, which has been plotted with the delay-time ($\tau = 7$ minutes) found by PICS.

The density measurements of the crystallizing solution give a crystallization isotherm which at low conversions cannot be described by the normal Avrami-Evans equation. However, when the delay time is introduced the Avrami exponent can be computed as $n = 1.5 \pm 0.1$ (figure 4). This conclusion agrees with the measurements of heterogeneous crystallization of PPO from the melt as done by Packer and Shariff¹¹. Here also a delay-time was found and an Avrami exponent $n = 1.6$. The exponent $n = 1.5$ can also be deduced from the measurements by optical microscopy of Van Emmerik and Smolders³, who found that the radii of the spheres growing in the solution increased with the square root of time (assuming a constant number of nuclei).

From the absence of additional dissymmetry during the first stages of growth as followed by PICS we conclude that in this stage we observe Rayleigh scattering. It is known that the crystallinity in the final material is low^{1,2}. The crystallization is possible here by solvent molecules which constitute part of the crystalline unit cell^{1,3}. The high amorphous content of the small particles makes it reasonable to neglect anisotropy in the scattering particles. The scattering is thus thought to arise from the higher density of the spheres. Of course in polymers which form more ideal crystallites one should make a correction for anisotropy.

Thus from the density measurements where we found that $n = 1.5$ we can expect that the light scattered will depend on t^3 after a certain delay-time. As is shown this is precisely what is found in these solutions.

The Avrami exponent found for these solutions shows that the growth is diffusion controlled. This means that material is transported from bulk solution to the crystal surface. Since the overall crystallinity in the spheres is low, this suggests that only parts of the macromolecules are able to crystallize. The fraction of the chain which can participate in crystallization and the time it takes for its formation out of disordered chains, will of course, be governed by the internal ordering ability of the macromolecular chain. The sequences of ordered segments have to diffuse towards each other. When after a previous phase separation the solution is heated for some time at a temperature in the region of the high end of the melting endotherm as found by DSC^{1,2}, the delay-time has disappeared. This type of crystallization can be explained as a "seeded" crystallization.

When the melting procedure is less rigorous (viz. not long enough) we obtain after pulsing back to 20°C at first a linear increase in scattering intensity. After passing the point to which the original crystallization had proceeded, a normal curvature takes over. The slope of the initial part of these curves is very much dependent on the original degree of crystallization. This effect can be explained by assuming incomplete melting of the crystallites and/or incomplete diffusion of crystallizable material from the area of the old crystallite into bulk solution. When this solution crystallizes again, crystallization probably occurs within the outline of the old crystallite. Because of the availability of material necessary for the growth within this area, crystallization resembles a condensation reaction. After the complete old volume has been crystallized the normal growth situation (diffusion controlled) is restored again. When the degree of conversion of the original crystallization is

higher, the area in which this phenomenon can occur is larger and the slopes are steeper. This crystallization in molten crystallite volumes has been observed for spherulites of other materials as well.

In these experiments all of the original scattering had disappeared before the second temperature jump was made. This, together with the prolonged induction times for the completely molten solution suggests that the crystallization of PPO involves a two step nucleation process.

It is probable that first a conformation change is needed before nucleation and growth of crystals can occur.

In the seeded experiments the crystals may have disappeared, but the material is still in the right conformation.

The experiments reported above are in agreement with DSC results reported earlier^{1,2}.

It is clear that the PICS light scattering technique can give very useful information about the first stages of nucleation from solution.

We thank dr. J. Goldsbrough and mr. B.W. Ready for carrying out part of the measurements.

REFERENCES

1. K.W. Derham, J. Goldsbrough and M. Gordon, *J. Pure and Appl. Chem.* **38**, 97 (1974).
2. D.M. Koenhen and C.A. Smolders, *J. Pol. Sci. part A-2*, in press.
3. P.T. van Emmerik and C.A. Smolders, *European Pol. J.* **9**, 931 (1973).
4. W.J. Dunning and others in: *Nucleation*, ed. A.C. Zettlemoyer. Dekker New York, 1969.
5. L. Mandelkern, *Crystallization of Polymers*, McGraw Hill, New York, 1964.
6. J.W. Kennedy, M. Gordon and G.A. Alvarez, *Polimery (Warsaw)* No. 10, 1464 (1975).
7. See for instances G. Oster in *Physical Methods of Chemistry*, Part III A. Interscience New York 1972.
8. D. Turnbull, *Solid State Physics*, Vol. 3, Academic Press, New York, 1956.
9. G. Oster, *J. Colloid Sci.*, **2**, 291 (1974).
10. P.T. van Emmerik and C.A. Smolders, *J. Polym. Sci. C* **38**, 73 (1972).
11. A. Packter and K.A. Sharif, *Polymer Letters* **9**, 435 (1971).
12. D.M. Koenhen and C.A. Smolders, *J. Pol. Sci. A-2*, in press.
13. E.P. Magré and J. Boon; *Proceeding of the IUPAC International Symposium, Leiden, 1970*, p. 835.

PHASE SEPARATION PHENOMENA IN SOLUTIONS OF POLY(2,6-DIMETHYL-1,4-PHENYLENE OXIDE). IV. THERMODYNAMIC PARAMETERS FOR SOLUTIONS IN A SERIES OF HOMOLOGOUS SOLVENTS: TOLUENE TO HEXYLBENZENE

D.M. KOENHEN, A. BAKKER, L. BROENS and C.A. SMOLDERS
Twente University of Technology, Dept. Colloid and Interface Science, Enschede, The Netherlands

SYNOPSIS

Melting points curves for solutions of poly(2,6-dimethyl-1,4-phenylene oxide) (PPO) in a series of homologous solvents, toluene to n-hexylbenzene have been obtained from visual and differential scanning calorimetry measurements.

The measured melting points were used to calculate interaction parameters. It was found that consistent values were obtained with the Flory-Hoffman melting point depression equation only if the assumption was made that the solvent forms part of the crystal lattice and using an adapted dependence of the melting enthalpy per polymer unit on the co-crystallizing solvent. The dependencies of the interaction parameters in the series of solvents are explained qualitatively with solubility parameter theory and with the Flory-Prigogine equation of state.

INTRODUCTION

It has been shown in previous papers in this series that the phase separation of solutions of PPO* in toluene is a crystallization phenomenon^{1,2,3}. Measurements of the thermodynamic parameters showed for these solutions an increase in the free enthalpy correction parameter g with polymer concentration¹. The role of the solvent in the crystallization is not made clear in previous work.

Thermodynamic parameters can be derived from melting point curves. This gives a possibility to test the hypotheses which may be put forward for the role of the solvent. It allows the determination of thermodynamic parameters for other solvent systems as well.

In this contribution the melting curves have been determined for PPO in the solvents toluene, ethylbenzene, n-propylbenzene, n-butylbenzene, n-pentylbenzene

* Registered trade mark of General Electric Company.

same lattice is used for both the polymer and the solvent this equation probably gives a configurational entropy which is somewhat too high.

A second contribution comes from free-volume effects. For this type of correction the corresponding states theory of Prigogine⁹ and Flory¹⁰ is used.

Another reason for deviations from the Flory-Huggins configurational entropy is polymer chain flexibility and back bending. It is customary to correct for all non-idealities with the correction parameter g in equation 1 introduced in this form by Koningsveld¹¹:

MELTING POINT DEPRESSION

The difference in chemical potential between a crystalline polymer segment and a polymer segment in the pure liquid state can be written as¹²:

$$\mu_u^c - \mu_u^o = - \Delta g_u^o = - (\Delta h_u^o - T \Delta s_u^o) \quad (2)$$

where the unit is defined as the polymer segment and Δg_u^o , Δh_u^o , Δs_u^o are the partial molar free-enthalpy, enthalpy and entropy of fusion per mole of pure polymer segment.

When we now put $\frac{\Delta h_u^o}{\Delta s_u^o}$ as T_m^o , this equation can be written as:

$$\mu_u^c - \mu_u^o = - \Delta h_u^o \left(1 - \frac{T}{T_m^o} \right) \quad (3)$$

The difference in chemical potential between a polymer unit in the solution and a polymer segment in the pure liquid state is given by:

$$\mu_u - \mu_u^o = RT \left[\frac{M_o}{M_n} \ln w + (1-w) \frac{M_o}{M_n} - (1-w) + \left(g_o + \frac{g_1}{T} + 2g_2 w \right) (1-w)^2 \right] \quad (4)$$

In this form this quantity is defined for M_o grams as being one mole. Hence for the difference in chemical potential per mole of polymer segment units, it should read:

$$\mu_u - \mu_u^o = RT \left[\frac{M_u}{M_n} \ln w + \frac{M_u}{M_n} (1-w) - (1-w) \frac{M_u}{M_o} + \frac{M_u}{M_o} \left(g_o + \frac{g_1}{T} + 2g_2 w \right) (1-w)^2 \right] \quad (5)$$

and n-hexylbenzene. These solvents are characterized by an increasing length of hydrocarbon chain on an aromatic phenyl ring. Normal alkanes are non-solvents for PPO, whereas aromatics are known as good solvents⁴. Thus in the series mentioned the solvent power decreases. This will of course effect the measured melting point curves and the thermodynamic parameters. Also there are consequences which can be drawn from the model of the crystals assumed. If the solvent is not entering the crystallite itself, the usual melting point theories can be applied. If the solvent forms part of the crystalline lattices as is the case with solvents such as α -pinene and decalin⁵ the theory has to be adapted. The purpose of this work was to see whether thermodynamic parameters (Δh_u^0 , T_m^0 , g) determined for PPO-toluene solutions, and combined with the measured melting point curves for the homologous solvent series could give a meaningful set of parameters for the series of solvents.

THEORETICAL CONSIDERATIONS

In order to describe polymer solution thermodynamics use is made of the well known Flory-Huggings equation⁶.

$$-\frac{\Delta G_m}{RT} = w_0 \ln w_0 + \sum \frac{M_0}{M_i} w_i \ln w_i + g w_0 \sum w_i \quad (1)$$

where ΔG_m is the free enthalpy of mixing for M_0 grams of solution, T is the temperature in K, R is the universal gas constant, w_0 and w_i are the weight fractions of solvent and polymer species, respectively, M_0 and M_i are the molecular weight of solvent and polymer, and g is the free enthalpy correction parameter.

This equation is given here in weight fractions as was proposed by Scholte⁷. The use of weight fraction is especially recommended when studying the same solution at different temperatures, because this concentration variable does not change with temperature as is the case with volume fractions. The original Flory-Huggins theory was derived on the basis of the lattice theory⁶. This means that every segment in the lattice is associated with a certain volume, hence volume fractions should be used. For generally encountered organic substances the molecular weight of a fixed volume segment is approximately the same⁸. This allows equation 1 to be used. In view of the approximation that the

In the last two equations the correction parameter g has been written as $g = g_0 + \frac{g_1}{T} + g_2 w$, where g_0 , g_1 and g_2 are supposed to be constants.

In the equilibrium state between polymer crystals and the polymer solution the following relation is valid.

$$\mu_u^c - \mu_u^o = \mu_u - \mu_u^o \quad (6)$$

Therefore we obtain as an expression for the melting point depression:

$$\frac{1}{T_m} - \frac{1}{T_m^o} = \frac{-R}{\Delta h_u^o} \left\{ \frac{M_u}{M_o} \ln w + (1-w) \frac{M_u}{M_n} - (1-w) \frac{M_u}{M_o} + \frac{M_u}{M_o} \left(g_0 + \frac{g_1}{T} + 2g_2 w \right) (1-w)^2 \right\} \quad (7)$$

In this equation the assumption has been made that Δh_u and Δs_u in equation 2 are independent from the temperature, which is not correct. This problem has been solved by Hoffman¹³, who showed that a correction term $\frac{T_m}{T_m^o}$ was necessary for the description of the chemical potential difference $\mu_u^c - \mu_u^o$ to correct for the temperature dependence of Δh_u and Δs_u below T_m^o . This results in the following equation for the lowering of the melting point.

$$\frac{\Delta h_u^o \left(\frac{T_m^o - T_m}{T_m^o} \right) T_m}{(T_m^o)^2} = -RT_m \left\{ \frac{M_u}{M_o} \ln w + (1-w) \frac{M_u}{M_n} - (1-w) \frac{M_u}{M_o} + \frac{M_u}{M_o} \left(g_0 + \frac{g_1}{T} + 2g_2 w \right) (1-w)^2 \right\} \quad (8)$$

So far the influence of crystal morphology has not been mentioned. Factors involving the crystal morphology have been evaluated for a similar system by Helms¹⁴. He found that the crystal morphology (surface enthalpy coordination numbers, fold length etc.) has not very much influence on the thermodynamic parameters (g). On the other hand the characteristic melting enthalpy and thermodynamic melting point are influenced. Since we do not have specific knowledge about the crystal morphology as such in the systems considered here, we use equations 7 and 8 and we regard Δh_u^o and T_m^o as characteristic values for a given morphology and not as thermodynamic equilibrium values.

This is justified when the factors involved in the morphology do not change too much in the series studied.

SOLVENT IN THE CRYSTAL LATTICE

When solvent enters the crystal lattice the situation becomes somewhat more complicated. It has been assumed that the solvent enters the crystal lattices at a fixed ratio, between solvent molecules and polymer segment units (solvent may stabilize helix formation). It is known that the crystallinity in these systems disappears on removal of the solvent by evaporation.

At the melting point the crystals (including the solvent) will be in equilibrium with the solution in which the crystal is immersed. When nearly all crystals have been melted, the concentration is effectively the net solution concentration. Theoretically it is possible to obtain a certain (though very low) degree of crystallinity until the solution concentration approaches 100 %.

The chemical potential of the solution is again given by equation 5 and the chemical potential of the crystal is again given by equation 3, and with the Hoffman correction equation 8 is obtained again. The parameters Δh_u^0 and T_m^0 of course are now characteristic for a given polymer (solvent) crystal and they will change with a change of solvent.

It is to be expected that Δh_u^0 decreases with increasing molecular weight (i. e. volume) of the solvent because the crystals obtained will have larger spacings per unit cell. If the total enthalpy per gram of crystals remains constant, Δh_u^0 will decrease because this value is defined per mole of polymer units. Of course the total melting enthalpy depends on intermolecular forces on the helix stability, but it is assumed here that these last effects do not exceed the first mentioned volume effect.

EXPERIMENTAL

VISUAL DETERMINATION OF MELTING POINTS

The appropriate amounts of polymer and solvents were weighed in a pyrex glass tube with an inner diameter of 3 mm. The contents were degassed and sealed as previously described¹. The sealed tubes were heated to a temperature at which the contents became homogeneous. The homogeneous solutions were cooled by only 1°C per day to obtain crystals of the highest possible order.

Then the tubes were heated again at a rate of $1^{\circ}\text{C}/\text{day}$ and the melting points were detected at the disappearance of the turbidity.

DSC DETERMINATIONS OF THE MELTING POINTS

The determinations were performed with a Perkin-Elmer DSC-1B differential scanning calorimeter. The solutions prepared as described above were quickly cooled to obtain a solid mass. The tubes were broken and a small amount (± 10 mg) of the solid mass, was transferred to the liquid-type sample pans and sealed. The sample pans were heated to a temperature at which complete dissolution was assured, held 1 day at that temperature, and checked for weight loss.

The sample pans which had a good seal were cooled down to room temperature at a rate of $1^{\circ}\text{C}/2$ hr.

The melting points were now detected by the end of the melting endotherm in the heating thermogram. The scanning speed was $16^{\circ}\text{C}/\text{min}$.

MATERIALS

Determinations were made with a polymer sample, which was characterized by $\bar{M}_n = 23,000$, $\bar{M}_w = 44,000$. The solvents used were of analytical grade.

RESULTS

The results for melting points curves are given in figure 1. Visual and DSC determinations agreed to within 1°C . As was expected the melting curves for the solvents with increasing length of hydrocarbon chain shift to higher temperatures.

For PPO solutions in toluene g_0 , g_1 and g_2 values have been evaluated in a previous paper ¹. This resulted in the values $g_0 = 0.58$, $g_1 = 0$ and $g_2 = 0.19$. Literature values for Δh_u° and T_m° for PPO crystals show a broad range of values ¹. Therefore we decided to evaluate these values directly from the toluene melting points.

With a computer optimization program, using in equation 8 the values $g_0 = 0.58$, $g_1 = 0$ and $g_2 = 0.19$ and the measured toluene melting point curve the value $\Delta h_g^{\circ} = \Delta h_u^{\circ}/120 = 11.84$ cal/g was obtained. The optimum in the calculations is that T_m° at which Δh_u° is a constant over the T_m° curve.

For equation 7 (the simple Flory equation) the same program was run, but we found unrealistic high T_m^0 values, coupled with very low Δh_u^0 values.

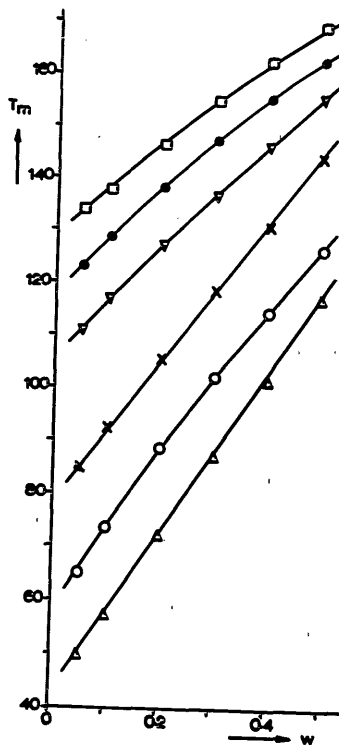


Fig. 1. Melting point curves for PPO in the homologous solvent series toluene to hexylbenzene. Δ toluene, \circ ethylbenzene, \times propylbenzene, ∇ butylbenzene, \bullet pentylbenzene, and \square hexylbenzene.

The above values found for Δh_u^0 and T_m^0 were now used to calculate the term $g_0 + 2g_2 w$ from equation 8 for the other solvents, using the experimental melting points (g_1 was set to zero for the complete series of solvents). The results for $g_0 + 2g_2 w$ versus w are presented in figure 2.

As can be seen here there is no linear relationship between $g_0 + 2g_2 w$ and concentration w as was found for toluene. This would mean that for solvents other than toluene consistent sets of g_0 and g_2 values could not be calculated.

Moreover the values for $g_0 + 2g_2 w$ are surprisingly low. In our analysis, considering solvent participation in the crystal lattice of the polymer to take place, an assumption has now to be made concerning the dependence of Δh_u^0 and T_m^0 on the molecular weight of the solvent, M_0 .

Since the g values themselves are sensitive to Δh_u^0 and less sensitive to T_m^0 it is assumed that Δh_u^0 will decrease proportionally with increasing molecular weight of the solvent, whereas T_m^0 will remain constant at 580 K, i. e.

$$\Delta h_g^0 \frac{M_0}{M_u} = \text{constant} = 11.84 \times \frac{92}{120} = 9.08 \text{ (cal/g)} \quad (9)$$

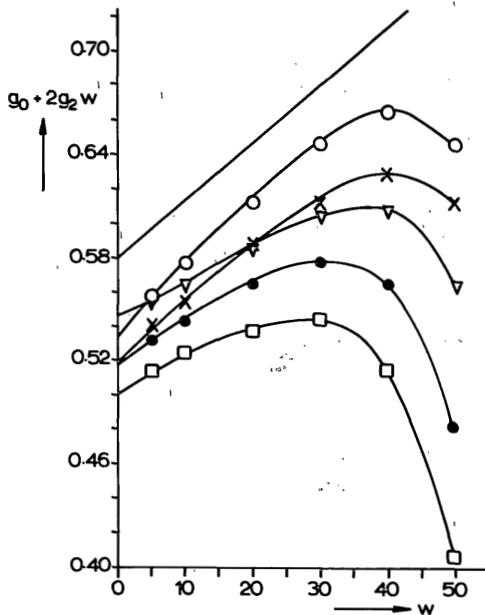


Fig. 2. Calculated curves for $g_0 + 2g_2 w$ for pure polymer crystals. — toluene, \circ ethylbenzene, \times propylbenzene, ∇ butylbenzene, \bullet pentylbenzene, and \square hexylbenzene.

The results for the calculation of $g_0 + 2g_2 w$ from equation 8 and using $T_m^0 = 580 \text{ K}$ and Δh_g^0 as given in equation 9 are given in figure 3.

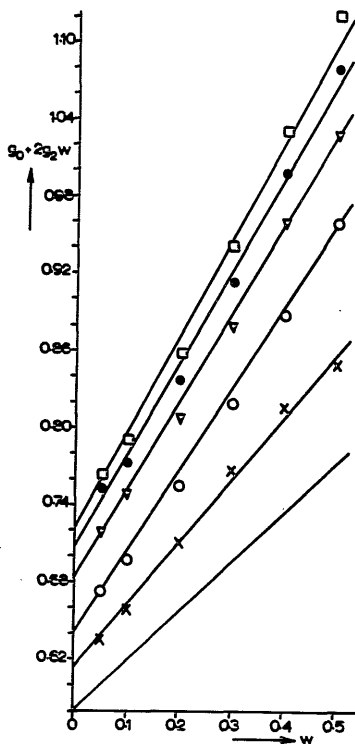


Fig. 3. Calculated curves for $g_0 + 2g_2 w$ with the assumption of co-crystallization by the solvents. — toluene, X ethylbenzene, O propylbenzene, ∇ butylbenzene, ● pentylbenzene, and □ hexylbenzene.

Consistent sets of g_0 and g_2 values which were calculated from figure 3 are given in table 1. As can now be seen from figure 3 and from table 1 there is an increasing concentration dependence in g for the solvent series studied. The concentration dependence of g values for solutions of PPO in toluene as well as in the other solvents can at least in part be explained by the equation of state theory of Flory and Prigogine^{9,10}.

Table 1. Calculated g_0 and g_2 values with the assumption of co-crystallization from the solvent.

	g_0	g_2	<u>correlation coefficient of curve</u>
ethylbenzene	0.61	0.25	0.997
n-propylbenzene	0.63	0.32	0.998
n-butylbenzene	0.67	0.35	0.998
n-pentylbenzene	0.70	0.38	0.998
n-hexylbenzene	0.71	0.41	0.997

Table 2 shows the results for the calculation of the interaction parameter g from the type of equation as proposed by Dayantis¹⁵, for the excess entropy

$$\Delta s_{\text{excess}} = -R \left\{ w_0 \ln \frac{\tilde{v}_0^{1/3} - 1}{\tilde{v}^{1/3} - 1} + w_0 c_1 \ln \frac{\tilde{v}_1^{1/3} - 1}{\tilde{v}^{1/3} - 1} \right\} \quad (10)$$

in which \tilde{v}_0 and \tilde{v}_1 are the characteristic volumes of solvent and polymer respectively, c_1 is the constant giving the number of degrees of freedom of the polymer segment compared to the solvent, \tilde{v} is the characteristic volume of the solution.

g values are calculated from:

$$\frac{\Delta s_{\text{excess}}}{R} = g w_0 w \quad (11)$$

and thus only represent an entropic correction.

Table 2. Calculated values of the correction parameter g from free volume theory. Assumptions: $\tilde{v}_0 = 1.2515$, $\tilde{v}_1 = 1.135$, $c_1 = 0.125$.

w	$g = g_0 + \frac{g_1}{T} + g_2 w$
0.05	0.362
0.1	0.366
0.2	0.376
0.3	0.386
0.4	0.397
0.5	0.408

We expect that the concentration dependence of g calculated with this theory will not be very sensitive to an increase in molecular weight of the solvent. There is still a different approach to obtain values for polymer-solvent interaction parameters: by using the solubility parameter theory. If there is no concentration dependence, the interaction parameter g can be calculated directly from the solubility parameter theory. To assume an interaction parameter which does not depend on the concentration would imply that only dispersion forces are present. The polar forces could then independently be accommodated in the concentration dependent term. We have calculated here the enthalpy correction parameter χ_H as:

$$\chi_H = \frac{V_0}{RT} (\delta_d^0 - \delta_d^1)^2 \quad (12)$$

using δ_d^1 value for PPO from Koenhen and Smolders¹⁶ and taking δ_d^0 values from van Krevelen⁸. Results are given in table 3.

Table 3. Calculated values for the enthalpic interaction parameter χ_H calculated with the solubility parameter theory. g_0 and g_2 values from table 1.

	δ_d^0	χ_H	(taken from table 1)	
			g_0	g_2
toluene	8.84	0.058	0.58	0.19
ethylbenzene	8.76	0.087	0.61	0.25
n-propylbenzene	8.73	0.108	0.63	0.32
n-butylbenzene	8.69	0.136	0.67	0.35
n-pentylbenzene	8.66	0.163	0.70	0.38
n-hexylbenzene	8.63	0.19	0.71	0.41

DISCUSSION

1. MELTING ENTHALPY AND MELTING TEMPERATURE

We could show above that no realistic values are obtained for the melting enthalpy and the melting temperature when using the simple Flory melting point depression theory. Obviously it is not allowed to neglect the variation of the melting enthalpy and entropy with temperature for these rather large melting point depressions. ($\Delta T \approx 200$ K).

The Δh_u^0 , T_m^0 values obtained with the Flory-Hoffman theory show values in the expected range. The Flory-Hoffman equation is used here in a slightly different form compared to earlier publications^{1, 17, 18}, because there the difference in definitions of the unit or the segment for solvent and polymer was neglected. In that case our calculations for toluene solutions would give $\Delta h_g^0 = 9.08$ cal/g. This value agrees well with the uncorrected values reported earlier¹. We now see that the correct value for toluene as solvent is $\Delta h_g^0 = 11.84$ cal/g.

2. INTERACTION PARAMETERS IN SOLUTION

The results for $g_0 + 2g_2$ w versus w calculated with equation (8) and $\Delta h_g^0 = 11.84$ cal/g give values for the series of solvents (fig. 2) which are contrary to the expectations, and therefore we believe that these values are not correct. When the assumption was made that the solvent forms part of the crystals and the simple dependence of Δh_u^0 on $\frac{M_u}{M_0}$ was introduced, straight lines were obtained for $g_0 + 2g_2$ w versus w which permitted the calculation of consistent g_0 and g_2 sets for each solvent.

It has to be stressed however, that it is in no way proven that the dependence we used has to be correct one, nor is the constancy of T_m^0 proven.

Since the final result of our calculations of solution parameters, derived from experimental melting point data and using an assumption on solvent co-crystallization, gives g_0 and g_2 values which show an increase with solvent molecular weight (as we had anticipated from solubility expectations), we think that this once more is an indication for the fact that solvent is built in in the lattice.

A part of the concentration dependence of g can be attributed to the equation of state contributions; as is shown in table 2. From the solubility parameter theory (equation 12 and table 3) it is shown that the enthalpic contribution to the interaction parameter increases with molecular weight of the solvent in the series studied. Since the enthalpic contribution for PPO solutions in toluene is nearly zero (literature 1 and table 3) the term $\frac{g_1}{T}$ was not used. (In general the enthalpic contribution is depicted as $A + B/T$). In the interpretation of our melting point curves however, it is difficult to distinguish between a concentration dependence and a reciprocal temperature dependence as was shown in a previous paper¹. An eventual contribution of $\frac{g_1}{T}$, induced by the changing enthalpic contribution over the solvent series, is incorporated

in the term $g_2 w$ because of the difficulty to discriminate between them ($1/T_m$ is linear in w).

The interaction parameter χ_H calculated with the solubility parameter concept for dispersion forces is given at one temperature (25°C) and it is not concentration dependent. The observed increase over the solvent series is in agreement with expected values and is also in good agreement with the increase in values for g_0 (table 3) from the melting point depression calculations.

Summarizing, the conclusion can now be drawn from the melting point depression curves that solvent is built in the crystal lattice. The thermodynamic polymer-solvent interaction parameters calculated from these curves with the appropriate assumptions are reasonable and can be explained qualitatively by solubility theories.

REFERENCES

1. D.M. Koenhen and C.A. Smolders, *J. Polym. Sci. A-2*, 15, 155 (1977).
2. D.M. Koenhen and C.A. Smolders, *J. Polym. Sci. A-2*, 15, 167 (1977).
3. D.M. Koenhen and C.A. Smolders, *J. Polym. Sci. C*, in press.
4. J. Brandrup and E.H. Immergut, *Polymer Handbook* 2nd ed.
5. E.P. Magré and J. Boon, Communication presented at the Microsymposium on Structure of Organic Solids, Prague, 1968.
6. P.J. Flory, *Principles of Polymer Chemistry*, Cornell University Press, Ithaca, N.Y., 1953.
7. Th. G. Scholte, *J. Polym. Sci.*, A-2, 8, 841 (1970).
8. D.W. van Krevelen, *Properties of Polymers*, Elsevier Publishing Company, Amsterdam, 1972.
9. I. Prigogine, *The molecular Theory of Solutions*, Interscience Publishers, New York, N.Y., 1957.
10. P.J. Flory, R.A. Orwoll and A. Vrij, *J. Amer. Chem. Soc.*, 86, 3515 (1964).
11. R. Koningsveld; *Advan. Coll. Interface Sci.*, 2, 151 (1968).
12. L. Mandelkern, *Crystallization of Polymers*, McGraw Hill Book Company, New York, N.Y., 1964.
13. J.D. Hoffman, *J. Chem. Phys.* 28, 1192 (1958).
14. J.B. Helms, Dissertation, Groningen, 1970.
15. J. Dayantis, *J. Polym. Sci. C-39*, 35 (1972).
16. D.M. Koenhen and C.A. Smolders, *J. Appl. Pol. Sci.* 19, 1163 (1975).
17. P.T. van Emmerik and C.A. Smolders, *J. Pol. Sci. C-39*, 311 (1972).
18. P.T. van Emmerik and C.A. Smolders, *Europ. Pol. J.*, 9, 293 (1973).

PHASE SEPARATIONS IN SOLUTIONS OF POLY(2,6-DIMETHYL-1,4-PHENYLENE OXIDE), V. VAPOUR PRESSURE AND MEMBRANE OSMOMETRY

A. BAKKER, D.M. KOENHEN and C.A. SMOLDERS
Twente University of Technology, Dept. Colloid and Interface Science, Enschede, The Netherlands

SYNOPSIS

Vapour pressure osmometry and high pressure membrane osmometry have been used as techniques for the determination of the interaction parameters for solutions of PPO in toluene. Vapour pressure osmometry proved to be a good method for these determinations in the concentration range 5 to 15 % by weight of PPO.

Membrane osmometry is a slow method but yields accurate results. The interaction parameters which have been determined are somewhat lower than those determined earlier by light scattering. On the whole the agreement however, is very good. From these measurements it could be shown that the temperature dependence of the interaction parameters in this system is very low.

The results for the phase separation behaviour is that liquid-liquid phase separation cannot be expected, whereas crystallization is possible. From the apparently low melting temperature found for the pure polymer, in relation to its T_g-value, it was concluded that this melting phenomenon is not the real crystalline melting point but that of a degenerate lattice. Together with X-ray observations for this and other systems with PPO this led to the conclusion that the crystals formed in solution contain the solvent molecule in the lattice.

INTRODUCTION

In this work we describe the determination of the thermodynamic correction parameter χ_w from the Flory-Huggins equation¹ using two different methods. These methods are vapour-pressure osmometry and high pressure membrane osmometry. In an earlier paper the χ_w and g parameters for the system PPO*-toluene have been determined from light scattering data². Introduction of these

* PPO is a trade mark of General Electric CO.

parameters in experimental melting point depression data suggested that the right order of magnitude of these χ_w and g values had been obtained. The concentration range covered however, was rather small ($w < 10\%$) and some confusion could have been roused by three different publications which give completely different values^{2, 3, 4}. The purpose of this work is to determine the thermodynamic parameters from independent methods, which do not have the same type of disturbances possible with light scattering. The data are here obtained over an extended concentration range as well. An understanding of the temperature and concentration dependence of the χ_w and g parameters is important for the use of these parameters in describing phase transitions in the solutions⁵. The influence of these factors on the liquid-liquid phase separation is qualitatively described by Van Emmerik and Smolders⁶. In the first articles in this series however, it was shown that crystallization is expected to occur^{2, 7, 8, 9}. The solvent is thought to take part in the crystal lattice. In this case it is even more important to know the concentration and temperature dependence of interaction parameters accurately to explain the special conformational features in this type of crystallization. For instance in helix formation it is known that interaction between solvent molecules and the polymer solution e.g. making use of a corresponding states theory, accurate data are necessary as well¹¹.

THEORETICAL

VAPOUR PRESSURE OSMOMETRY

The principle of this method is the determination of a temperature difference between a drop of polymer solution and a drop of pure solvent. This temperature difference is induced by solvent condensation which occurs because of a difference in vapour pressure between the solution and the pure solvent. The temperature differences involved are compared with the heats measured from a solution of a known low molecular weight substance which obeys Raoult's law, and thus has a known vapour pressure lowering. The calibrating substances used to determine the vapour pressure lowering from the heat of condensation of the solvent can be benzil, methylstearate or glucosepentaacetate. Because these substances are supposed to behave ideally in the concentration range used, the method is often employed as a means of determining the number average molecular weight of polymers. This determination makes use of extrapolation to zero concentration where the polymer solution behaves ideally as well.

In this work however, we do not extrapolate to zero concentration and the polymer solution does not behave ideally at the concentrations measured. Thus we have to determine the actual vapour pressure lowering of the polymer solution by comparison with the effect for the ideally behaving calibrating substances mentioned.

For the chemical potential difference of the solvent in the solution and in the pure state, we have¹²:

$$\Delta\mu_o = RT \ln P_1/P_1^o + B(P_1 - P_1^o) \quad (1)$$

and for the solutions of low molecular weight substances at not too high concentration:

$$P_1 = X P_1^o \quad (\text{Raoult's law}) \quad (2)$$

where R is the gas constant, T is the temperature in Kelvin, B is the virial coefficient of toluene, P_1 the vapour pressure of the solution, P_1^o the vapour pressure of the solvent, and X is the mole fraction of toluene.

Thus:

$$\Delta\mu_o = RT \ln X_A + B P_1^o (X_A - 1) \quad (3)$$

B can be calculated from the following relation¹³:

$$B = 2278\{0690-310(e^{-1250/T}-1)-0,169(e^{1205/T}-1)-2921(e^{-253,05}-1)\} \quad (4)$$

From the measurements of the calibrating substance $\Delta\mu_o$ can be obtained for different concentrations of this substance. For the polymer solution of a known concentration the $\Delta\mu_o$ of the solution is set equal to the $\Delta\mu_o$ for the calibrating substance with a concentration giving the same recorder reading. From the latter concentration $\Delta\mu_o$ can then be calculated.

The χ_w parameter can now be calculated from the Flory-Huggins equation for $\Delta\mu_o$:

$$\chi_w = \frac{\Delta\mu_o/RT - \ln(1-w) - (1 - \frac{M_o}{M_n})w}{w^2} \quad (5)$$

where w is the weight fraction of polymer in the solution.

HIGH PRESSURE MEMBRANE OSMOMETRY

Membrane osmometry is often used as a means of determining the number average molecular weight of polymers as well as is the case for vapour pressure osmometry. In addition to this, osmometry has frequently been used to determine the thermodynamic parameters of polymer solution^{11, 14}. At higher concentrations however, the osmotic pressures which develop are much higher than those commonly used for molecular weight determinations. This is why we use the indication high pressure membrane osmometry for this method. In the principles of the methods there is no difference.

$$\Delta\mu_0 = \pi V_0 \quad (6)$$

where V_0 is the molar volume of the solvent and π is the osmotic pressure. When π is measured χ_w values can again be determined from the combined equations 5 and 6.

EXPERIMENTAL

VAPOUR PRESSURE OSMOMETRY

For the measurements use was made of a commercial Knauer instrument. For the calibration substance benzil was chosen, of which solutions in toluene were made with concentrations between 74×10^{-5} and 9806×10^{-5} mole/kg. Temperatures of 35.1; 39.3; 53.5; 64.5 and 75.6 °C were used. For concentrations below 10 % polymer pearl thermistors were used, for concentrations in excess of 10 % universal thermistors were used. The amplifier was set at range 64 at concentrations until 10 %, at 32 for concentrations from 10-15 % and at 8 for 15-20 % PPO.

The recorder used was a Kipp BD5 apparatus; sensitivity range was set at 1 mV. All the solutions of both benzil and toluene were made up from the same batch of analytical grade toluene. The PPO used had a number average molecular weight of between 19.000 and 24.000 as determined with this instrument and 23.000 as determined by low pressure osmometry.

Before the solutions were syringed into the instrument the solutions were thermostated to within 1 °C of the temperature used in the instrument. Instrument rea-

dings were always taken after 5 minutes.

HIGH PRESSURE OSMOMETRY

A membrane osmometer was constructed with a design as given in figure 1. This design is very similar to that used by Flory et al. but it has better filling and sealing characteristics. Pressure was given by compressed air or nitrogen over a mercury column. Membranes used were common commercial regenerated cellulose membranes. Temperatures used were 39.1; 45.4; 53.5; 64.6 and 74.5 °C.

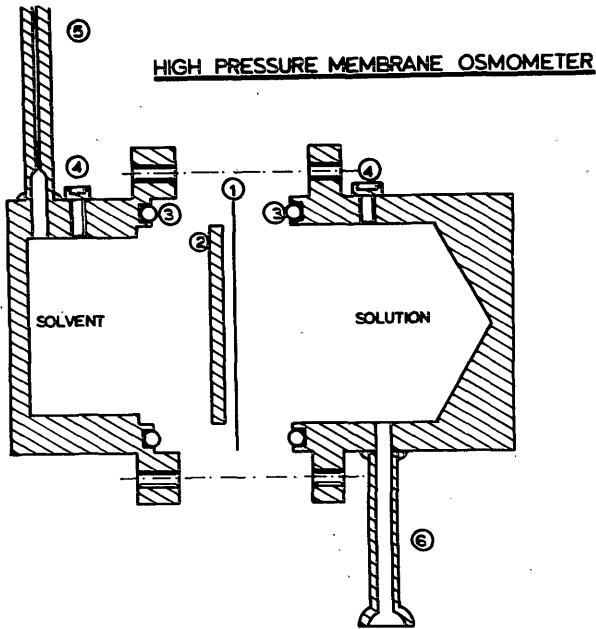


Fig. 1. High pressure membrane osmometer. 1 membrane, 2 porous steel plate, 3 O-rings, 4 filling ports, 5 glass capillary, 6 mercury filled U-tube

RESULTS

VAPOUR PRESSURE OSMOMETRY

From the measurements at different concentrations of benzil for every temperature given above, a calibration curve of temperature difference (arbitrary recorder units Δn) versus concentration is obtained (figure 2)

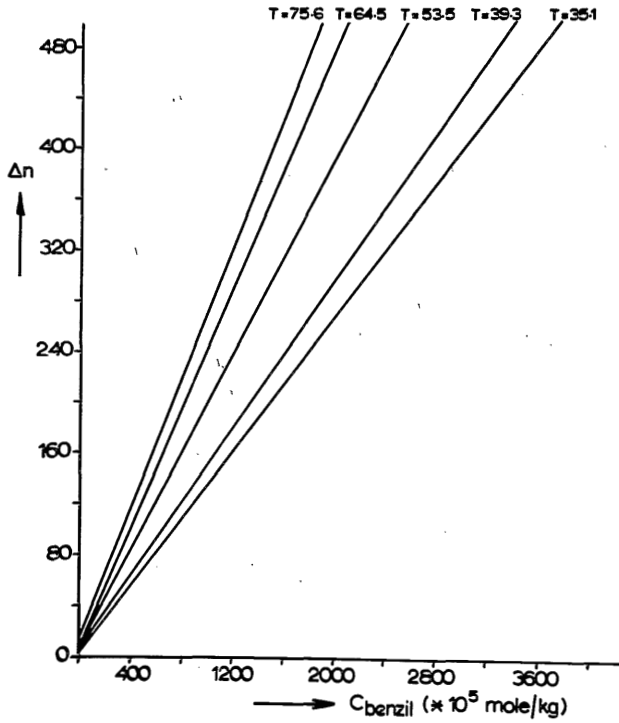


Fig. 2. Calibration curves for the vapour pressure osmometer for benzil solutions at different temperatures.

For a specific polymer solution now a value Δn_p is measured. For this Δn_p the corresponding concentration of benzil (1-X) is obtained from figure 2 and $\Delta \mu_o$ can be calculated. In tabel 1 the results are shown.

Table 1. Thermodynamic parameters from vapour pressure osmometry

temperature °C	polymer concentration weight fraction	comparable concentration benzil mole/kg $\times 10^5$	chemical potential $\Delta\mu_0 \times 10^{-6}$ erg/mole	interaction parameter χ_w	error in χ_w
35.1	0.005033	27.30	0.6453	0.3	0.33
	0.009264	69.40	1.640	0.19	0.11
	0.019457	168.40	3.979	0.30	0.030
	0.050151	689.30	16.30	0.344	0.007
	0.095424	2086.40	49.44	0.364	0.003
39.3	0.005033	23.00	0.5512	0.4	0.364
	0.009264	50.00	1.198	0.39	0.12
	0.019457	145.70	3.439	0.35	0.032
	0.050151	657.10	15.75	0.356	0.007
	0.095424	2050.30	49.25	0.368	0.003
	0.145309	4371.40	105.4	0.389	0.002
53.5	0.005033	33.00	0.8265	0.1	0.29
	0.009264	74.00	1.853	0.1	0.10
	0.019457	178.50	0.4469	0.27	0.027
	0.050151	698.20	17.49	0.341	0.006
	0.095424	2147.00	53.92	0.358	0.003
	0.145309	4839.00	122.1	0.369	0.003
64.5	0.019454	224	5.797	0.16	0.035
	0.050151	770	20.15	0.311	0.008
	0.095424	2101	54.56	0.362	0.003
	0.145309	5134	133.9	0.356	0.009
	0.200510	10159	267.3	0.36	0.0122
75.6	0.009264	66.60	1.780	0.2	0.1397
	0.019454	237.20	6.341	0.13	0.037
	0.050151	814.30	21.79	0.298	0.008
	0.095424	2171.10	58.22	0.355	0.004
	0.145309	4626.90	124.6	0.37	0.16
	0.200510	8125.40	220.0	0.410	0.009

Errors in the measurements do occur during the determination of the calibration curve figure 2 and in the determination of Δn_p for the polymer solution. These errors can be converted to errors in X in the following way:

$$\Delta x = \frac{\text{standard error of estimate of calibration curve}}{\text{slope of curve}}$$

When the standard deviation in a series of measurements is larger than the standard error of estimate for the calibration curve, the following relation is valid:

$$\Delta x = \frac{\text{standard deviation of measured values}}{\text{slope of curve}}$$

These relations are valid when the error in making up the benzil and PPO concentrations is negligibly small, which condition is satisfied here.

Another source of errors which is contained in $\Delta\chi_w$ is the uncertainty in M_n . At low concentrations it has to be expected that errors caused by the instrument become notable. This effect then appears because of the very small signals at these low concentrations. These effects (see table 1) have not been evaluated in this work.

In figures 3 and 4 dependencies of χ_w on concentration and temperature are given.

MEMBRANE OSMOMETRY

The results for the membrane osmometry are given in table 2.

Table 2. Thermodynamic parameters from high pressure membrane osmometry

t °C	w -	π g/cm ²	$-\Delta\mu^0 \times 10^{-6}$ erg/mole	χ -
39.1	0.050	151.2	16.13	0.349
45.5	0.050	155.0	16.61	0.347
53.5	0.050	157.6	17.04	0.346
39.5	0.100	499	53.1	0.371
53.6	0.100	506	54.9	0.374
64.5	0.100	513	56.3	0.375
53.4	0.150	1148	124	0.379
64.6	0.150	1151	126	0.383
74.6	0.150	1172	130	0.383
53.4	0.200	2018	219	0.401
64.6	0.200	2059	226	0.398
74.5	0.300	4183	465	0.46*

* Not reliable due to some leakage from the cell.

DISCUSSION

Vapour pressure osmometry proves to be a reliable method which gives the right magnitude of interaction parameters. At low concentrations ($w < 5\%$) the method becomes inaccurate. This also occurs at concentrations above $\pm 15\%$ where the thermistors are not linear any more, and the viscosity of the solution prohibits the syringing. Between these concentrations the method is easy to use and quick. For normal vapour pressure measurements this concentration range would be very difficult, experimentally.

Membrane osmometry is known to be more accurate. Here equilibrium is obtained after a relatively long time (24 hours). Thus the method is rather slow. The pressures which have to be applied (up to 3 atm) present sealing problems. With membrane osmometry the limiting factors are the pressures and the temperature which can be applied for the membrane used. For the system PPO-toluene with cellulose membranes this means that temperatures had to be lower than 80°C and concentrations less than 30% .

From table 1 and 2 one can see that the values obtained from vapour pressure osmometry show a larger spreading than the values from membrane osmometry. Both methods give values which are somewhat lower than those obtained by light scattering experiments in previous work.

We believe that the membrane osmometry values obtained here are the best published for the system PPO-toluene. In the case of light scattering always the problem of water and dust removal from the solutions is present². A small amount of these last components gives higher light scattering values for χ_w . The distinct dependence on concentration and the relative insensitivity of χ_w towards temperature is given by all three methods. From the membrane osmometry data values for g_0 and g_2 can be calculated. We found $g_0 = 0.498$ and $g_2 = 0.163$ while g_1 is taken to be zero. These values once again show that no liquid-liquid phase separation has to be expected, because when these values are inserted in the Flory-Huggins equation no inflection points can be calculated in the ΔG_m versus w curves. For the calculations based on the experimental melting point curves as given in previous work⁹ these g_0 , g_2 values have the effect that the Δh_u^0 values become higher and T_m^0 is somewhat lower. ($\Delta h_g^0 = 14.4$ cal/g; $T_m^0 = 531.5$ K) compared to $\Delta h_g^0 = 11.4$, $T_m^0 = 580$ K. The g_0 and g_2 values to be calculated for PPO in the other solvents (ethylbenzene to hexylbenzene) are correspondingly lower. These values were calculated with the assumption $g_0 = 0.58$ and $g_2 = 0.19$ for PPO in toluene in previous work⁹

The other conclusions however, are unaffected.

It has often been found that T_m^o values for crystals of PPO lie between 513 K and 545 K. This gives a ratio T_g/t_m from 0.91 - 0.83^{4, 5, 15}.

In comparison with other polymers, including poly(1,4-phenylene oxide)¹⁶ and poly(2,6-diphenyl-1,4-phenylene oxide)^{17, 18} this is unexpectedly high.

In DSC measurements a melting endotherm is measured at around 523 K, for "as received" polymer. This polymer probably has been made by oxidative polymerization¹⁹, followed by a coagulation step. We have also found that rapid coagulation in non-solvents of a different nature like diethylether, methanol or hexane gives the same DSC melting endotherm and a very weak X-ray pattern. The melting endotherm and the same weak X-ray pattern is also observed if wet crystalline mats of PPO in α -pinene are treated with non-solvents with the loss of the original strong X-ray pattern. When the wet mats of α -pinene crystals are dried in vacuum or air all crystallinity is lost²⁰.

It is known that in the α -pinene crystals the α -pinene forms part of the crystal lattice. Crystals grown from toluene show the same behaviour. From these observations the conclusion can be drawn that the melting point measured for the pure polymer in DSC is not the real crystalline melting point but the melting point of a degenerate crystal structure or a partly ordered glassy state. The melting points are this low because in the crystals the solvent forms a part of the lattice and on drying the structure is lost. The real melting point for pure PPO must be at higher temperature as in indicated by the work of Boon and Magre²¹ who measured a T_m of 603 K for stretch crystallized PPO and the work of Packter and Shariff²² who measured $T_m = 623$ K in their heterogeneous ratios for T_g/T_m . Probably PPO has internal constraints, which prohibit the crystallization to a great extent in the pure state. These constraints can possibly be attributed to the meta-substitution which is always present as can be seen from the 815 cm^{-1} peak in infrared spectra²³.

When the solvent is incorporated in the lattice these constraints could be cancelled.

REFERENCES

1. P. J. Flory, *Principles of Polymer Chemistry*, Cornell Univ. Press, Ithaca, 1953.
2. D. M. Koenhen and C. A. Smolders, *J. Pol. Sci. A-2*, 15, 155 (1977).
3. A. R. Schultz and C. R. McCullough, *J. Pol. Sci. A-2*, 10, 307 (1972).
4. P. T. van Emmerik and C. A. Smolders, *J. Pol. Sci., C*, 38, 73 (1972).
5. R. Koningsveld, *British Polym. J.*, 7, 435 (1975).
6. P. T. van Emmerik and C. A. Smolders, *Eur. Pol. J.* 9, 157 (1973).
7. D. M. Koenhen and C. A. Smolders, *J. Pol. Sci. A-2*, 15, 167 (1977).
8. D. M. Koenhen and C. A. Smolders, *J. Pol. Sci. C*, in press.
9. D. M. Koenhen and C. A. Smolders, submitted to *J. Pol. Sci.*
10. L. Mandelkern, *Crystallization of Polymers*, McGraw Hill, New York, N. Y. 1964.
11. B. E. Eichmger and P. J. Flory, *Trans. Faraday Soc.*, 64, 2035 (1968).
12. W. J. Moore, *Physical Chemistry* 5th ed. Longman, London 1972.
13. A. P.I. 23-2 (33.1110)-h, page 1.
14. P. J. Flory, H. Daoust, *J. Polym. Sci.* 25, 429 (1957).
15. F. E. Karasz, J. M. O'Reilly, H. E. Bair and R. A. Kluge, paper presented at the 155th Natl. ACS Meeting 1968.
16. J. Boon and E. P. Magré, *Die Makromol. Chem.* 126, 130 (1969).
17. J. Boon and E. P. Magré, *Die Makromol. Chem.* 136, 269 (1970).
18. W. Wrasidlo, *Macromolecules* 4, 642 (1971).
19. A. S. Hay, *Adv. Pol. Sc.* 4, 496 (1967).
20. E. P. Magré and J. Boon, Scientific Communication IIIrd Microsymposium "Structure of Organic Solids", Prague, 1968.
21. E. P. Magré, private communication.
22. A. Packter and K. A. Shariff, *J. Polym. Sci., Polym. Letters* 9, 435 (1971).
23. A. Savolainen, Ph. D. thesis, Helsinki (1974).

The Determination of Solubility Parameters of Solvents and Polymers by Means of Correlations with Other Physical Quantities

D. M. KOENHEN and C. A. SMOLDERS, *Twente University of Technology, Enschede, The Netherlands*

Synopsis

Correlations of solvent solubility parameters with molar attraction constants and with properties like surface tension, dipole moment, and index of refraction have been explored. From relations found to be valid for solvents, it is possible to calculate the solubility parameters for polymers. A relation between the dispersion contribution to the surface energy of polymers (a measurable quantity) and the dispersion solubility parameter of polymers has been found which is similar to a relation established for low molecular weight substances.

INTRODUCTION

Predicting the energy of mixing of solvents and polymers from properties of the pure substances is an alluring prospect. In recent years, good progress has been made with methods based on the solubility parameter concept proposed by Hildebrand and others.¹ This theory relates the energy of mixing to the energies of vaporization of the pure components:

$$\frac{\Delta E_{\text{mix}}}{\phi_1\phi_2} = V_m(\delta_1 - \delta_2)^2 \quad (1)$$

$$\delta = [C.E.D.]^{1/2} = \left[\frac{\Delta E_{\text{vap}}}{V_m} \right]^{1/2}$$

where ΔE_{mix} = energy of mixing (or enthalpy, if ΔV_{mix} is zero), ϕ_1, ϕ_2 = volume fractions of the components, V_m = average molar volume based on mole fractions, δ_1, δ_2 = solubility parameters, $C.E.D.$ = cohesive energy density, and ΔE_{vap} = energy of vaporization.

This theory has been developed for mixing of nonpolar substances. However, many of the solvents and polymers in common use are polar, i.e., have dipole moments and/or capabilities for hydrogen bonding. It is clear that these factors should be included in the theory.

The first step was made by Prausnitz et al.,^{2,3} who divided the energy of vaporization into a nonpolar, dispersion part and a polar part. They were able to calculate a nonpolar solubility parameter λ and a polar solubility parameter τ . Hansen^{4,5} divided the polar part τ into a dipole-dipole contribution and a hydrogen bonding contribution, both of which could be determined through solubility

experiments with polymers. In this article, we will use the notation introduced by Hansen⁴):

$$\delta^2 = \delta_d^2 + \delta_p^2 + \delta_h^2 \quad (2)$$

where δ_d = solubility parameter due to dispersion forces, δ_p = solubility parameter due to dipole forces, and δ_h = solubility parameter due to hydrogen bonding (or in general due to donor-acceptor interactions).

Chen⁵ showed that the contribution to the energy of mixing in polymer solutions caused by dispersion forces and dipole forces could be taken together to one enthalpy correction parameter χ_H (a Flory-Huggins-type correction parameter),

$$\chi_H = \frac{V_m}{RT} [(\delta_{d1} - \delta_{d2})^2 + (\delta_{p1} - \delta_{p2})^2] \quad (3)$$

which, together with the δ_h 's, could describe the solubility characteristics.

The two last-mentioned theories produce good predictions for the solubility of polymers.

The determination of the solubility parameters of many substances, however, is still a difficult and laborious undertaking. A new approach in recent literature has been to find correlations between solubility parameters $\delta(\delta_d, \delta_p, \delta_h)$ and other physical properties of the substance.

In this work we have explored possible correlations of the solubility parameters with molar attraction constants and with properties like surface tension, dipole moment, and index of refraction. Since it is obvious that not all contributions to molecular interactions affect both ΔE_{vap} and the physical properties mentioned in a parallel way, our main purpose was to improve existing relationships between them.

RELATION BETWEEN SURFACE TENSION AND COHESIVE ENERGY DENSITY

Using a Lennard-Jones potential for the interaction between the molecules, one can derive⁷

$$\gamma_L = \left(1 - \frac{n_s}{n}\right) \frac{\epsilon}{a} \quad (4)$$

in which γ_L = surface tension, n_s = coordination number in the surface layer, n = coordination number in the bulk phase, a = cross-sectional area per molecule, and ϵ = minimum potential in a L-J potential curve. If the area per molecule is proportional to $V_m^{2/3}$, as for spherical molecules, and if ΔE_{vap} (= $V_m \cdot C.E.D.$) is proportional to ϵ , the following relation holds

$$C.E.D. = A \left(\frac{1}{V_m}\right)^{1/3} \gamma_L \quad (5)$$

in which A is a constant.

This relation has also been derived by some other approaches.^{1,8,9,10} These derivations make use of a spherical symmetric type of potential around a molecule, in most cases explicitly a Lennard-Jones potential. This potential, however, is not valid for interactions between molecules in polar substances,¹¹ i.e.,

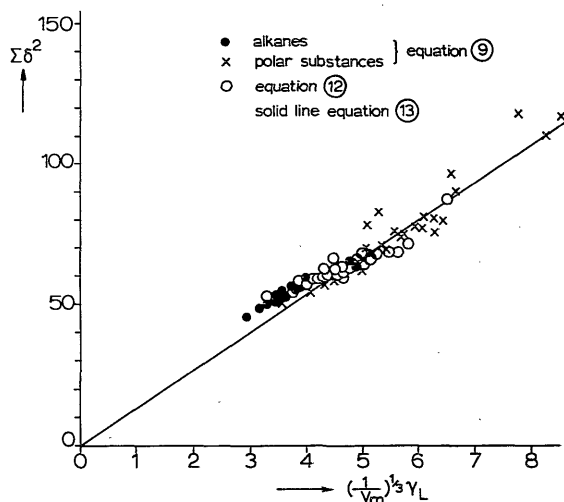


Fig. 1. Relation between surface tension and solubility parameters for solvents.

substances where dipole-dipole and hydrogen bonding forces act. Hence eq. (5) is found to be valid for *nonpolar liquids only*.

Beerbower¹⁰ used the division of the different contributions to the *C.E.D.* according to Hansen⁵ in a computer analysis and arrived at the following relationships, rewritten in the form of eq. (5):

$$\delta_a^2 + 0.632 \delta_p^2 + 0.632 \delta_h^2 = 13.9 \left(\frac{1}{V_m} \right)^{1/3} \gamma_L \text{ for nonalcohols} \quad (6)$$

$$\delta_a^2 + \delta_p^2 + 0.06 \delta_h^2 = 13.9 \left(\frac{1}{V_m} \right)^{1/3} \gamma_L \text{ for most alcohols} \quad (7)$$

and

$$\delta_a^2 + 2\delta_p^2 + 0.481 \delta_h^2 = 13.9 \left(\frac{1}{V_m} \right)^{1/3} \gamma_L \text{ for acids, phenols and amines} \quad (8)$$

In our least-squares analysis of solvent data, we find that the relation

$$\delta_a^2 + \delta_p^2 = 13.8 \left(\frac{1}{V_m} \right)^{1/3} \gamma_L \quad (9)$$

fits practically all substances listed in Table I, with a correlation coefficient of 0.99 and a standard error of estimate 5.6 for $\delta_a^2 + \delta_p^2$ (Fig. 1). Exceptions are some cyclic compounds, acetonitrile, carboxylic acids, and polyfunctional alcohols.

The reason for the absence of δ_h in this relationship, which is also valid for monofunctional hydrogen bonding substances, is probably the fact that the interactions responsible for liquid-vapor interfacial energy do not involve the breaking of hydrogen bonds; see also eq. (7).

Bagley et al.¹¹ showed recently that the contribution to the cohesive energy from hydrogen bonds depends on temperature only, at least at pressures not too far removed from atmospheric. The contributions of dispersion and dipolar forces are shown to be volume dependent.¹¹ When the vapor pressure at an

TABLE I
Solubility Parameters, Surface Tensions, Molar Volumes, and Calculated Values of Solvents

Substance	δ_d^a	δ_p^a	δ_h^a	γ^b	$V_m,^b$ cc/mole	$(1/V_m)^{1/3}\gamma$	$\delta_d^2 + \delta_p^2 + \delta_h^2$ CED = δ_d^2
Methanol	7.42	6.0	10.9	22	40.7	6.39	91.1 204
Ethanol	7.73	4.3	9.5	22	58.5	5.67	78.2 168
<i>n</i> -Propanol	7.75	3.3	8.5	22.62	75.0	5.37	71.0 143.2
<i>n</i> -Butanol	7.81	2.8	7.7	23.38	91.8	5.19	68.8 122.1
2-Eth. butanol	7.70	2.1	6.6	24.32	123.2	4.90	63.7 107.3
Meth. isob. carb.	7.47	1.6	6.0	22.63	127.2	4.51	58.4 94.4
Cyclohexanol	8.50	2.0	6.6	33.91	106.0	7.18	76.3 119.8
2-Butoxyethanol	7.76	3.1	5.9	27.4	132	5.39	69.8 104.6
Cellosolve	7.85	4.5	7.0	28.2	97.8	6.13	81.9 130.9
Diethylether	7.05	1.4	2.5	16.50	104.8	3.51	51.7 57.9
Furan	8.70	0.9	2.6	23.38	72	5.63	76.4 83.3
Diethyl sulfide	8.25	1.5	1.0	24.5	108.2	5.15	70.3 71.3
Dimethylsulfoxide	9.00	8.0	5.0	42.86	71	10.37	145.0 170.0
Acetone	7.58	5.1	3.4	22.27	73.9	5.31	83.5 95.0
Methyl ethyl ketone	7.77	4.4	2.5	23.04	90.2	5.15	79.7 86.0
Acetophenone	8.55	4.2	1.8	37.72	117.1	7.72	90.7 94.0
Tetrahydrofuran	8.22	2.8	3.9	26.4	74.0	6.30	75.4 90.6
Ethyl acetate	7.44	2.6	4.5	22.99	98.5	4.99	62.1 82.4
Acetonitrile	7.50	8.8	3.0	27.55	52.9	7.35	133.7 142.7
Butyronitrile	7.50	6.1	2.5	25.84	87.0	5.85	93.5 99.7
Nitromethane	7.70	9.2	2.5	34.98	54.0	9.27	143.9 150.2
Nitroethane	7.80	7.6	2.2	32.13	71.3	7.76	118.6 123.4
2-Nitroprop.	7.90	5.9	2.0	29.29	86.9	6.62	97.2 101.2
Aniline	9.53	2.5	5.0	42.79	91.1	9.52	97.1 122.1
Nitrobenzene	8.60	6.0	2.0	42.00	102.3	8.99	101.0 113.9
Dimethylformamide	8.52	6.7	5.5	35.2	77.0	8.29	117.5 147.1
Diprop. amine	7.50	0.7	2.0	22.28	136.9	4.33	56.7 60.7
Diethylamine	7.20	1.1	3.0	19.39	103.2	4.14	54.5 63.5
Pyridine	9.25	4.3	2.9	36.33	80.4	8.43	104.1 112.5
Carbon tetrachloride	8.65	0	0	26.15	97.1	5.70	74.8 74.8
Chloroform	8.65	1.5	2.8	26.53	80.7	6.15	77.1 84.9
Trichloroethylene	8.78	1.5	2.6	28.8	90.2	6.43	79.3 86.1
Chlorobenzene	9.28	2.1	1.0	31.37	102.1	6.72	90.5 91.5
α -Bromonaphthalene	9.94	1.5	2.0	44.2	140.0	8.53	101.1 105.1
Benzene	8.95	0.5	1.0	28.18	89.4	6.31	80.4 84.1
Toluene	8.82	0.7	1.0	27.92	106.4	5.90	78.3 79.3
Ethyl benzene	8.70	0.3	0.7	28.48	123.1	5.73	75.8 76.3
Hexane	7.27	0	0	17.91	131.6	3.52	52.8 52.4
Cyclohexane	8.18	0	0	24.38	108.7	5.61	66.9 66.9
Pentane	7.05	0	0	15.48	116.104	3.17	49.7 49.7
3-Methylpentane	7.13	0	0	17.60	130.611	3.47	50.8 50.8
3-Methylhexane	7.29	0	0	19.30	146.714	3.66	53.1 53.1
2-Methylbutane	6.75	0	0	14.46	117.38	2.95	45.6 45.6
2-Methylpentane	7.13	0	0	16.87	132.875	3.31	50.8 50.8
Heptane	7.50	0	0	19.80	147.456	3.75	56.3 56.3
Octane	7.54	0	0	21.14	163.530	3.87	56.9 56.9
Decane	7.74	0	0	23.37	195.905	4.02	59.9 59.9
Cyclopentane	8.10	0	0	21.82	94.713	4.79	65.6 65.6
Ethylcyclohexane	7.96	0	0	25.14	143.141	4.81	63.4 63.4
2-Methylhexane	7.22	0	0	18.80	148.576	3.33	52.1 52.1
2-Methylheptane	7.34	0	0	20.14	164.607	3.67	53.9 53.9
Acetic acid	7.10	3.9	6.6	27.3	57.1	7.09	65.6 109.2
Formic acid	7.0	5.8	8.1	37	37.8	11.07	82.6 148.3
Butyric acid	7.30	2.0	5.2	26.6	92.5	5.88	57.3 84.3

^a Hansen.^{5,13}

^b Riddick and Bunger.³⁶

interface has moderate values, γ_L therefore depends only on dispersion and dipolar forces. These forces also determine the internal pressure of a liquid¹¹ $P_i = \delta_a^2 + \delta_p^2$, so eq. (9) is in fact a relation between internal pressure and surface tension.

On the other hand, in the expression for the *C.E.D.* ($C.E.D. = \delta_a^2 + \delta_p^2 + \delta_h^2 = \Delta E_{vap}/V_m$), δ_h cannot be omitted, since during evaporation of liquids toward dilute vapor, hydrogen bonds are being broken. Hence a relation between *C.E.D.* and γ_L , eq. (5), is not to be expected, unless $\delta_h = 0$.

Equation (9), of course, is not valid for polyfunctional alcohols which can form three-dimensional "networks" in bulk but not in the surface region. The other substances that deviate from eq. (9) have solubility parameters which are placed rather arbitrarily,¹³ especially the carboxylic acids and cyclic compounds.

The δ parameters of cyclic molecules, being assessed by solubility experiments on polymers, are even more uncertain; these molecules "exhibit enhanced interaction affinity compared to flexible aliphatic molecules, because they act to separate the polymer chains and thus reduce interchain forces."¹⁴

In view of the uncertainties in the solubility parameters,* especially in δ_p and δ_h , eq. (9) applied to all types of solvents is just as accurate in predicting γ_L values as the three Beerbower relations (6)–(8) for separate series of solvents.

The contribution of the dispersion forces is nearly the same in both approaches; generally this contribution is the most important one.

Equation (9) is applicable to substances with zero δ_p values (hydrocarbons) and to those with finite δ_p and δ_h values (polar molecules). This suggests that relations of the form

$$\delta_a^2 = A \left(\frac{1}{V_m} \right)^{1/3} \gamma_L^d \quad (10)$$

where γ_L^d = part of γ_L due to dispersion forces, and

$$\delta_p^2 = A \left(\frac{1}{V_m} \right)^{1/3} \gamma_L^p \quad (11)$$

where γ_L^p = part of γ_L due to dipole forces, might be valid.

For a check of these relationships, γ_L^d values have been determined by application of the homomorph concept: A homomorph is a hydrocarbon counterpart of the same size and shape, at the same reduced temperature $T_R = T/T_{critical}$ (T and T_{cr} in K).

From literature data on hydrocarbons,¹⁵ a homomorph chart for γ_L^d has been constructed (Fig. 2) which can be used for liquids that have simple linear saturated hydrocarbons as a homomorph. Knowing V_m and T_R of a substance, one can directly read γ_L^d from Figure 2. In Table II, the γ_L^d values found for several substances of this kind are shown, together with δ_a^2 values obtained from recent homomorph charts for δ_a .^{3,16} The equation obtained by least-squares analysis of data from Table II is (Fig. 1)

$$\delta_a^2 = 13.2 \left(\frac{1}{V_m} \right)^{1/3} \gamma_L^d \quad (12)$$

with a correlation coefficient 0.99 and standard error of estimate 3.5.

* See for a discussion on this matter reference 16. We have used Hansen's tables unless otherwise stated.

TABLE II
Dispersion Solubility Parameter, Dispersion Contribution
of Surface Tension, and Total Surface Tension of Solvents

Substance	δ_d^2	γ_L^d , dyne/cm	γ_L , dyne/cm
Methanol	60	16	22
Ethanol	60.4	17	22
<i>n</i> -Propanol	60.7	19	22.6
<i>n</i> -Butanol	60.7	20.5	23.4
Pentanol-1	61.9	22.4	25.6
Propylene glycol	67.5	23	72
Ethylene glycol	71.2	22	46.5
Butanediol-1,4	68.0	23.5	37.8
Ethyl lactate	62	22.5	28.8
Butyl lactate	61	24	
Diethylene glycol	63	21.5	48.5
Dipropylene glycol	68	25	
2-Butoxyethanol	62.0	23	27.4
Cellosolve	62	21	28.2
Diacetone alcohol	63	23	31
Methylcellosolve	63	20.5	
Diethyl ether	52.5	15.5	16.5
Methylal	57	17	21
Diethyl sulfide	61	20.5	24.5
Dimethylsulfoxide	88.8	27	42.8
Acetone	59	18	22.3
Methyl ethyl ketone	59.3	19	23
Ethyl acetate	57.8	18.5	23.0
Butyl acetate	58.5	22	25
Acetonitrile	64.3	19	27.6
Butyronitrile	65.7	21.5	25.84
Nitromethane	67.6	20.5	34.9
Nitroethane	65.8	21.5	32.13
Dimethylformamide	69.7	24	35.2
Dipropylamine	57.5	20.5	22.7
Diethylamine	56	17.5	19.4
Chlorobutane	59	19.4	

In view of the fair agreement between the value of the numerical constant in equations (9) and (12), one can conclude that

$$\delta_d^2 + \delta_p^2 = A \left(\frac{1}{V_m} \right)^{1/3} \gamma_L \quad (13)$$

where A is about 13.5 and also

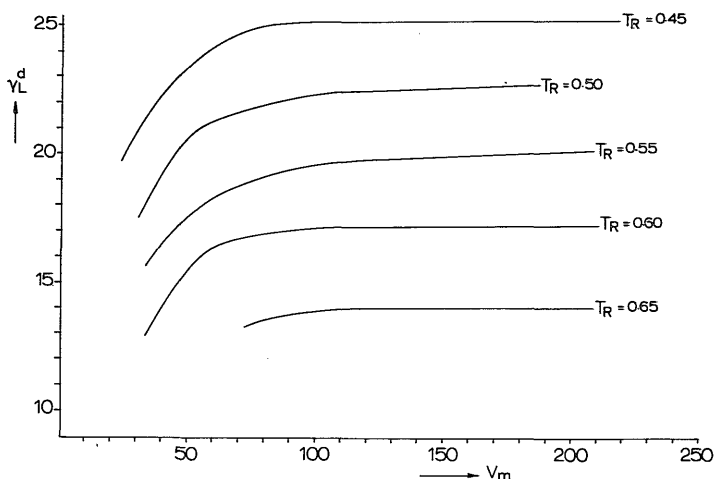
$$\gamma_L = \gamma_L^d + \gamma_L^p \text{ and } \gamma_L^h \approx 0 \quad (14)$$

for most substances.

Obviously, values of γ_L^d calculated by Panzer¹⁷ using

$$\gamma_L^d = 0.0715 V_m^{1/3} \delta_d^2 \quad (15)$$

agree with values found in this work, when the error of estimates are taken into consideration. With the establishment of eq. (12) we have shown that this calculation of γ_L^d is justified.

Fig. 2. Homomorph chart for determination of γ_L^d .

CALCULATION OF THE DISPERSION CONTRIBUTION WITH MOLAR ATTRACTION CONSTANTS

From tables of molar attraction constants of characteristic groups in molecules,¹⁸ it is possible to estimate the solubility parameter with the equation

$$\delta = \frac{\sum F_i}{V_m} \quad (16)$$

where F_i = molar attraction constant of a specific group i . Since Hansen⁴ has made a separation in contributions to the *C.E.D.*, one should expect the following relationships to hold:

$$\delta_d = \frac{\sum F_{id}}{V_m} \quad (17A)$$

$$\delta_p = \frac{\sum F_{ip}}{V_m} \quad (17B)$$

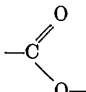

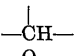
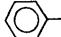
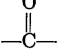
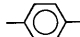
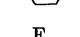
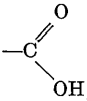
$$\delta_h = \frac{\sum F_{ih}}{V_m} \quad (17C)$$

where F_{id} , F_{ip} , F_{ih} are the molar attraction constants for dispersion-, dipole-, and hydrogen-bond forces, respectively.

Dispersion Contribution F_{id}

We have derived the molar attraction constants for the dispersion contributions F_{id} with the help of δ_d values taken from Hansen.^{4,5} Results are given in Table III. The constants appear to be truly additive, within the errors inherent to the determination of δ_d values by the homomorph concept and by solubility experiments as performed by Hansen (up to 1 Hildebrand unit in δ_d).¹⁶

TABLE III
 Molar Attraction Constants (Dispersion Contribution) F_{id}

Group	$F_{id}, \frac{\text{cal} \cdot \text{cc}^{1/2}}{\text{mole}}$	Group	$F_{id}, \frac{\text{cal}^{1/2} \cdot \text{cc}^{1/2}}{\text{mole}}$
—CH ₂ —	139		193
CH ₃ —	201	—N— H	70
—OH	99		800
	51		
	159		738
—C≡N	218		659
—NO ₂	215	F —C— F	160 ^a
	200		

^a van Krevelen.¹⁸

Polar Contribution F_{ip}

As an example of a polar group, the —OH alcohol group was chosen. The molar attraction constants calculated with δ_p 's appear to be of constant magnitude when only one —OH group is present in the molecule. When two or more of these groups are present in the same molecule, the contribution of each —OH group to the attraction constant F_{ip} —(OH) decreases considerably (Table IV).

This, of course, can be expected to depend on the distance and mutual orientation of the groups. Therefore it is not possible to define molar attraction constants for dipole forces when more than one polar group is present in the molecule.

 TABLE IV
 Molar Attraction of One-OH Group (Polar Contribution) F_{ip}

In substance	F_{ip} —OH, $\frac{\text{cal}^{1/2} \cdot \text{cc}^{1/2}}{\text{mole}}$
Methanol	244
Ethanol	232
<i>n</i> -Propanol	246
<i>n</i> -Butanol	256
<i>n</i> -Pentanol	248
2-Ethylbutanol-1	259
2-Ethylhexanol-1	251
1,3-Butanediol	218
Glycerol	145

Contribution of H-Bonds F_{ih}

The energy of a special type of hydrogen bond E_h can be taken as a constant,¹⁹ which may be different for different H-bonded compounds. For the energy of one —OH group, Hansen^{5,13} used 5000 cal/mole and he found

$$\delta_h = \sqrt{E_h \cdot A/V_m} = \sqrt{5000 A/V_m} \quad (18)$$

where A is the number of —OH groups in the molecule. Since $\Sigma F_{ih} = V_m \delta_h = \sqrt{V_m} 5000 A$, the molar attraction constant F_{ih} for a H-bonding group in a homologous series would depend on molar volume, which makes H-bonding contributions to F_i intractable. Equation (18) can be used, however, if the energies for different types of H bonds or acceptor/donor complexes are known.²⁰

We can conclude from this section that (a) the molar dispersion attraction constants $F_{i,d}$ (Table III) enable one to calculate δ_d for liquids and polymers; (b) since constant values for $F_{i,p}$ and $F_{i,h}$ cannot be defined, the prediction of the total solubility parameter δ from attraction constant contributions is of limited value.

RELATION BETWEEN INDEX OF REFRACTION (n_D) AND δ_d

Sewell²¹ has already searched for a relationship between the *C.E.D.* and the index of refraction. The main idea is that the interaction energy between non-polar molecules is dependent on the polarizability (London dispersion forces). The polarizability can, on the other hand, be described by the Lorentz-Lorentz equation:

$$\frac{4}{3} \pi N/V \alpha = \frac{n_D^2 - 1}{n_D^2 + 2} \quad (19)$$

where n_D = refractive index, N = number of molecules per cc, and α = average polarizability per molecule.

Sewell found a correlation between the *C.E.D.* and $(n_D^2 - 1)/(n_D^2 + 2)$ with *C.E.D.* values calculated from Small's tables.^{18,23} Using the separation of *C.E.D.* in three contributions, we expect a relationship between δ_d and n_D even for polar substances, in which relation the interference of polar and hydrogen bonding forces has vanished.

The right-hand side of eq. (19) is almost a linear function of n_D in the region of n_D values observed (n_D between 1.3 and 1.6). This is also true for n_D^2 (see Fig. 3) and therefore one of these functions can be used with equivalent results. The relation found to be valid here for the substances of Table V is

$$\delta_d = 9.55n_D - 5.55 \quad (20)$$

with correlation coefficient 0.90 and standard error of estimate 0.32. This relation resembles very much the relationships found by Papazian²² and by Holmes²³ between the surface tension and the dielectric constant or the square of the index of refraction.

Equation (13) suggests that a factor $V_m^{1/6}$ might occur in eq. (20). This dependence on V_m has not been evaluated in this study because of the minor importance of this factor in the range of molar volumes studied. For more accurate studies, however, incorporation of this dependence of V_m might be recommendable.

TABLE V
 Index of Refraction, Dipole Moment, and Related Solubility Parameters for Solvents

Substance	Index of refraction n_D^a	Dispersion solubility par. δ_2^b	Dipole moment μ (D) ^c	Polar solubility par. δ_p^d
Methanol	1.32840	7.42	1.70	6.0
Ethanol, 99.9%	1.36140	7.73	1.69	4.3
<i>n</i> -Propanol	1.38556	7.75	1.68	3.3
<i>n</i> -Butanol	1.3993	7.81	1.66	2.8
Pentanol-1	1.4100	7.81	1.7	2.2
Propylene glycol	1.4329	8.24	2.25	4.6
Ethylene glycol	1.4318	8.25	2.28	5.4
Cyclohexanol	1.46477	8.50	1.86	2.0
Ethyl lactate	1.4124	7.80	2.4	3.7
2-Butoxyethanol	1.41980	7.76	2.08	3.1
Oxitol (Cellosolve)	1.4077	7.85	2.08	4.5
Diacetone alcohol	1.4235	7.65	3.24	4.0
Diethyl ether	1.35243	7.05	1.15	1.4
Furan	1.42140	8.43	0.71	0.9
Dioxane	1.42241	8.55	0.45	0.9
Methylal	1.35335	7.35	0.74	0.9
Carbon disulfide	1.62799	9.97	0.06	0
Dimethylsulfoxide	1.4783	9.00	3.9	8
γ -Butyrolactone	1.4348	9.26	4.12	8.1
Acetone	1.35868	7.58	2.69	5.1
Acetophenone	1.53423	8.55	2.69	4.2
Tetrahydrofuran	1.40716	8.22	1.75	2.8
Ethyl acetate	1.37239	7.44	1.88	2.6
<i>n</i> -Butyl acetate	1.3900	7.67	1.84	1.8
Isoamyl acetate	1.4007	7.45	1.82	1.5
Acetonitrile	1.34411	7.50	3.44	8.8
Butyronitrile	1.3838	7.50	3.57	6.1
Nitromethane	1.38118	7.70	3.56	9.2
Nitroethane	1.39193	7.80	3.60	7.6
2-Nitropropane	1.39439	7.90	3.73	5.9
Aniline	1.58628	9.53	1.51	6.0
Nitrobenzene	1.5500	8.60	4.03	6.0
Dimethylformamide	1.43047	8.52	3.86	6.7
Dipropylamine	1.4043	7.50	1.03	0.7
Diethylamine	1.3854	7.30	1.11	1.1
Morpholine	1.4542	8.89	1.50	2.4
Cyclohexylamine	1.45926	8.35	1.26	1.5
Pyridine	1.51016	9.25	2.37	4.3
Carbon tetrachloride	1.4600	8.65	0	0
Chloroform	1.4460	8.65	1.15	1.5
Ethylene chloride	1.4448	8.50	1.86	2.6
Methylene chloride	1.42416	8.52	1.14	3.1
1-1,1-Trichloroethane	1.4379	8.25	1.57	2.1
1-Chlorobutane	1.4021	7.95	1.90	2.7
Trichloroethylene	1.4767	8.78	0.8	1.5
Chlorobenzene	1.52481	9.28	1.54	2.1
<i>o</i> -Dichlorobenzene	1.55145	9.35	2.27	3.1
α -Bromonaphthalene	1.6580	9.94	1.29	1.5
Benzene	1.50112	8.95	0	0.5
Toluene	1.49693	8.82	0.31	0.7
Xylene	1.49722	8.65	0.45	0.5

(continued)

TABLE V (continued)

Substance	Index of refraction n_D^a	Dispersion solubility par. δ_d^b	Dipole moment μ (D) ^c	Polar solubility par. δ_p^d
Ethylbenzene	1.49588	8.70	0.37	0.3
Styrene	1.54682	9.07	0.13	0.5
Tetralin	1.54135	9.35	0.60	1.0
Hexane	1.37486	7.24	0.085	0
Cyclohexane	1.426223	8.18	0	0
Acetic acid	1.3719	7.10	1.68	3.9
Formic acid	1.37140	7.00	1.82	5.8
Butyric acid	1.3980	7.30	1.65	2.0
Benzaldehyde	1.5455	9.15	2.77	4.2

^a Values from Riddick and Bunger³⁶ and *Handbook of Chemistry and Physics*.³⁷

^b Values from Hansen.^{5,13}

^c Values from Riddick and Bunger³⁶ and McClellan.²⁵

^d Values from Hansen.^{5,13}

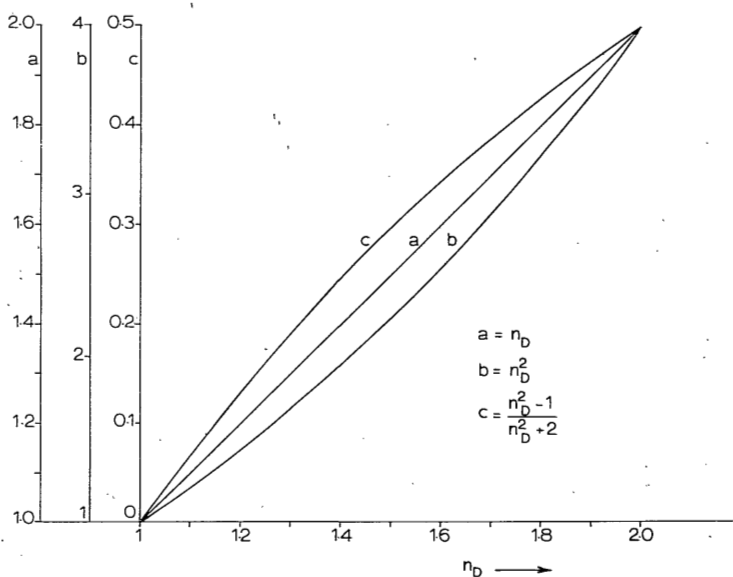


Fig. 3. Some functions of n_D .

RELATION BETWEEN THE DIPOLE MOMENT (μ) AND δ_p .

In order to calculate the contribution of permanent dipoles to the cohesive energy density, Hansen⁵ has used the formula proposed by Böttcher²⁴:

$$\delta_p^2 = \frac{12108}{V_m^2} \frac{\epsilon - 1}{2\epsilon + n_D^2} (n_D^2 + 2)\mu^2 \tag{21}$$

where ϵ = dielectric constant and μ = dipole moment.

Another, and more simple empirical relationship has been proposed by Beerbower:¹⁶

$$\delta_p = A' \frac{\mu}{V_m^{1/2}} \quad (22)$$

When the statistical thermodynamical derivation of Bonn and van Aartsen⁹ is used, including the Keesom potential for dipole-dipole interaction (which in fact is not justified),¹² the following relation can be found:

$$\delta_p = A'' \frac{\mu^2}{V_m^{3/2}} \quad (23)$$

Empirically we found a linear relationship between δ_p and the square root of the right-hand side of eq. (23):

$$\delta_p = A''' \frac{\mu}{V_m^{3/4}} \quad (24)$$

When δ_p values are taken from Hansen,^{5,14} we found for 59 solvents (Table V)

$$\delta_p = 50.1 \frac{\mu}{V_m^{3/4}} \quad (24a)$$

with a correlation coefficient 0.99 and a standard error of estimate 0.38. For the relation of Beerbower, eq. (22), these solvents give

$$\delta_p = 18.3 \frac{\mu}{V_m^{1/2}} \quad (22a)$$

with a correlation coefficient 0.97 and a standard error of estimate 0.50. We may conclude here that either of the relations (24a) or (22a) can be used to calculate δ_p values.

APPLICATION TO POLYMERIC SYSTEMS

Applying the relations found in the preceding sections to polymeric systems⁸ we have been able to predict δ_d values for polymers from n_D and F_{id} data, respectively. If the dipole moment of the polymer is known, we are able to predict δ_p of the polymer also. Furthermore, since a particular type of hydrogen bond appears to have a constant energy, we can calculate δ_h from this energy and the molar volume of a segment, using eq. 18.

Dispersion Contribution to the *C.E.D.* for Polymers from F_{id} and n_D

In Table VI, the δ_d values for several polymers are given, calculated from F_{id} , eq. (17a), and from n_D , eq. (20). As can be seen from the table, δ_d values for polymers with polar groups attached to the phenylene ring like in poly(2,6-dimethyl-1,4-phenylene oxide) have not been included in the calculations from F_{id} . There were not enough δ_d values of low molecular weight analogs available to incorporate the effect of the phenylene ring on the additive value F_{id} for an attached polar group. A shift to somewhat higher F_{id} values is expected, as is the case for the additive constants for the molar refraction (R), calculated by Goedhart.²⁵

TABLE VI
Solubility Parameters and Other Physical Properties of Polymers

Polymer	n_D	$\mu(D)$	V_{m_2}	γ^d	δ_d from F^{id} eq. (17a)	δ_d from n_D , eq. (20)	δ_p from μ , eq. (24a)	δ_h from eqs. (18), (27)
Polyethylene	1.483	0 ^b	32.8	35	8.47	8.61	0	0
Polystyrene	1.591	0.26 ^c	99	44	9.37	9.64	0.42	1.0
Poly(tetrafluoroethylene)	1.298 ^a	0 ^d	50	19.5	6.2	6.84	0	0
Polyacrylonitrile	1.514	2.75 ^d	44.8	—	9.11	8.91	7.9	3.3
Poly(2,6-dimethyl-1,4-phenylene oxide)	1.567	0.88 ^d	111.7	—	—	9.41	1.3	2.4
Poly(methyl methacrylate)	1.490	1.30-1.90 ^c	85.6	50.5 ^b	8.57	8.68	± 2.8	3.8
Nylon 6.6	1.530	2.8 ^d	211.5	—	—	9.06	± 2.5	6.0
Poly(vinyl chloride)	1.539	1.67-1.75 ^c	45.1	—	—	9.15	4.9	1.5
Poly(ethylene terephthalate)	1.580	1.44 ^d	144.5	53 ^b	—	9.54	1.7	4.2

^a Calculated with additive constants from molar refraction as proposed by Goedhart.²³

^b Private communication, Bargeman.²⁴

^c From McClellan.²⁴

^d Estimated; 80% of corresponding monomer value.

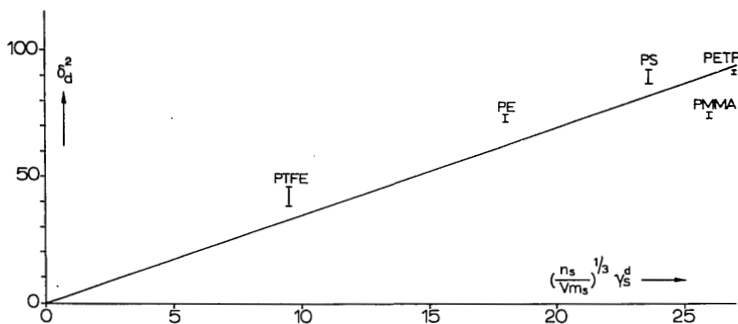


Fig. 4. Relation between dispersion part of the surface tension and the solubility parameters for polymers.

Relation Between δ_d^2 and γ_s^d for Polymers

In the case of polymers, the molar volume derivations based on spherical molecules are not valid, and therefore one cannot use the factor $(1/V_m)^{1/3}$ from eq. (5). Wu²⁷ has proposed an approach for polymers in which he used an effective cross-sectional area to obtain the factor between the *C.E.D.*, calculated with attractive constants,²⁸ and the γ_c value of Zisman.²⁹ Equation (5) then becomes

$$C.E.D._s = A \left(\frac{n_s}{V_{ms}} \right)^{1/3} \gamma_c \quad (25)$$

where *C.E.D.*_s = *C.E.D.* of a segment, $V_{ms} = V_m$ of a segment, and n_s = number of atoms in a segment.

The *C.E.D.* values calculated by Wu, using the attractive constants of Small,²⁸ do not represent true dispersion contributions; neither are the values of the critical surface tensions for polar polymers based on dispersion contributions.³⁰ Therefore, the relation we propose for polymers must be analogous to eq. (10) and reads

$$\delta_d^2 = A \left(\frac{n_s}{V_{ms}} \right)^{1/3} \gamma_s^d \quad (26)$$

where γ_s^d is the dispersion contribution part of the free surface energy of the polymer. Values of γ_s^d are known for nonpolar polymers,³¹ and in two cases immersion calorimetry has been performed on polar polymers to obtain λ_s^d values.³⁴

In Figure 4, a graphic representation of eq. (26) is given, where values of Table VI have been used. The constant *A* found by least-squares fitting has the value 3.4; because of a different geometric factor, this constant deviates from the one found in eq. (12). The correlation is good, but more data are necessary and we hope that they will become available soon.

Polar Contribution to the *C.E.D.* for Polymers, δ_p

The measured average dipole moments of polymers²⁶ are generally 70–90% of the dipole moments of the corresponding monomer unit. For polymer μ values not to be found in the literature, we have estimated the dipole moment at 80% of the dipole moment of the monomer.

The δ_p 's calculated with eq. (24a) are given in Table VI.

The Hydrogen-Bonding Parameter δ_h for Polymers

It is argued above that the energy for a hydrogen bond should be known in order to make an estimate of δ_h . The energy for the H bond in alcohols has been given as 5 kcal/mole. For the energy of the amide H bond, we have used the value of 3.9 kcal/mole given by Pimentel and McClellan.¹⁹

For esters, nitriles, monochloro, ether, and cyclic compounds, we have used values of E_h compiled by Beerbower and Hansen:²⁰

$$E_h = \delta_h^2 V_m \quad (27)$$

E_h = enthalpy of an H bond or donor/acceptor group

—ester group	about 1250 cal/mole
—nitrile group	about 500 cal/mole
—ether group	about 550 cal/mole
—monochloro substituent	about 100 cal/mole
—phenylene ring	about 100 cal/mole

The results of calculations of δ_h for some polymers, using the above E_h values of H bond types are given in Table VI.

DISCUSSION

In the foregoing sections, we have discussed relations between solubility parameters and other physical properties, and the possibility of determining the solubility parameters with additive constants. From the relations established, it is possible to determine the solubility parameters (δ_p , δ_d , δ_h) for solvents and polymers. Especially for the latter group of substances, this is a very important result, because otherwise time-consuming determinations (solubility or swelling experiments) must be made.

We have demonstrated that only the dispersion contribution to the *C.E.D.* can be calculated with a molar attraction constant. The values of F_{id} which we found for $-\text{CH}_3$ and $-\text{CH}_2-$ equal those reported by Allen, Gee, and Wilson³² for *n*-alkanes. The value of δ_d for polyethylene calculated with these values also compare quite well with the value obtained by extrapolation of the δ_d of *n*-alkanes to infinite chain length.³² The literature values for F_t ¹⁸ used in the calculation of the total solubility parameter always represent some kind of compromise, especially when hydrogen bonds occur. The solubility parameters calculated with these values can be considered as highly approximate only. For nonpolar substances, these δ values are apparently too low. Our solubility parameter components (δ_d , δ_p , δ_h) for polymers have been calculated from relationships based on solvent data of Hansen. Therefore, it is better to compare our values with his.³³

This is possible by making plots of solubility spheres similar to those Hansen used to obtain his values. Because δ_d values especially cover only a narrow range ($\delta_d \approx 7-10$), the solubility spheres are usually occupied only for a small part by coordinates (δ_d , δ_p , δ_h) of solvent solubility parameters. It is therefore possible to envelope these points by a solubility sphere with different center coordinates (δ_d , δ_p , δ_h of the polymer) and a different radius. When the radius increases, the center coordinates must shift in the direction of the empty part of the solubility sphere.

Although the polymer solubility parameters given by Hansen³³ can therefore be only approximate, his method of plotting can be used to check polymer δ values obtained in different ways: these values have to be the center of a solubility sphere which envelopes the coordinates of the solvents in which the polymer is soluble, and which excludes the coordinates of the nonsolvents. The values given in Table VI satisfy this condition.

The difference between δ_d from F_{id} and from n_D in Table VI is within the confidence limit of twice the standard error of estimate (~ 0.6 Hildebrand).

Although solubility parameters are a very helpful instrument to estimate polymer swelling and solubility, it should be emphasized that they reflect the attractive forces in the pure substances only. Interactions not expected by combining separate δ -parameter values may arise, especially so for hydrogen bonds.

Chen⁶ has shown that upon mixing, the dispersion and dipolar forces can be taken together to one parameter χ_H and that the hydrogen-bonding forces need to be taken into consideration separately. Donor-acceptor complexes are known to be formed when an electron donor group can come into contact with an acceptor group. In a pure substance which is of electron-donating type, δ_h may be small. When, however, this substance is mixed with a substance which is electron accepting (also δ_h small), strong hydrogen bonds will be the result.

We feel that these shortcomings of the solubility parameter theory can be overcome if it becomes possible to extend Drago's³⁵ theory for the prediction of the enthalpy of donor-acceptor complexes to solvent and polymer-solvent mixtures.

The authors are indebted to Dr. D. Bargeman for many enlightening discussions during the preparation of this manuscript.

References

1. J. H. Hildebrand, and R. L. Scott, *The Solubility of Non-Electrolytes*, 3rd ed., Dover, New York, 1949.
2. R. F. Blanks and J. M. Prausnitz, *Ind. Eng. Chem., Fundam.*, **3**, 1 (1964).
3. R. F. Weimer and J. M. Prausnitz, *Hydrocarbon Process. Petrol. Refiner*, **44**, 237 (1965).
4. C. M. Hansen, *J. Paint Technol.*, **39**, 104 (1967).
5. C. M. Hansen and K. Skaarup, *J. Paint Technol.*, **39**, 511 (1967).
6. S. A. Chen, *J. Appl. Polym. Sci.*, **15**, 1247 (1971).
7. A. S. Michaels, *A.S.T.M. Technical Publication*, **340**, 3 (1963).
8. R. E. Cuthrel, *Polym. Preprints*, **11**(2), 488 (1970).
9. R. Bonn and J. J. van Aartsen, *Eur. Polym. J.*, **8**, 1055 (1972).
10. A. Beerbower, *J. Colloid Interfac. Sci.*, **35**, 126 (1971).
11. E. B. Bagley, T. P. Nelson, and J. M. Scigliano, *J. Paint Technol.*, **43**, 35 (1971).
12. J. C. Melrose, *J. Colloid Interfac. Sci.*, **28**, 403 (1968).
13. C. M. Hansen, Dissertation, Danish Technical Press, Copenhagen, 1967.
14. J. L. Varsano and S. G. Seymour, *J. Pharm. Sci.*, **62**, 92 (1973).
15. A. P. I. Selected Values of Properties of Hydrocarbons and Related Compounds, Texas A & M University, Texas, 1971.
16. A. Beerbower and J. R. Dicky, *A.S.L.E. Trans.*, **12**, 1 (1969).
17. J. Panzer, *J. Colloid Interfac. Sci.*, **44**, 142 (1973).
18. D. W. van Krevelen, *Properties of Polymers*, Elsevier, Amsterdam, 1972.
19. A. McLellan and G. Pimentel, *The Hydrogen Bond*, Freeman, San Francisco, 1960.
20. C. M. Hansen and A. Beerbower, *Encyclopedia of Chemical Technology*, Supplement Volume 1971, Wiley, New York 1971, p. 889.
21. J. H. Sewell, R. A. E. Technical Report No. 66185, June 1966.

22. H. A. Papazian, *J. Amer. Chem. Soc.*, **93**, 5634 (1971).
23. C. F. Holmes, *J. Amer. Chem. Soc.*, **95**, 1014 (1973).
24. C. F. Böttcher, *The Theory of Electric Polarisation*, Elsevier, Amsterdam, 1952.
25. D. J. Goedhart, Communication Gel Permeation Chromatography International Seminar, Monaco, Oct. 12-15, 1969.
26. A. L. McClellan, *Tables of Experimental Dipole Moments*, Freeman, San Francisco, 1963.
27. S. Wu, *J. Phys. Chem.*, **72**, 3332 (1968).
28. P. A. Small, *J. Appl. Chem.*, **3**, 71 (1953).
29. W. A. Zisman, in *Adhesion and Cohesion*, J. Weiss, Ed., Elsevier, Amsterdam, 1962.
30. W. R. Good, *J. Colloid Interfac. Sci.*, **44**, 63 (1973).
31. F. M. Fowkes, *Ind. Eng. Chem.*, **56**(12), 40 (1964).
32. G. Allen, G. Gee, and G. J. Wilson, *Polymer*, **1**, 456 (1960).
33. C. M. Hansen, *J. Paint Technol.*, **39**, 505 (1967).
34. D. Bargeman, private communication.
35. R. S. Drago, *Structure and Bonding*, Vol. 15, Coordinative Interactions, Berlin, 1973.
36. J. A. Riddick and W. B. Bunger, *Organic Solvents*, Wiley-Interscience, New York, 1970.
37. R. C. Weast, *Handbook of Chemistry and Physics*, 48th ed.

Received April 16, 1974

Revised August 13, 1974

Phase Separation Phenomena During the Formation of Asymmetric Membranes

D. M. KOENHEN, M. H. V. MULDER,* and C. A. SMOLDERS, *Twente University of Technology, Enschede, The Netherlands*

Synopsis

The formation of membranes from two systems has been studied. In the system polyurethane-dimethylformamide-water, the mechanism for the formation of the sponge-like structure proves to be a liquid-liquid phase separation with nucleation and growth of the diluted phase. This mechanism has been confirmed for the system modified polystyrene-polyisoprene-polystyrene/*o*-dichlorobenzene/(methanol-water). Crystallization and gelation is discussed. The membranes prepared showed hyperfiltration activity. The mechanism proposed here is believed to be valid for other systems, too.

INTRODUCTION

Loeb and Sourirajan¹ were the first to develop a method for preparing asymmetric ("high flux") membranes for the application of desalination by reverse osmosis. These membranes consist of an extremely thin selective layer (0.1-0.2 μm) backed by a porous substructure in which sometimes finger-like cavities can be present. In principle, these asymmetric membranes were obtained by the following procedure: After casting a solution of cellulose acetate (CA) on a glass plate, the volatile solvent (acetone) was allowed to evaporate for a short time, followed by immersion in a precipitating agent (for instance, water). Heat treatment of the final membrane will improve the salt rejection.

Many investigations have been dedicated to elucidate the formation mechanisms of the asymmetric structure of the membranes. These investigations cover roughly the following approaches: (1) An explanation is given of the phase transition, or phase inversion, during the formation of the membrane structure. (2) An explanation for the final asymmetric structure is brought in relation to physical quantities of the materials used and the conditions in which the membranes are prepared.

In the first group of investigations, several authors explained the formation of the sponge-like structure in a way very similar to the colloidal demixing theory described by Bungenberg de Jong.² To this group of authors belong Maier and Scheuermann,³ Keilin,⁴ and Kesting.⁵ In the mechanism described, spherical droplets or micelles are formed in which the mass of the polymer molecules is concentrating at the exterior surfaces. Subsequently, the micelles will contact each other and form polyhedra. The process is completed by further polymer

* Present address: Wafilin B. V., Hardenberg, The Netherlands.

desolvation, syneresis, and capillary depletion. Strathmann, Scheible, and Baker,⁶ making use of ternary phase diagrams, described how the polymer-rich phase separates from a supersaturated solution to form spherical solid droplets, which can grow and agglomerate to form an interconnected solid structure. In a later report, Strathmann et al.⁷ revised this mechanism in such a way that the precipitated polymer-rich phase remains fluid for some time and agglomerates to form finally a solid polymer matrix.

In the second group of investigations, Frommer and Lancet⁸ and Strathmann et al.⁷ have related the final asymmetric structure to the rate of precipitation. When the rate of precipitation is low, a sponge-like structure will be obtained. These authors also studied the formation of finger-like cavities which are often found in asymmetric membranes. They concluded that the formation of finger-like cavities, growing in the fluid layer, is generally associated with a high rate of precipitation.

Matz⁹ explained the formation of finger-like cavities on the basis of changing surface tension during the coagulation step. The surface tension of the polymer-rich phase increases through loss of the solvent, while the surface tension of the aqueous phase will decrease. At the point where these surface tensions are equal, the interface is very sensitive to distortion and cavity formation is easily initiated. Growth can occur through diffusion of the solvent into these cavities.

Another explanation was proposed by Strathmann et al.⁷ who stated that the homogeneous skin layer cracks through shrinkage of the polymer-rich phase and cavities can develop. Growth of cavities proceeds by shrinkage of the polymer matrix which is caused by inflow of nonsolvent.

Much the same type of coagulation process which occurs during the formation of asymmetric membranes is encountered during the wet-spinning process of synthetic polymer fibers. The presence of finger-like cavities in the fibers has been reported, for instance, for wet-spun acrylic fibers^{10,11} and for nylon 6 and polyurethane.¹²

According to Gröbe et al.¹¹ the mass transfer will be favored in places of the polymer-poor phase. The number of these places is given by statistical distribution. The phase separation front will move faster in these places because of the faster exchange of solvent and nonsolvent. Because there is nonsolvent present in the polymer-poor dilute phase, solvent can reduce its chemical potential by diffusing into it.

Eventually, the cavity will contain so much of the solvent that the composition is below the precipitation threshold. Coagulation at the boundary of the cavity will then be retarded. Solvation of the polymer molecules in the solution, just outside the cavity, is lowered by diffusion of the solvent into the cavity. Therefore, transfer of the polymer will occur to surrounding places by creep; eventually, complete desolvation will take place.

In this paper, we will report on experiments done in our laboratory to obtain more information concerning the phase separation involved in the membrane formation. Originally, this work was started to provide insight in the coagulation process as a part of a program on wet-spun fibers. Later, it appeared to us that it would also be applicable to the processes occurring during the formation of asymmetric membranes. The demixing process will be discussed taking the line of the thermodynamics and kinetics of phase equilibria in polymer solutions.

THEORETICAL CONSIDERATIONS

Liquid-Liquid Phase Separation

The Gibbs free enthalpy of mixing of a polymer and a solvent can be described with the Flory-Huggins equation¹³ which is expressed here in weight fractions:

$$\frac{\Delta G_m}{RT} = w_0 \ln w_0 + \sum_i \frac{M_0}{M_i} w_i \ln w_i + g \sum w_i \cdot w_0 \quad (1)$$

in which ΔG_m = free enthalpy of mixing, R = universal gas constant, T = absolute temperature, w_0 = weight fraction of solvent, w_i = weight fraction of polymer species i , M_0 = molecular weight of the solvent, M_i = molecular weight of the polymer species i , and g = empirical correction factor. The first two terms on the right-hand side of eq. (1) give the entropy of mixing. This entropy is small compared with the mixing of low molecular weight substances through the factor

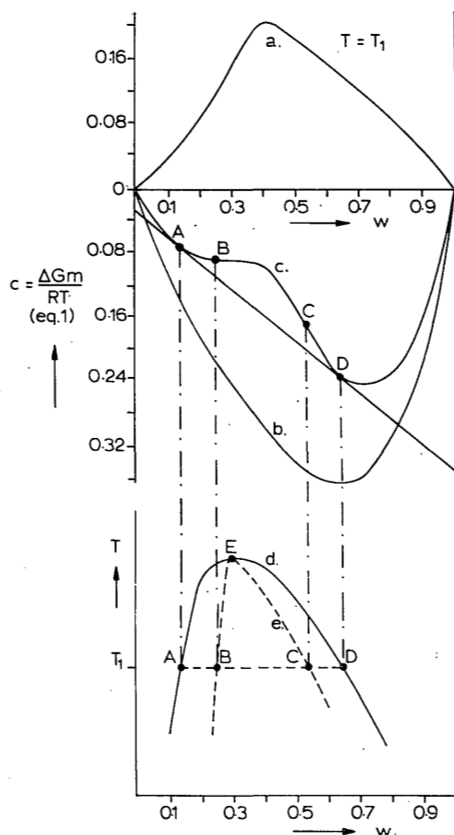


Fig. 1. Schematic representation of the free enthalpy components given by eq. (1) and the corresponding phase diagram for a binary system with liquid-liquid phase separation: curve a, $g \sum w_i w_0$; curve b, $w_0 \ln w_0 + \sum_i (M_0/M_i) w_i \ln w_i$; curve c, $\Delta G_m/RT$; curve d, cloud point curve, curve e, spinodal.

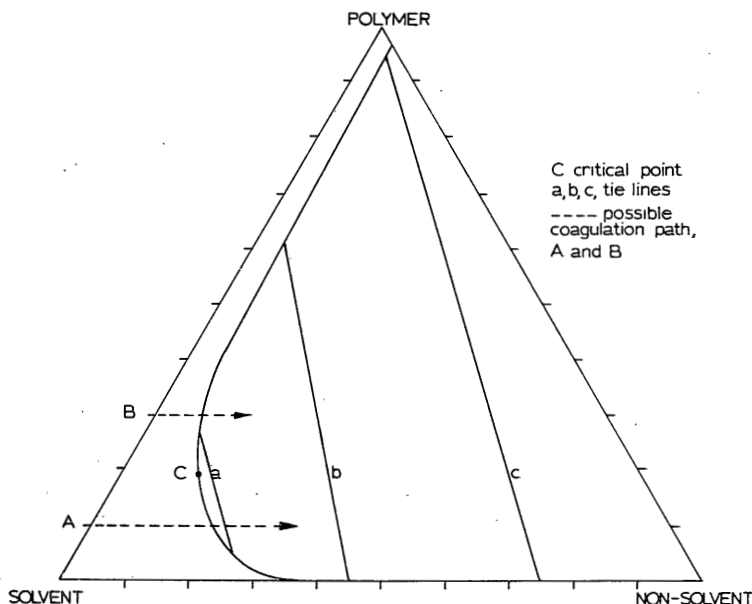


Fig. 2. Schematic phase diagram for a ternary system.

M_o/M_i . Because this entropy of mixing is small, a small endothermic enthalpy of mixing or some other nonideality, together represented by the positive term $g \sum w_o w_i$, can cause a phase separation.

The situation in such a case is given schematically in Figure 1, where points A and D are the common tangents of the ΔG_m curve. These concentrations A and D have identical chemical potentials and form phases in equilibrium. The points B and C are the points of inflection of the G_m curve. Any composition between points A and D can lower its free enthalpy of mixing by separating into phases of compositions A and D. Lines connecting the compositions of the coexisting phases (A-D, etc.) are called tie lines. At point E, the compositions are the same and the tie line is a point, the critical point. Compositions between A and B on one side of the demixing region and C and D on the other side are metastable and only give demixing when a nucleus is formed having a composition which is close enough to the composition at the other end of the demixing gap. These nuclei grow further until a complete demixing into phases A and D has taken place. This mechanism is called nucleation and growth.

The compositions between the points of inflection B and C are unstable to the very small fluctuations which are always present. Such compositions would give instantaneous demixing, the so-called spinodal demixing. This type of demixing, however, is difficult to obtain in fluid systems because in most cases nucleation and growth will occur in passing the metastable region.

In a system which is composed of a polymer and one or more solvents and nonsolvents, which is the case in membrane preparation, there are more degrees of freedom. The phase diagram of a ternary system consisting of a polymer, a

solvent, and a nonsolvent is most conveniently given by the so-called isothermal sections (Fig. 2). When a polymer solution is coagulated with a nonsolvent as in membrane preparation, we can assume that after the initial skin formation, the overall polymer concentration in the membrane is constant, while the concentration of solvent decreases and that of nonsolvent increases.

In a system as illustrated in Figure 2, a solution of, say, 10% polymer passes the border of the two-phase region at the diluted side of the critical point, whereas a solution of 30% enters this region at the opposite side of the critical point. In the first case, nuclei of the concentrated phase will be formed with a large difference in composition from the original solution, and the diluted phase will change continuously in composition, getting more and more dilute. In the latter case, nuclei of the diluted phase will be formed while the concentrated phase can change continuously. Thus, in nucleation and growth, we have two possibilities: (A) nucleation and growth of the concentrated phase, and (B) nucleation and growth of the diluted phase

The consequences for the morphology in the final coagulated polymer solution are obvious. In case A, one expects spheres of the concentrated phase dispersed in a dilute solution. In case B, one expects spheres of a dilute solution surrounded by concentrated polymer solution matrix. When the precipitation process has come to an end, the concentration of polymer in the concentrated phase has become very high, i.e., the polymer has solidified and the following morphologies can exist: In case A, a latex is obtained which in principle has no mechanical strength. Through coalescence or sticking of the polymer spheres, an open-pore structure can be obtained which could have some strength. In case B, spherical cells will be formed.

Crystallization

Crystallization is another type of phase separation which is possible in solutions of macromolecules. From dilute solutions, some polymers can crystallize in the form of lamellar single crystals being about 100 Å thick and often many microns in the lateral directions. In these crystals, the polymer chains are oriented normal to be plane of the lamella and are arranged in a folded manner.¹⁶ From concentrated solutions, more complicated crystal structures can be obtained, reminiscent of the familiar spherulites obtained by crystallization from the melt. The melting points of these crystallites can be described qualitatively by the Flory melting point depression theory.¹³

When the concentration is high or when the crystallites are small, many links between different polymer molecules are formed, and a homogeneous but cloudy gel can be obtained. These gels are thermoreversible, and the melting points can also be described by the Flory theory.¹⁷ The gel structure is thought to be composed of the familiar fringed micelles. Often, the formation of helices is involved in the crystallization and gelling process.^{18,19,20} Gelation can also occur in solutions of the well-known membrane material cellulose acetate.²¹ These considerations will be of importance for the solidification (gelation) of concentrated polymer regions in membranes, like the "skin" at the surface of the membrane, or the concentrated polymer phase which forms the matrix in the porous part of the membrane.

EXPERIMENTAL

Materials

Two different types of membranes have been prepared: (a) from polyurethane (PU) (Estane 5701 F1), and (b) from a modified polystyrene-polyisoprene-polystyrene (SIS) block copolymer (CARIFLEX TR 1108). All of the solvents used were of analytical grade.

Cloud Points

Cloud points were determined in well-homogenized PU solutions. Homogeneous mixtures of polyurethane-dimethylformamide were prepared by the method also used by Van Emmerik and Smolders.²²

The appropriate amounts were weighed in small Pyrex glass tubes which were degassed, flushed with nitrogen, degassed again, and sealed under vacuum at liquid nitrogen temperature. The sealed glass tubes were heated, if necessary, in an oil bath to approximately 80°C for at least 24 hr in order to obtain homogeneous liquid mixtures.

Phase separation points were usually determined by cooling or heating the thermostat bath 1°C every hour or 1°C every 10 min.

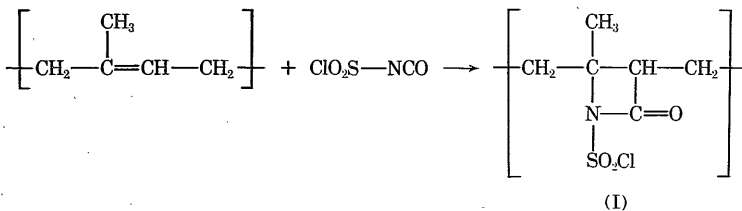
Optical Microscope Studies

The phase separation of polyurethane was examined with a Olympus EH microscope. A drop of polymer solution is placed between two microscope slides. By means of a hypodermic syringe, water is placed near the edge. Photographs are taken of the interface at certain time intervals.

Membrane Preparation

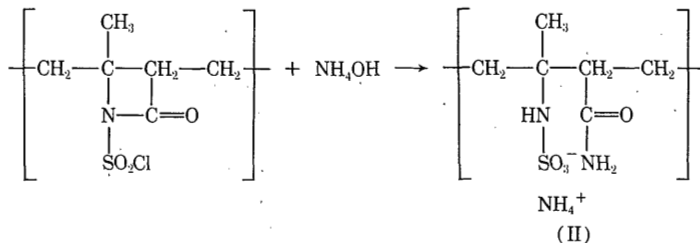
PU Membranes. PU membranes were prepared from 15–30% polyurethane solutions in DMF. The solution was cast on a glass plate and, after a short evaporation time, immersed in a coagulation bath. Water and different ratios of DMF/water solutions were used as precipitation media.

Ionic Membranes. These were prepared from polystyrene-polyisoprene-polystyrene (SIS) block copolymer which was modified as follows.²³ To a 10% SIS solution in toluene, N-chlorosulfonyl isocyanate (NCSI) was added at room temperature. Below, the reaction of the polyisoprene middle block with NCSI is shown schematically:



The molar ratio of NCSI added to isoprene was 60%. After isolation of the product, the polymer was dissolved in 1,2-dichlorobenzene.

A 15% solution of compound I in 1,2-dichlorobenzene was cast on a glass plate. After a certain evaporation time, the cast polymer was immersed into a water/methanol (20/80) bath. In order to prevent extensive swelling, crosslinks were introduced by immersing the membrane in a 2% hexamethylenediamine solution in toluene at room temperature. In a final step, the membrane was modified by immersing it at room temperature in a concentrated (4M) ammonia solution in which hydrolysis occurs, giving polymer II:



Scanning Electron Microscope Studies

Cross sections of the membranes were examined with a JEOL-JSM U3 scanning electron microscope (SEM). Samples were prepared by cryogenic breaking followed by freeze drying (or etching) and coating the sample with a charge-conducting layer according to a technique developed earlier.¹²

Hyperfiltration Experiments

Hyperfiltration experiments were carried out in a stirred Amicon high-pressure cell, Type 420, at an operating pressure of 40 atmospheres. In each experiment, a 3000 ppm NaCl solution was used as feed solution. The concentrations in feed and product were determined by specific resistance measurements using a conductivity cell.

RESULTS

In the quasi-ternary system of polyurethane-dimethylformamide-water, quasi-binary sections were chosen for which the following phase transitions were studied.

Liquid-Liquid Phase Separation

In the first place, a range of polymer solutions with a constant ratio of dimethylformamide-water were studied. When a homogeneous solution is cooled, cloudiness appears at a certain temperature. The appearance of the cloudiness is not dependent on the rate of cooling; and when the solution is centrifuged, two liquid layers can be obtained in the tube. By heating the phase-separated solution, the system becomes homogeneous again at the same temperature. Hence, a liquid-liquid phase separation is obtained in these experiments. The cloud

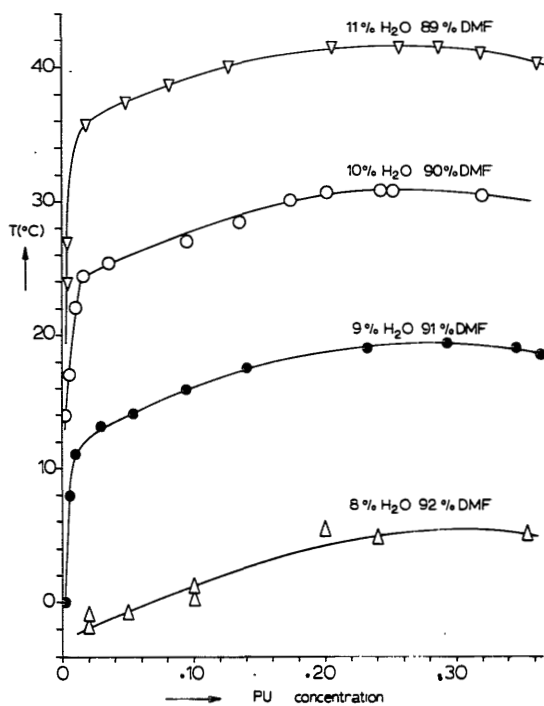


Fig. 3. Cloud point curves in the system PU/DMF/H₂O.

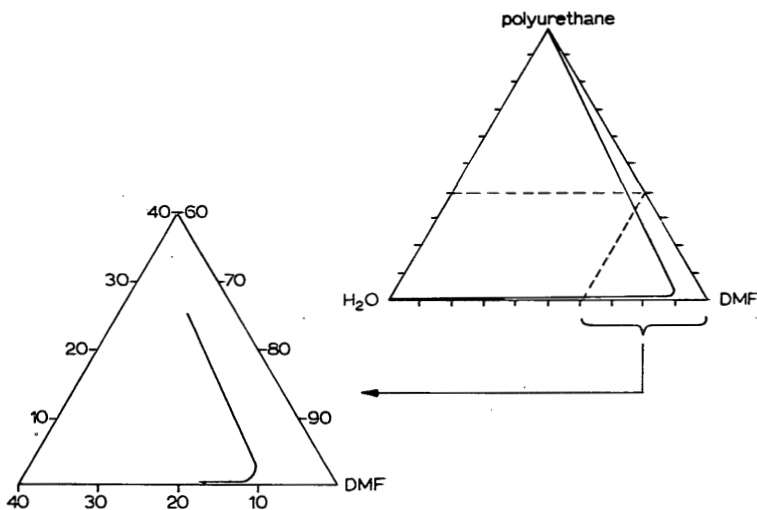


Fig. 4. Ternary diagram for PU/DMF/H₂O at 20°C.

point curves obtained for several quasi-binary sections (this means different ratios of dimethylformamide–water as solvent) are given in Figure 3. In Figure 4, these data have been plotted in a ternary diagram for one temperature (25°C).

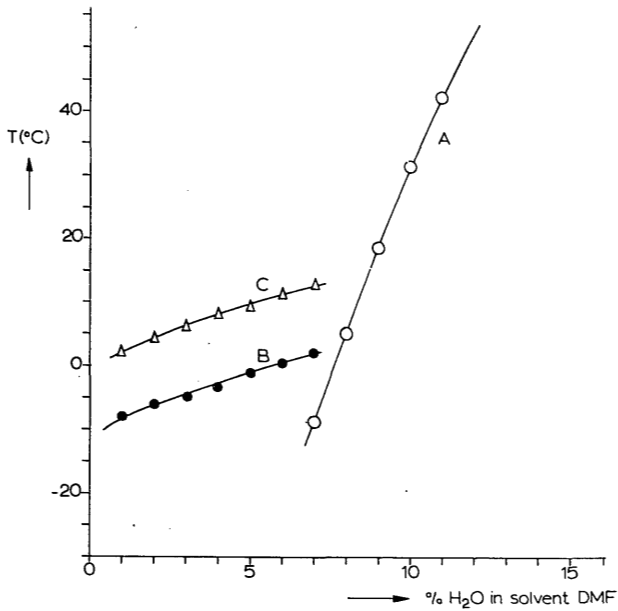


Fig. 5. Phase behavior at low water content in the system PU/DMF/H₂O for a polymer concentration of 25%.

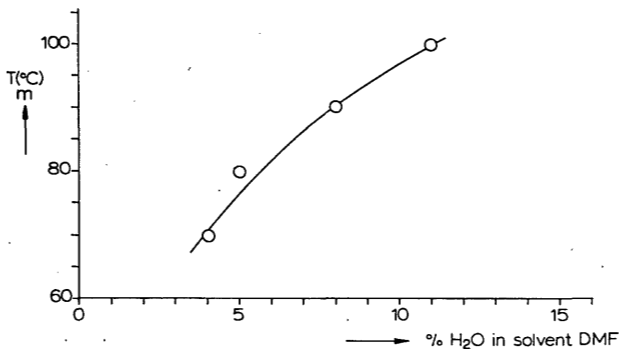


Fig. 6. Gel melting points in the system PU/DMF/H₂O for a polymer concentration of 50%.

If plotted against the increasing concentration of water at one polymer concentration (25%), curve A in Figure 5 is obtained.

Crystallization

If there is less than 8% water in the solvent, the PU solution becomes turbid at a temperature which is dependent on the cooling rate. In Figure 5, curve B corresponds to a very low cooling rate (1°C per 24 hr). At faster cooling rates, this curve is shifted to lower temperatures.

The phase-separated solution remains fluid. On heating the phase-separated solution, the turbidity disappears again at a temperature corresponding to curve

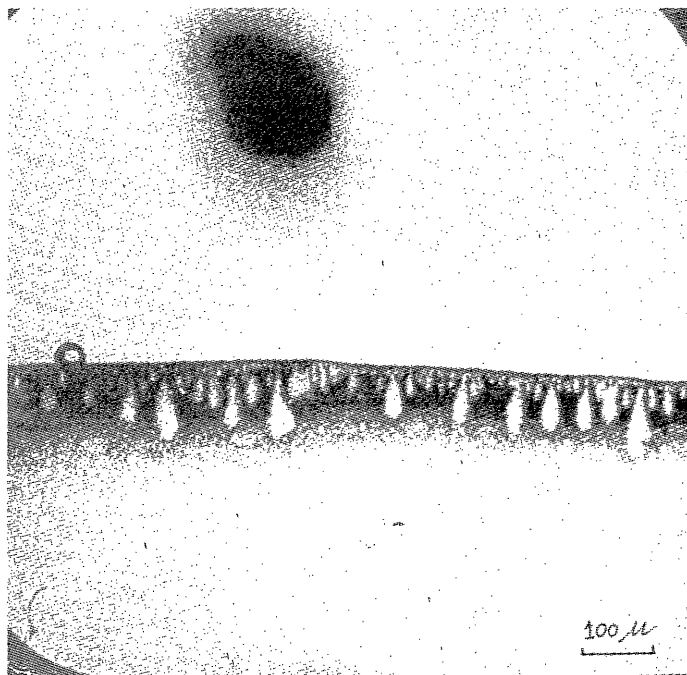


Fig. 7. Coagulation front 8 sec after contact with water (PU concentration 25%), as observed with an optical microscope.

C. This gap between cooling and heating curve clearly indicates crystallization, in which undercooling is quite common.¹⁶ At high polymer concentration, gelation occurs; the kinetics of gelation depend on water content and temperature. The gel is elastic and opaque. Upon heating, the gel becomes fluid at a certain temperature (the gel melting point). In differential scanning calorimetry (DSC), an endothermic peak is obtained on heating. In Figure 6, the gel melting points determined by DSC measurements are given for gels with a polymer content of 50%.

Morphology and Kinetics

By means of an optical microscope, the coagulation process was studied. Figure 7 was taken 8 sec after water was added. A higher magnification of the coagulation front is given in Figure 8. In Figures 9, 10, and 11, which were taken at time intervals of 1 sec, coalescence of droplets can be seen to occur.

In Figure 12, a scanning electron microscope photography of a membrane obtained from the system PU in DMF, coagulated in water, is shown. Figure 13 shows a SEM micrograph of a demixed solution in which the polymer concentration was very low (0.5% PU). It is obvious that the structure differs from that in Figure 12. In Figure 14, a scanning electron microscope photograph of a membrane obtained from the system modified SIS/1,2-dichlorobenzene/water-methanol is shown.

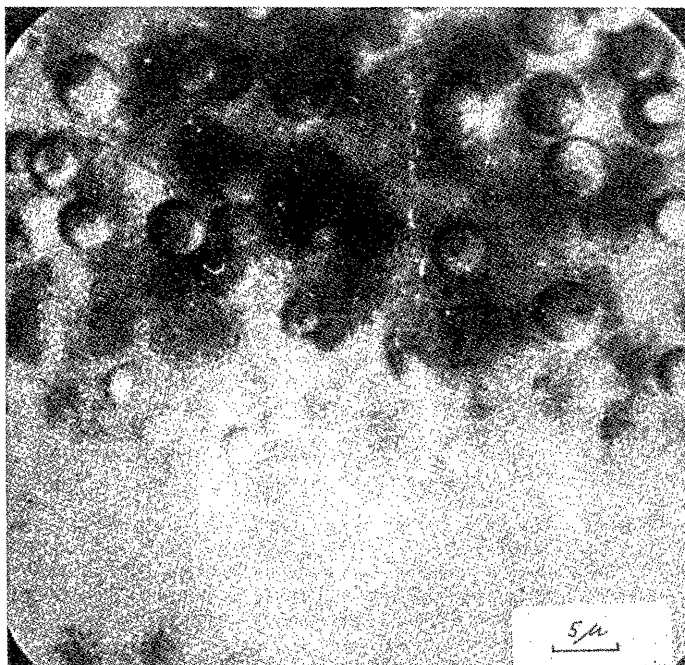


Fig. 8. High magnification of the coagulation front shown in Fig. 7.

As can be seen from Figure 15, the penetration distance of the coagulation front (the liquid-liquid demixing front, not that of the finger-like cavities) is proportional to \sqrt{t} . The penetration rate of the coagulation is of the same magnitude here as in the system cellulose acetate-dimethylformamide-water.⁸

Hyperfiltration Experiments

Hyperfiltration experiments were carried out as described. Typical results of the polyurethane membranes were a salt rejection of 21% and a flux of 1.1 cm/hr. The modified SIS membranes showed a salt retention of 62% and a flux of 2.4 cm/hr. The membrane performances have not been optimized as yet.

DISCUSSION

The combination of the optical microscope photographs (Figs. 7-11) and the SEM photographs (Figs. 12 and 14) shows that what is visible as a droplet during the demixing under the microscope is in the final membrane a spherical void in the sponge-like area. The photographs of the coalescent droplets also show that at that particular stage of the coagulation, both phases can still be fluid. The SEM photograph of the product of the coagulation process at very low (0.5%) polymer concentration (Fig. 13) shows spherical polymer particles. Following the theoretical section on liquid-liquid phase separation, nucleation and growth of the diluted phase occurs in the first case (Fig. 12).

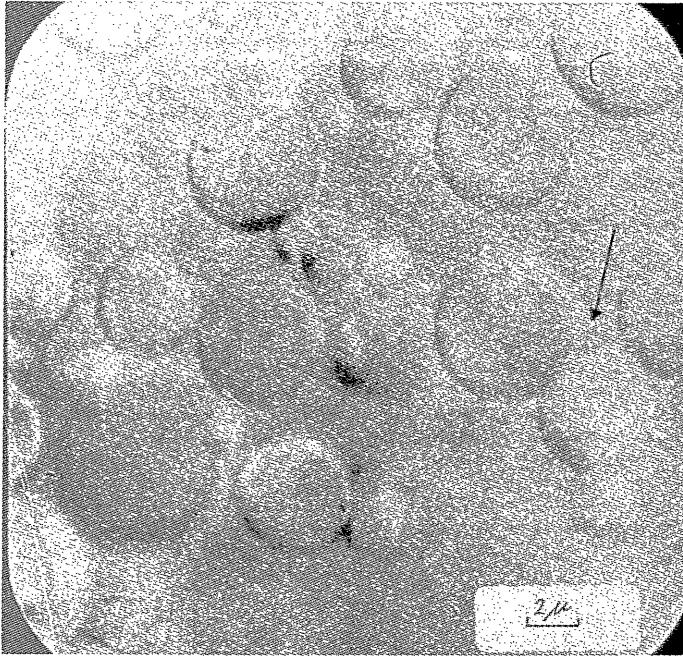


Fig. 9. Coalescence of droplets, optical microscope.

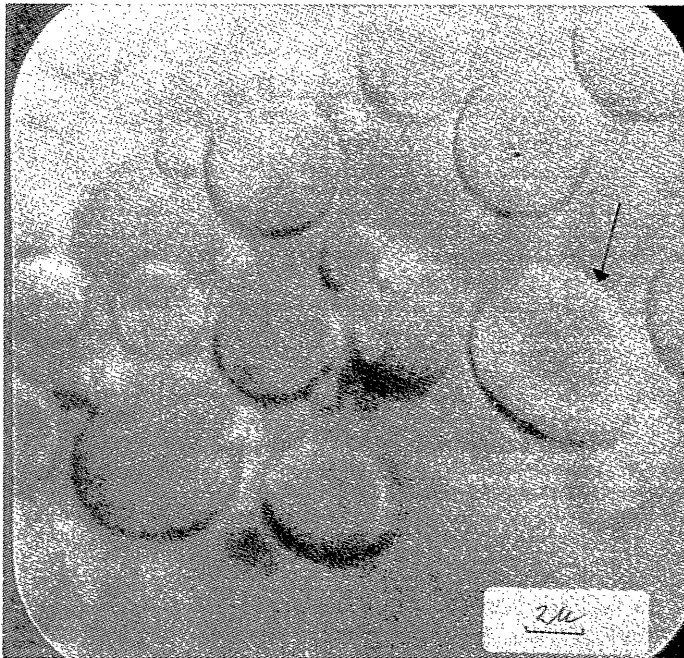


Fig. 10. Coalescence of droplets. Picture taken 1 sec after Fig. 9.

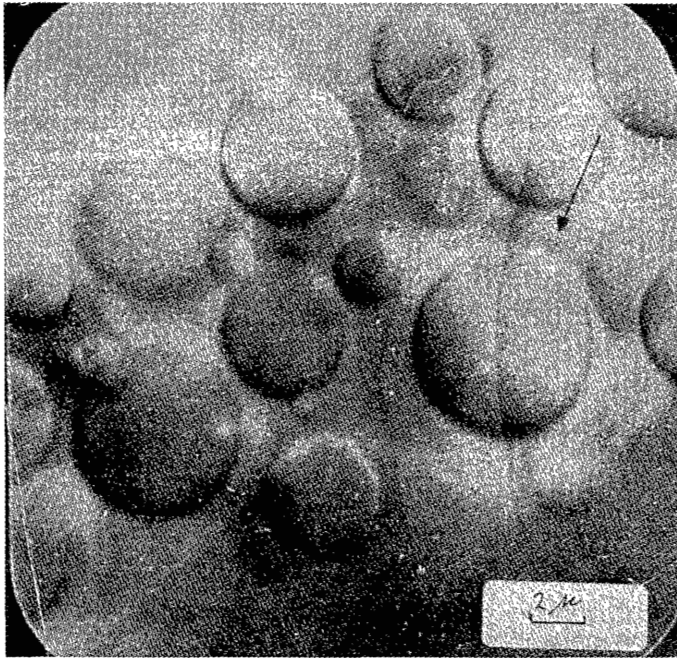


Fig. 11. Coalescence of droplets. Picture taken 1 sec after Fig. 10.

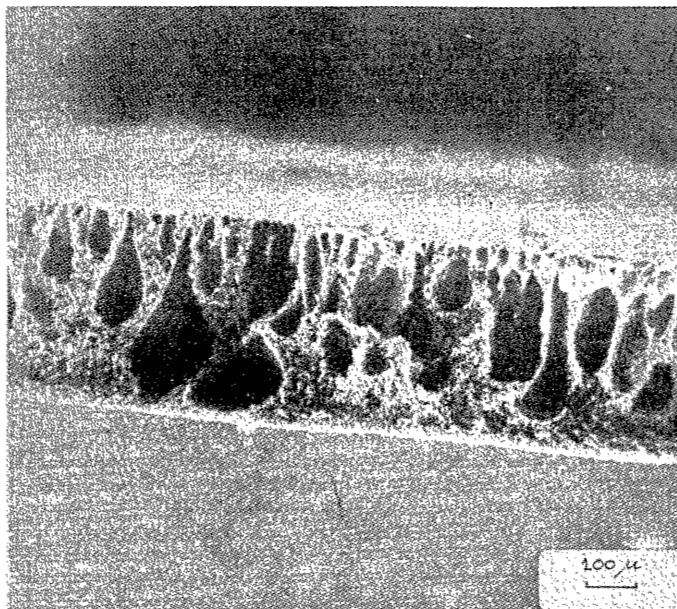


Fig. 12. Hyperfiltration membrane obtained from the system PU/DMF/H₂O (SEM photograph).

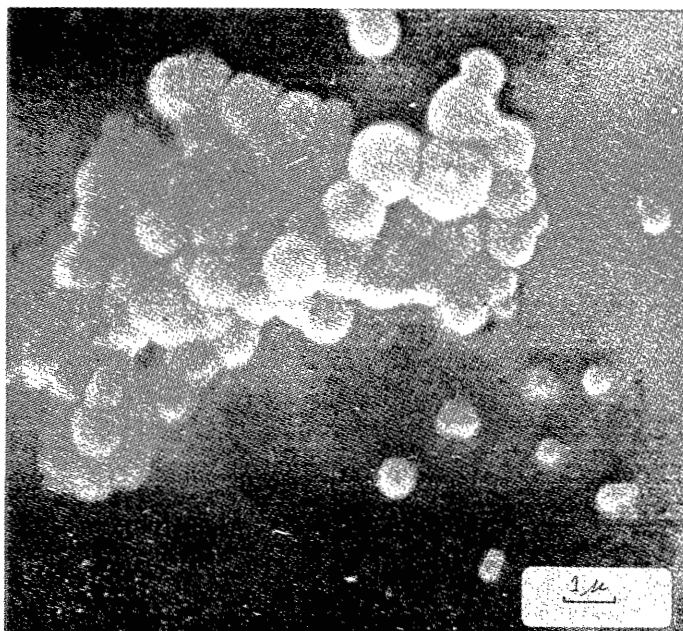


Fig. 13. SEM photograph of the latex particles which occur after the coagulation of a very diluted PU solution.

In the latter case (Fig. 13), nucleation and growth of the concentrated phase has occurred. Nucleation and growth of the diluted phase is observed for the PU system as long as the polymer concentration is above 5%. Therefore, the critical point in Figure 4 lies at a rather low polymer concentration (<5% PU).

The SEM photograph of the SIS membrane shows the same sponge-like structure which originates from nucleation and growth of the diluted phase. The structure observed for our membranes has also been found in other types of membranes.^{7,8,24} The explanation of the presence of the finger-like cavities given by Gröbe et al.¹¹ seems the most probable for this type of systems. This opinion is mainly based on the observation made by several authors that these fingers can penetrate the solution further than the coagulation front, without causing direct coagulation in the areas between these fingers.^{8,11,25,26}

This observation excludes, as the usual mechanism, the cracking of the surface skin layer or the disturbance of this layer and occlusion of nonsolvent. Moreover, the explanation of Gröbe et al. is in agreement with the results of Frommer et al.⁸ who found a bigger chance to obtain finger-like cavities when the nonsolvent and the solvent show a high affinity (big exothermic heat of mixing). This means a large driving force for diffusion of the solvent into these fingers. Frommer also found that the fingers could only grow in the liquid polymer solution. The number of finger-like cavities should be diminished when the difference in chemical potential of the solvent in the polymer solution and the nonsolvent is

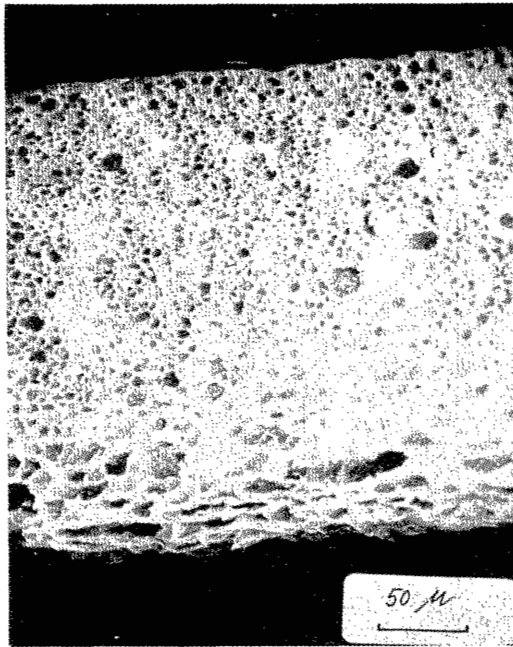


Fig. 14. SEM photograph of a membrane obtained from the system modified SIS/1,2-dichlorobenzene/(water-methanol):

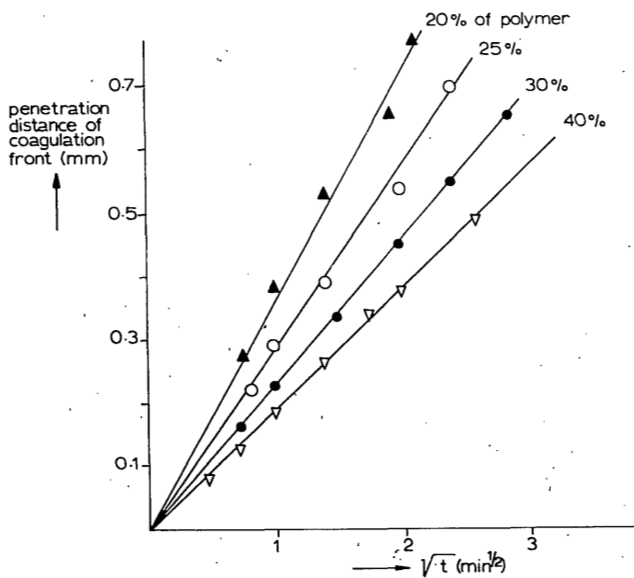


Fig. 15. Penetration of the coagulation front in the PU/DMF/H₂O system.

lowered. Frommer achieved this by salt-gelling, while we found that in the polyurethane system, adding solvent (DMF) to the nonsolvent (water) was effective in this respect. This effect was also found by Strathmann.⁷

In the SIS system, the solvent (1,2-dichlorobenzene) is not miscible with water, and miscibility is achieved only after adding methanol to the nonsolvent solution. Thus, the affinity between solvent and nonsolvent is low, and a membrane without finger-like cavities is the result (Fig. 14). Of course, the above reasoning can only be approximate because the affinities between solvent and polymer and nonsolvent and polymer have been left out of consideration.

The difficulty in the explanation given by Matz⁹ is that the surface tensions (valid for the interface between the substance and air) do not give direct information about the interfacial energy between the polymer solution and coagulation bath. Furthermore, it should be argued that the interface becomes less sensitive when the viscosity increases through the loss of solvent to the coagulation bath. At any rate, the explanation is not consistent with the experimental data which show that adding solvent to the coagulation bath gives fewer finger-like cavities.

The penetration of the coagulation front inward is proportional to \sqrt{t} . This is in agreement with all the diffusion equations derived for such situations.^{7,25,27,28,29} When the liquid-liquid phase separation has proceeded through the formation of spherical droplets or finger-like cavities, the polymer matrix will gradually become more concentrated until it eventually solidifies. We feel that the tendency of a polymer solution to crystallize and/or form a gel when high enough in concentration could be very important for the final membrane performance. Indeed, it has been found in cellulose acetate membranes that the ordering in the skin is an important variable.^{6,30}

A different type of mechanism might be operative typically for skin formation. Since, in general, the top layer of the film has a higher concentration by the evaporation of solvent and because the rate of phase separation is very high for this layer, in direct contact with nonsolvent, the mechanism of spinodal demixing (see theoretical section) cannot be excluded. The result is a favorable fine-mazed polymer network, intertwined by the fine pores. Crystallization in polymer regions may also follow here.

CONCLUSIONS

The general mechanism for the membrane formation by coagulation in nonsolvents follows the following scheme:

a. Direct desolvation of a top layer (skin) where most likely gelation takes place (especially when an evaporation step is performed before coagulation).

b. Liquid-liquid phase separation in the solution below the skin. In most instances, nucleation and growth of the diluted phase occurs. In this case the polymer forms the continuous matrix, and the final structure after complete desolvation is the typical sponge-like structure. When the difference in chemical potential for the solvent between the polymer solution and the nonsolvent is large, finger-like cavities also occur.

The authors are grateful to Mr. A. Bakker for carrying out a part of the experiments described in this paper.

References

1. S. Loeb and S. Sourirajan, *Advan. Chem. Ser.*, **38**, 117 (1962).
2. M. G. Bungenberg de Jong, *Kolloid-Z.*, **80**, 221 (1937).
3. K. H. Maier and E. A. Scheuermann, *Kolloid-Z.*, **171**, 122 (1960).
4. B. Keilin, Office of Saline Water, Res. Dev. Rept. 117, Aug. 1964.
5. R. E. Kesting, *Synthetic Polymeric Membranes*, McGraw-Hill, New York, 1971.
6. H. Strathmann, P. Scheible, and R. W. Baker, *J. Appl. Polym. Sci.*, **15**, 811 (1971).
7. H. Strathmann, K. Kock, P. Amar, and R. W. Baker, *Desalination*, **16**, 179 (1975).
8. M. A. Frommer and D. Lancet, in *Reverse Osmosis Membrane Research*, H. K. Lonsdale and H. E. Podall, Eds., Plenum Press, New York, 1972.
9. R. Matz, *Desalination*, **10**, 1 (1972).
10. J. P. Craig, J. P. Knudsen, and V. F. Holland, *Text. Res. J.*, **32**, 435 (1962).
11. V. Gröbe, G. Mann, and G. Duwe, *Faserforsch. Textiltech.*, **17**, 142 (1966).
12. D. M. Koenhen, M. A. de Jongh, C. A. Smolders, and N. Yücesoy, *Colloid Polym. Sci.*, **253**, 521 (1975).
13. P. J. Flory, *Principles of Polymer Chemistry*, Cornell University Press, Ithaca, N.Y., 1953.
14. J. W. Cahn, *Trans. Met. Soc. AIME*, **242**, 166 (1968).
15. C. A. Smolders, J. J. van Aartsen, and A. Steenbergen, *Kolloid-Z.Z. Polym.*, **243**, 14 (1971).
16. L. Mandelkern, *Crystallization of Polymers*, McGraw-Hill, New York, 1964.
17. P. H. Morgan and G. S. Park, *Faraday Disc. Chem. Soc.*, **57**, 38 (1975).
18. D. Eagland, P. Dilling, and R. G. Wheeler, *Faraday Disc. Chem. Soc.*, **57**, 181 (1975).
19. T. A. Bryce, A. A. McKinnon, E. R. Morris, D. A. Rees, and D. Thorn, *Faraday Disc. Chem. Soc.*, **57**, 221 (1975).
20. D. S. Reid, T. A. Bryce, A. H. Clark, and D. A. Rees, *Faraday Disc. Chem. Soc.*, **57**, 230 (1975).
21. V. M. Averyanova and G. N. Tunofeyeva, 12th IUPAC Microsymposium on Macromolecules cont. F4, 1973.
22. P. T. van Emmerik and C. A. Smolders, *J. Polym. Sci. C*, **38**, 73 (1972).
23. P. M. van der Velden, M. H. V. Mulder, L. van der Does, and C. A. Smolders, *Polym. Letters*, **14**, 5 (1976).
24. G. J. Gittens, P. A. Hitchcock, and G. E. Wakley, *Desalination*, **12**, 813 (1966).
25. M. E. Epstein and A. J. Rosenthal, *Text. Res. J.*, **36**, 813 (1966).
26. M. van Hilten, T. H. Twente, Report 1973.
27. D. R. Paul, *J. Appl. Polym. Sci.*, **12**, 383 (1968).
28. H. Jost, A. Gröbe, and H. Klare, *Faserforsch. Textiltech.*, **14**, 522 (1963).
29. A. Rende, *J. Appl. Polym. Sci.*, **16**, 585 (1972).
30. R. Matz, *Desalination*, **12**, 273 (1973).

Received December 15, 1975

SUMMARY

In this thesis work on some aspects of phase separation phenomena in polymer solutions is reported.

In the first chapter a general introduction is given on the importance of phase separations in polymer solutions. The different types of phase separations which are possible are discussed. Of course the thermodynamics of polymer solutions have received a great deal of attention. The first part of the thesis is devoted to solutions of poly(2,6-dimethyl-1,4-phenylene oxide) in aromatic solvents (mainly toluene).

The thermodynamic correction parameter in the Flory-Huggins equation (g) has been determined (Chapter II) by a light scattering method (for PPO in toluene). This gave the relationship for g , $g = 0.58 + 0.19 w$. With this parameter it proved to be possible to describe the phase separation as a crystallization phenomenon. However it was not possible to describe a liquid-liquid phase separation with this parameter. In differential scanning calorimetry experiments it appeared that these solutions were indeed able to crystallize. From two distinct endothermic peaks (dependent on thermal history) it was concluded that possibly two different modifications of crystallites exist (Chapter III). Measurements of the kinetics of the phase separation with the Pulse Induced Critical Scattering method revealed (Chapter IV) that there is a distinct induction time connected with the phase separation. This is also an indication for crystallization, probably in two succeeding steps. For the same polymer in the homologous solvent series toluene/*n*-hexylbenzene the thermodynamic correction parameters were calculated, using experimentally determined melting point curves. Only when the assumption was made that the solvent is built in the PPO crystal lattice, reasonable values for the correction parameter were obtained (Chapter V).

The last chapter on PPO solutions (Chapter VI) describes the determination of the thermodynamic correction parameter g from vapour pressure osmometry and high pressure membrane osmometry. The correction parameter appeared not to be very dependent on the temperature, but here the concentration dependence was noted as well. The values for membrane osmometry were $g_0 = 0.498$ and $g_2 = 0.163$. Whereas membrane osmometry proved to be the most reliable method, vapour pressure osmometry proved to be a very quick method, which

is very usable in a certain concentration range (5% and 15%). From these lower values of g and the very ratio for T_g/T_m found in this system it was concluded that the T_m usually found was not the thermodynamic melting point, but the melting of a degenerated structure, while in real crystals solvent is co-crystallizing into the lattice. With the hypothesis of a crystallization of PPO by a solvent stabilized helix structure, all the observed phenomena can be explained.

Chapter VII describes the relations between solubility parameters for polymer and solvents and other physical quantities as index of refraction, surface tension and dipole moments. Also some additive constants have been determined for the calculation of solubility parameters.

Chapter VIII describes the formation mechanism of asymmetric membranes. In the explanation of the formation mechanism, the phase separations which are described above, are used.

SAMENVATTING

In dit proefschrift wordt het onderzoek naar enkele aspecten van fase-scheidingen in polymeeroplossingen beschreven.

In het eerste hoofdstuk wordt een algemene inleiding gegeven over de betekenis van fase-scheidingen in polymeeroplossingen. De verschillende typen fase-scheidingen die mogelijk zijn worden besproken.

Natuurlijk heeft de thermodynamica van polymeeroplossingen een belangrijk deel van de aandacht gekregen. Het eerste deel van het proefschrift is gewijd aan oplossingen van poly (2,6 dimethyl-1,4 phenyleen oxide) in aromatische oplosmiddelen (hoofdzakelijk toluen).

De thermodynamische correctie parameter in de Flory-Huggins vergelijking (g) is bepaald (Hoofdstuk II) met een lichtverstrooiings methode (voor PPO in toluen). Dit leverde de relatie voor g , $g = 0,58 + 0,19w$. Met deze parameter bleek het mogelijk om de fase-scheiding te beschrijven als een kristallisatie-verschijnsel. Het was met deze parameter echter niet mogelijk een vloeistof-vloeistof fase-scheiding te beschrijven.

Uit Differentiele Scanning Calorimetrie experimenten bleek dat deze oplossingen inderdaad in staat waren te kristalliseren. Uit twee aparte endotherme pieken (afhankelijk van thermische geschiedenis) werd geconcludeerd dat er misschien twee verschillende modificaties kristallen bestaan (Hoofdstuk III).

Meting van de kinetiek van de fase-scheiding met de Pulse Induced Critical Scattering methode onthulde (Hoofdstuk IV) dat er een aparte inductie tijd verbonden is met de fase-scheiding. Dit is tevens een aanwijzing voor kristallisatie, waarschijnlijk in twee opeenvolgende stappen.

Voor het zelfde polymeer werd in de homologe oplosmiddelen reeks toluen / -n-hexyl benzeen de thermodynamische correctie parameter berekend, daarbij gebruik makend van experimenteel vastgestelde smeltpunt curves.

Alleen wanneer de onderstelling werd gemaakt dat het oplosmiddel was ingebouwd in het PPO kristal rooster, werden redelijke waarden voor de correctie parameter verkregen (Hoofdstuk V).

Het laatste hoofdstuk over PPO oplossingen (Hoofdstuk VI) beschrijft de bepaling van de thermodynamische correctie parameter g door middel van damp druk osmometrie en hoge druk membraan osmometrie. De correctie parameter bleek niet erg afhankelijk te zijn van de temperatuur, maar hier werd ook de concen-

tratie afhankelijkheid aangetroffen.

De waarden voor membraan osmometrie waren $g_0 = 0,498$ en $g_2 = 0,163$.

Terwijl membraan osmometrie de meest betrouwbare methode bleek te zijn, was de damp druk osmometrie een erg snelle methode, die goed bruikbaar is in een bepaald concentratie gebied (5% en 15%). Uit deze lage waarden voor g en de zeer hoge verhouding voor T_g/T_m gevonden voor dit systeem, werd geconcludeerd dat de T_m die gewoonlijk gevonden wordt niet het thermodynamische smeltpunt is, maar het smelten van een gedegenerende structuur, terwijl in echte kristallen het oplosmiddel mee in het rooster uitkristalliseert.

Met de hypothese van een uitkristalliseren van PPO in een door oplosmiddel gestabiliseerde helix structuur kunnen alle waargenomen verschijnselen verklaard worden.

Hoofdstuk VII beschrijft de relaties tussen oplosbaarheidsparameters, oplosmiddelen en andere fysische grootheden zoals brekingsindex, oppervlakte spanning en dipoolmomenten. Ook zijn enkele additieve constanten bepaald voor de berekening van oplosbaarheidsparameters.

Hoofdstuk VIII beschrijft het mechanisme van de vorming van asymmetrische membranen. In de verklaring van het vormings-mechanisme zijn de hierboven beschreven fase-scheidingen gebruikt.

Curriculum Vitae

DIRK MARINUS KOENHEN werd op 13 juni 1949 te Lathum (gem. Angerlo) geboren. In 1966 behaalde hij het HBS-B diploma aan "Het Rhedens Lyceum" te Velp (Gld). De studie aan de Technische Hogeschool Twente werd in september 1966 aangevangen. In september 1970 werd het baccalaureaatsdiploma behaald met als hoofdvak procestechniek. In juni 1973 werd het ingenieursdiploma behaald met als hoofdvak grensvlak- en kolloïdchemie.

Van juli 1973 tot juli 1977 was hij in dienst bij de Technische Hogeschool Twente als wetenschappelijk ambtenaar. In deze periode is het onderzoek ten behoeve van dit proefschrift verricht.

Vanaf 1 juli 1977 is hij in dienst van Wafilin B.V. te Hardenberg.

IF YOU DON'T BELIEVE ME, YOU'LL SEE IT WHEN THE EGGS
ARE FRIED

(cit. CERVANTES)

